HILT CRC

Australian Government
Department of Industry, Science and Resources

Cooperative Research Centres Program

Final Project Report

RP3.004
INTERMEDIATE PRODUCT EXPORTS FOR AUSTRALIA-CHINA GREEN STEEL

An outlook on exports of iron ore and green iron into decarbonised Chinese steel making value chains with a cost-minimising optimisation model

AUTHOR(S):

Jorrit Gosens, Alireza Rahbari, John Pye, Frank Jotzo
Heavy Industry Low-carbon Transition Cooperative Research Centre, ANU

DATE: MAR/25
HILT CRC REPORT 2025/197

HILTCRC.COM.AU

HILT CRC

Australian Government
Department of Industry, Science and Resources

Cooperative Research Centres Program

RP3.004
INTERMEDIATE PRODUCT EXPORTS FOR AUSTRALIA-CHINA GREEN STEEL

PROJECT NUMBER

RP3.004

AUTHOR(S):

Jorrit Gosens, Frank Jotzo
Heavy Industry Low-carbon Transition Cooperative Research Centre, ANU Crawford School of Public Policy & Zero-Carbon Energy for the Asia-Pacific (ZCEAP) Initiative

Alireza Rahbari, John Pye
Heavy Industry Low-carbon Transition Cooperative Research Centre, ANU School of Engineering & Zero-Carbon Energy for the Asia-Pacific (ZCEAP) Initiative

ADDRESS BLOCK:

Crawford School of Public Policy, 132 Lennox Crossing, J.G. Crawford Building, The Australian National University, Canberra ACT 2600

School of Engineering, 35A Science Road ACT 2600 Australia, Craig Building, The Australian National University, Canberra ACT 2600

Heavy Industry Low-carbon Transition Cooperative Research Centre, Lot Fourteen, Corner North Tc and Frome Rd, Adelaide SA 5000

ACKNOWLEDGEMENTS:

The work has been supported by the Heavy Industry Low-carbon Transition Cooperative Research Centre whose activities are funded by its industry, research and government Partners along with the Australian Government's Cooperative Research Centre Program. Jorrit Gosens and Frank Jotzo's involvement in this project were made possible through co-sponsoring by an anonymous private donor. The purchase of CRU data was made possible by a grant from the research spoke on Energy Transition of the Australian Centre on China in the World (CIW). This is HILT CRC Document 2025/197

OTHER MATTERS:

PROJECT PARTNERS:

The Australian National University
Curtin University
FMG Procurement Services Pty Ltd Industry
Grange Resources (Tasmania) Pty Ltd Industry
Onesteel Manufacturing Pty Limited
Minerals Research Institute of Western Australia
Roy Hill Holdings Pty Ltd

EXECUTIVE SUMMARY

China produces well over half of the world's steel and is the largest consumer of Australian iron ore, being the destination for a little over 80% of Australian iron ore exports. China's plans for decarbonisation include a reduction in steel demand and a greater use of recycled steel scrap, both of which can impact demand for (Australian) iron ore. Remaining future demand for primary steel will have to be met through decarbonised steel making pathways, with green hydrogen-based direct reduction currently the most likely pathway to produce green iron.

The existing cost-competitiveness of relatively low-grade Australian ores, and Pilbara ores in particular, is largely based on their suitability for use in the Blast Furnace - Basic Oxygen Furnace (BF-BOF) route. Whether these ores will remain cost-competitive for decarbonised steel making pathways, compared to the generally higher quality ores from e.g., Brazil, Sweden, Canada, or new suppliers in Guinea, remains unclear. This is because the more mature green steel production pathway of Hydrogen DRI - Electric Arc Furnace (H_2DRI-EAF) typically requires higher grade ores with > 65% iron content. Ores with lower Fe content can still be directly reduced, but require an additional melting step to remove impurities, via the less mature hydrogen DRI - Electric Smelter Furnace - Basic Oxygen Furnace (H_2DRI-ESF-BOF) pathway, or improvement via beneficiation processes.

A second issue requiring further investigation is whether the processing of Australian iron ore into iron or steel could competitively be done in Australia. Although Australia has high labour costs, it also has excellent solar and good wind resources that could potentially drive down renewable electricity and green hydrogen production costs, which form a large component of the production cost of green iron.

The aim of HILT research project RP3.004 is to assess the implications of decarbonising the Australia-China steel supply chain on the greenhouse gas emissions, and cost-competitiveness of Australian exports of ore, steel, or intermediate products. This report focuses on the techno-economics of various possible exports, including direct shipping ore, beneficiated ores, HBI, pig iron, or steel from Australia, into future Chinese green steel value chains. A lifecycle analysis of emissions in these supply chains is provided in a separate report, and a synthesis of project outcomes is provided in a non-technical brief.

This report describes the development and initial results from a cost-minimising source-and-sink optimisation model developed for RP3.004. Critically, the model takes into account differences in ore quality from mines around the world, and how this influences processing costs in different pathways. We do so by developing process models for different conventional and decarbonised production pathways that consider how different compositions of ore influence energy and raw material requirements etc., in different processing steps. This is combined with an optimisation model that considers 1) the cost of all mining, inputs of energy and raw materials, 2) the CapEx and OpEx required in different processing steps, and 3) transport costs between different centres of production and demand. Cost data is sourced from CRU, the industry benchmark for this data, which provides global coverage of both the mining and steelmaking industries.

This model offers insight into the relevance of ore quality in green steel making value chains, the cost competitiveness of different ores in EAF and ESF production routes, and the production cost of green hydrogen required to make Australian green iron competitive in Chinese value chains. Using baseline cost data, our model results suggest that Chinese demand for Australian iron ore will decline if forecasted reductions in steel demand and increases in scrap supply materialise. By 2035, our model forecasts Australian exports of iron ore to China to fall by about 260 Mt, with bigger reductions if China implements very ambitious green steel targets due to a preference for higher quality ores. By 2050, sharp reductions in primary steel production driven by increased reliance on scrap in China are expected to lead to significant reductions in Chinese demand for iron ore, to as little as 250 Mt, with as little as 60 Mt of that demand supplied by Australia. These trends depend on whether or not the reduction in steel demand and increased supply of scrap will develop as strongly as forecasted, whether China develops sufficient EAF or ESF capacity to process the green iron required to meet total steel demand via either route, on top of EAF capacity to recycle all that scrap, and the technical feasibility of meeting demand for all types of steel with recycled steel scrap.

The results highlight the role for further technology development, such as novel technologies for beneficiation or reduction via electrolysis of ores, in improving the competitiveness of Australian ores in a future Chinese market for green steel. They also highlight the importance of exploring the development of green iron markets beyond China, as the results presented here say nothing about the cost-competitiveness of Australian green iron production for supply into the Japanese, Korean, Indian, Taiwanese, European, or other markets. Further work will be carried out in HILT project RP3.009 using this model to identify the cost-competitiveness of Australian green iron, or alternatively iron used in green steel making value chains, in those other global markets. That follow-up project will also identify critical points at which cost reductions or technology improvements could improve the competitiveness of Australian iron ore or green iron in such potential global markets, and interrogate how different policy mechanisms could help improve this competitiveness.

The cost-competitiveness of Australian green iron production in future green steel value chains will depend most strongly on the production cost of green hydrogen, relative to key competitors in Latin-America, the MENA region, etc., and relative to Chinese domestic production. Results suggest that green iron production would occur entirely in China at hydrogen cost parity between Australia and China. However, at a cost differential of just A$0.50/kg of green hydrogen, Chinese demand for Australian green iron increases to 300 Mt, slowly climbing to about 450 Mt if the cost differential is as large as A$1.25/kg H_2. The challenge then is for development of low-cost renewable energy projects, or for government assistance, including in the form of a Hydrogen Production Tax Incentive, to drive down the production cost sufficiently to realise such a cost differential. These hydrogen production costs need further

investigation, which is planned or a future iteration of the model, utilising modelling methodology developed for Australia under the HILT CRC RP2.006 project, and will consider more locally specific hydrogen production costs estimates for e.g., the Pilbara, other regions in Western Australia, South Australia, Tasmania, etc. This future work would allow us to better quantify the supply side support required to maintain demand for Australian ores.

Lastly, our model results show that the Electric Smelter Furnace will be of key importance to the cost-competitiveness of Australian iron ore in future green steel value chains, regardless of whether the production of iron occurs in Australia or China. Our model suggests that in scenarios with high green steel demand in China, Australian iron ore consumption would climb together with ESF capacity, from near zero in scenario with no or very little ESF capacity, to 380 Mt of Australian iron ore consumption in a scenario with an ESF capacity of 400 Mt or above. It is therefore imperative that Australian industry and government work to stimulate the technological development of the ESF, which is currently still in the demonstration stage, and help support their industrial-scale rollout. This may mean developing ESF processing capacity domestically, or convincing customers in China or other key markets that investment in ESF capacity are worthwhile.

CONTENTS

1. INTRODUCTION

Global plans for decarbonisation will inevitably have to deal with steelmaking emissions, which make up about 7 to 9 per cent of global emissions. China stands out, producing and consuming well over half of all steel globally, and relying on emissions heavy blast furnaces to a higher degree than other major steel making nations. As a result, Chinese steelmaking emissions account for as much as 16 per cent of total domestic emissions[1]. China is also the largest consumer of Australian iron ore, being the destination for a little over 80% of Australian iron ore exports[2].

China's plans for decarbonisation include a reduction in steel demand and a greater use of recycled steel scrap, the supply of which is expected to grow significantly over the next few decades. These two developments can be expected to put pressure on demand for iron ore consumption and therefore imports, including from Australia. Further pressure on demand for Australian iron ore can be expected to come from a greater diversification of suppliers, including towards newly developed deposits in Guinea[1].

Both in China as well as any other steelmaking location globally, hydrogen based production routes are generally considered the most viable pathway to deep emission cuts for remaining primary steel making[3,4].

The existing cost-competitiveness of Australian ores, and Pilbara ores in particular, is largely based on their suitability for use in the Blast Furnace - Basic Oxygen Furnace (BF-BOF) route. The green steel making pathway with the highest TRL level currently is the hydrogen direct reduced iron (DRI) - Electric Arc Furnace (H_2DRI-EAF) pathway, though this route requires DRI with very low gangue content, i.e., made with ores with very high iron grades. An alternative pathway, a two-step steelmaking process via the hydrogen DRI - Electric Smelter Furnace - Basic Oxygen Furnace (H_2DRI-ESF-BOF) pathway can handle high gangue content iron ores, although it is currently at a lower TRL[5,6].

A switch to green steelmaking could have an impact on demand for iron ores with different compositions: some ores may not be suitable to the H_2DRI-EAF pathway at all, as they can not be beneficiated to the required Fe grade. In both the H_2DRI-EAF and H_2DRI-ESF-BOF pathway, iron ore composition will affect energy consumption, flux requirements, and iron losses either in the beneficiation step or to slag in the steelmaking step, amongst others[5,6].

These trends: lower steel demand and greater scrap supply, diversification towards new suppliers, and a switch to green steel making processes, will all affect demand for Australian ores. A particular issue that requires investigation is the competitiveness of low-grade Pilbara ores in the novel green steel making processes, versus higher grade ores from Brazil, Guinea, or elsewhere.

A second issue requiring further investigation is whether the processing of Australian ore into iron or steel could competitively be done in Australia. Although Australia has high labour costs, it does also have excellent solar and good wind resources that could potentially help drive down renewable electricity and green hydrogen production costs[4], which form a large component of the production cost of green iron[5]. The switch to green steel making potentially makes it more economical to split iron and steel making steps over different locations, as renewable energy costs are highly location dependent, and long-distance transport of green power or hydrogen is more technically challenging and more costly than long-distance transport of fossil fuels[7].

Questions over the suitability of Australian ores for green steel making, and the potential benefits to onshoring upstream processes, mean that the prospect for Australia becoming a low-cost producer of green iron remains unclear. The primary aim of this report is to assess the techno-economics of various options for Australian exports into a Chinese market that would demand increasing amounts of green steel. We consider different options for organising the value chain between Australia and China, including the possibility of exports of direct shipping ore, beneficiated ores, iron, or steel from Australia.

The assessment combines process modelling for different conventional and decarbonised production pathways, to assess how iron ores with different compositions would influence energy and flux requirements, slag production, and losses of iron etc., in different processing steps. We use cost data from the iron ore and steel cost models[8,9] developed by CRU, a reputable supplier used by much of the iron ore mining industry, that cover the global iron and steelmaking industries. The iron ore data from CRU has global coverage on the iron ore type (hematite, goethite, magnetite), composition, and production cost. This data is combined in an optimisation model that considers the cost of all mining, inputs of energy etc, the CapEx and OpEx required in different processing steps, as well as transport costs between different centres of production and demand.

This modelling framework allows us to assess who will supply iron ore into a future Chinese market for green steel, as well as via what processing pathways, and in what location it will be most economically processed. This type of model can assist future strategic decision making, including by helping policymakers understand viable leverage points to improve the preconditions for this industry to develop and be retained in Australia. This report was produced as part of RP3.004. A separate report under this same project provides Life-Cycle Analysis of GHG emissions for each of the different possible supply chain configurations between Australia and China. A synthesis report provides a non-technical summary and messages for policy makers.

2. PREVIOUS RESEARCH AND LITERATURE

The decarbonisation of the steelmaking sector has been the subject of much research in recent years. The most relevant previous research for the questions investigated in this report are those studies that have pointed at the possibility of re-organised global value chains for global iron- and steelmaking, with energy intensive processing steps closer to locations with abundant and cheap renewable energy.

This question of whether new locations could become dominant suppliers in global green steelmaking value chains has been investigated in a string of reports that have come out over the past two or three years. A good number of these reports have a specific focus on the feasibility of green iron production in Australia using Australian ores. It does deserve to be noted that this is already a recalibration on earlier work, which had a greater focus on the production of steel in Australia[4,10,11], or on the production and exports of green hydrogen for processing iron ore and other industrial uses elsewhere[12–14].

The studies that have engaged with the question of re-organised value chains for producing green iron and steel in new, renewable energy rich locations, have typically had one or more shortcomings that we attempt to address in the current work.

First, the large majority of studies only consider a Hydrogen DRI - Electric Arc Furnace (H_2DRI-EAF) pathway for green hydrogen-based steel making. This matters as the EAF pathway is generally considered to require DRI with very low gangue content, meaning it requires iron ore with very high Fe grades; typically 67% or higher[15]. This is an issue as it may not be feasible for the bulk of Australian iron ores to meet this high Fe grade, either because the beneficiation process required to improve low grade ores would have such poor recovery rates that very large amounts of ore would need to be mined to produce a single ton of product, or because these ores contain a relatively high mix of goethite and hematite, limiting their theoretical maximum Fe grade to below the required level. The alternative Hydrogen DRI - Electric Smelter Furnace - Basic Oxygen Furnace (H_2DRI-ESF-BOF) pathway can handle high gangue content iron ores, and would enable the use of Pilbara or other low grade ore for green steel making[5,6]. Reports that focus on the EAF pathway for green steel production without an ESF step would practically exclude any consideration of Pilbara ores being used, and is therefore not suited to investigate Australia's role in future green steel value chains. Beyond concerns over Australian participation, the global supply of DR grade ores is, and will very likely remain, limited and may never be able to cover demand if all future green steel were produced via this H_2DRI-EAF pathway[15,16].

Second, a large majority of studies use simplified mining cost and ore quality data, typically a single value for the cost of mining for any location in the world, and a single, often non-defined, composition of iron ore. This matters as the cost-competitiveness of different locations for green iron production may be largely dependent on local renewable energy production cost and the related production cost of green hydrogen. Differences in local mining costs matter as well, with about a factor of 4 difference in production costs between producers at the lower and higher ends of the global cost curve[17,18]. Ore qualities are also a strong driver of cost-competitiveness, as explained in the next two points. The, sometimes very, limited granularity on mining costs fails to capture the relative competitiveness of different mines within individual or even between different countries.

Third, previous studies all go to some length in describing detailed cost components considered for individual iron or steelmaking processing steps (see an overview in Table 1). The very large majority of this work, however, considers typical or average values for many of the energy and raw material inputs in each of these processes. This matters, as process inputs depend on the composition of the feedstock (DRI or ores) and these differences substantially influence resulting steel production costs[5], e.g., the amount of flux and power consumption required to melt DRI in an EAF process, as are the losses of iron to slag,. Use of an average power consumption per ton of steel, regardless of ore composition, ignores these differences. Ore composition determines energy and raw material consumption in most processing steps, as we will detail in our methodology section.

Fourth, a particular processing step that deserves additional attention is the beneficiation step, which is almost always ignored or highly simplified in previous work. The process of beneficiation involves separating iron from gangue components and allows upgrading of an iron ore to higher Fe grades in order to improve the price fetched for it. The separation is not a perfect process, however, and the product stream will still contain some gangue whilst some iron will be lost to the waste stream. How much of the iron is lost, or the weight recovery, depends on a number of factors. Most important is the form of iron oxide, mostly whether it is a magnetite, hematite, or goethite ore; the former is much more amenable to magnetic separation, which is relatively efficient (higher weight recovery) than methods available for other types of ore[6,19,20]. Weight recovery rates are also dependent on the way iron oxide and gangue components are mixed in the iron ore matrix, with finer grain sizes, as is typical in Pilbara hematite ores, making it more difficult to separate the two[21]. Lastly, the level of upgrading matters, with weight recovery still relatively high with limited levels of upgrading, but falling quickly as upgrading is pushed closer to the theoretical maximum Fe grade, which is in itself a function of the ore quality[5,6]. As explained in the previous point, the composition of the product used in iron and steelmaking influences energy and raw material consumption, affecting economic performance. Beneficiation can improve overall steelmaking cost when the reduced consumption of energy and other raw materials in downstream processing outweigh the losses (due to limited weight recovery) in the beneficiation step, and the associated additional costs to mine more material to make up for those losses[5].

Lastly, the selection of countries that are included in the assessment matters for results when assessing which is the most cost-competitive location for green iron production. This is typically not a very big issue, as most studies do include a wide variety of potential new locations for iron production, typically locations with high current levels of iron ore production and good quality renewable energy resources, as well as countries with very high shares of current global steelmaking output or capacity. Some studies however simply

exclude key Asian steel producers such China, India, Korea, or Japan, from their assessment, limiting their utility in comparing cost-competitiveness of importing green iron versus domestic production in these countries.

For a summary of recent work on the potential for global green iron trade to emerge, and how they handle these issues, see Table 1.

In our analysis here, we consider the possibility of producing iron via the H_2DRI-EAF as well as the H_2DRI-ESF-BOF pathways. Exports of iron can occur as HBI, produced from DRI, or as pig iron granules, produced from the ESF hot metal. In importing countries, either of these products can be consumed in EAF or BOF steelmaking pathways, with limitations on the acid gangue content of the DRI or pig iron processed in the EAF. We consider that H_2DRI can be produced both with blue or green hydrogen, but we consider the steel resulting from production with blue hydrogen as being fossil fuel based, and not as green steel.

We use mining cost and ore composition data from CRU Group, a company that provides business intelligence on the global mining and other sectors, whose iron ore cost model is considered the industry benchmark.

We develop process sub-models for each of the relevant iron and steel making processes that considers iron ore, or iron, composition in determining energy and raw material consumption, as well as slag production and iron losses. This includes a beneficiation sub-model that considers iron ore properties in determining weight recovery rates.

Our analysis is strongly focused on the future Australia-China trade relation in green iron, given the relevance of this relationship in current iron ore trade as well as current and expected future levels of steel production in China. As potential producer locations supplying the Chinese market with green iron, we consider three different regions in China, in the North, the South, and the West, as well as Australia and a number of key potential competitors, specifically Brazil and Chile, and Egypt and the UAE.

TABLE 1. REVIEW OF EARLIER STUDIES ON FUTURE GREEN IRON SUPPLY CHAINS

Study	Focus	Green steel pathways	Ore cost and quality assumptions	Process models consider iron ore quality	Beneficiation considered	Producer locations considered
Bilici et al., Global trade of green iron as a game changer for a near-zero global steel industry[22]	Possibility of competitive supplies of green iron in new producer locations	EAF and ESF pathways, electrolysis, CCUS	No indication of costs of mining or ore qualities used; model focuses on energy costs	No, model does not vary energy or raw material consumption levels with ore composition	Not modelled	Wide range of current iron ore exporters plus key steelmaking markets
Ellersdorfer et al., Unlocking new export opportunities[23]	Potential of Australia to become a supplier of green iron ore, green iron, or green steel	EAF pathways: NG-DRI-EAF and H_2DRI-EAF	Single global cost value for iron ore; no mention of different qualities of ore from different producers	No, model does not vary energy or raw material consumption levels with ore composition	Included as a cost component in mining but recovery rates not modelled	Major iron ore producers: Australia, Brazil, Sweden, and key markets: Europe, China, and India
Devlin et al., Global green hydrogen-based steel opportunities[24]	Possibility of competitive supplies of green iron in new producer locations	H_2DRI-EAF pathway only	Single global cost value for iron ore; no mention of different qualities of ore from different producers	No, model does not vary energy or raw material consumption levels with ore composition	Not modelled	Wide range of current iron ore exporters plus key steelmaking markets
Cao et al., Prospects of regional supply chain relocation for iron & steel industry decarbonization[25]	Potential of Australia to become a competitive supplier of green iron to Japan	EAF pathways: EAF scrap recycling, NG-DRI-EAF and H_2DRI-EAF	No indication of costs of mining or ore qualities used	No, model documentation does not suggest energy or raw material consumption is varied with ore composition	Not modelled	Australia, Japan
MRIWA, Western Australia's Green Steel Opportunity[26]	Economics and emissions of value chains for decarbonised steelmaking value chains with processing steps split between Western Australia and key importers	Exports of green iron ore, pellets, and HBI. Green steelmaking via the EAF pathway. ESF pathway not considered	Single representative quality and cost Pilbara hematite and Mid West magnetite ore	Selection of energy or raw material inputs varying with ore quality, e.g., flux but not power consumption or slag production in the EAF	Yes, to a single level of 63% for the hematite and 68% for the magnetite ore value chains	Western Australia plus typical export markets
RMI, Green iron corridors[6]	Possibility of competitive supplies of green iron in new producer locations	Both EAF and ESF pathways: H_2DRI-EAF H_2DRI-ESF-BOF H_2DRI-ESF-EAF	Single CapEx and OpEx values for mining globally, no consideration of composition beyond Fe grade	Selection of energy or raw material inputs varying with ore quality, e.g., hydrogen but not power and heat consumption in DRI making	Yes, weight recovery is modelled but unclear whether more than a selection of product grades is used in modelling	Wide range of current iron ore exporters plus key steelmaking markets, but ignores China, India in quantitative assessment
WWF & Deloitte, Forging Futures[27]	Potential of Australia and other countries to become a competitive supplier of	EAF pathways: EAF scrap recycling,	Ore mining costs as a single value per country, no mention of quality	Not considered or not defined	Mentioned as a model component but no weight recovery relation defined	Wide range, Pilbara, other Australia, USA, Canada, MENA, but not in key

	green iron to the APAC region	NG-DRI-EAF and H_2DRI-EAF	considerations beyond differentiation between hematite and magnetite			consumer countries (China, Japan, Korea, etc)
Bataille et al., Net-zero steel project[28]	Transition of steelmaking facilities to decarbonised steelmaking technologies, and future location of green iron production	EAF pathways: EAF scrap recycling, NG-DRI-EAF and H_2DRI-EAF	Single global cost value for iron ore; no mention of different qualities of ore from different producers	No, single values for energy and material inputs for any ore quality	Yes, report mentions any ore via the DRI-EAF pathway needs to be 67% Fe but does not specify weight recovery modelling	Wide range, global facility level detail covering iron ore exporting and steel producing countries
Mission Possible Partnership Steel Sector Transition Strategy Model[29]	Transition of steelmaking facilities to decarbonised steelmaking technologies, and future location of green iron production	EAF and ESF pathways, electrowinning, smelting reduction, CCUS	Single global cost value for iron ore; no mention of different qualities of ore from different producers	No, model does not vary energy or raw material consumption levels with ore composition	No, or not defined in model documentation	Wide range of 12 global regions, covering current iron ore exporters plus key steelmaking markets, though no exports of iron
Mandala, Growing Australia's iron advantage[30]	Potential of Australia and other countries to become a competitive supplier of green iron to the APAC region	EAF pathways: EAF scrap recycling, NG-DRI-EAF and H_2DRI-EAF	No indication of costs of mining or ore qualities used	No, model documentation does not suggest energy or raw material consumption is varied with ore composition	No, or not defined in model documentation	Wide range of current iron ore exporters plus key steelmaking markets

3. METHODOLOGY

3.1 OVERVIEW

The model developed under this project combines process modelling with an optimisation model to determine cost-optimal routes to supply a given demand for steel.

The model focuses on the Australia-China trade relationship in iron ore or future exports of green iron. China is the sole location with any demand for steel in the current iteration of the model, with demand levels exogenously determined, separately for steel and green steel. Production of iron ore can occur in any location worldwide, whilst production of iron and steel can occur in China, Australia, as well as a select number of possible competitor regions.

The core of the optimisation model is a node-and-link network that represents global production facilities (mines, beneficiation plants, iron and steelmaking steps) and the transport links between them. The optimisation problem minimizes costs for mining, transportation, OpEx and CapEx, as well as all energy and material inputs into iron and steel making processing.

The process models for all relevant iron and steel making process steps explain how energy and material inputs, as well as losses of iron in beneficiation or to slag, are dependent on ore type and composition, and are described in detail below in section 3.6.

The optimisation model tracks the transport of resources over the links in the network, starting with ore supplied by several hundred different mines, with this ore either flowing into beneficiation nodes, or straight into iron making processes, and then into steel making process nodes. The optimisation model, its objective and the constraints are described in more detail in section 3.7. In order to limit the number of resources tracked, we choose to limit the beneficiation step to a distinct number of beneficiation levels, i.e., final Fe grades. This is further explained in section 3.8. Cost assumptions are explained in section 3.9 and our data sources used are listed in section 3.10.

We first explain the scope of the model in terms of iron and steelmaking processes considered in section 3.2, the regions considered in section 3.3., the iron ore qualities and beneficiation levels considered in section 3.4, and the resources tracked throughout the model network in section 3.5.

3.2 IRON AND STEELMAKING PROCESSES CONSIDERED

The model contains a node-and-link flowchart that represents global production and consumption regions in Chinese steel supply chain and the transport links between them. A flowchart of a generic production centre, which is replicated in each production region in our model, is provided in Figure 1.

The key process routes considered in our model are listed in Table 2.

Any of these routes can use either direct shipping ore, or beneficiated material. Ore, HBI, pig iron granules, scrap, and steel can be imported and exported. Beneficiation is an optional step in any of the routes, and can only occur at the mine site, i.e., prior to any export.

We consider two types of ports with different handling equipment, being dry bulk ports (with handling equipment for granular material, with ore, HBI and pig iron shipped via such ports in this model), and neo-bulk ports (for goods that can't be containerized and are handled as individual units, with steel and scrap shipped via such ports in this model), with substantially different associated costs.

TABLE 2. IRON AND STEELMAKING PROCESSES CONSIDERED IN OUR MODEL

Route #	Process in country of ore origin or iron producing country	Process in China	Exported product
1	Mining, beneficiation	Blast furnace – BOF	Iron ore
2	Mining, beneficiation	Grey or blue DRI – EAF	Iron ore
3	Mining, beneficiation, green DRI – EAF	None	Steel
4	Mining, beneficiation, green DRI – ESF – BOF	None	Steel
5	Mining, beneficiation, green DRI – HBI	ESF – BOF	HBI
6	Mining, beneficiation, green DRI – HBI	EAF	HBI
7	Mining, beneficiation, green DRI – ESF	ESF – BOF	Pig iron
8	Mining, beneficiation, green DRI – ESF	EAF	Pig iron

3.3 REGIONS CONSIDERED

The generic production centre, presented in the flowchart in Figure 1. is replicated in a number of global regions. This includes Australia, China (separated into 3 regions), and two key Latin American and MENA production locations.

In the current iteration of the model, the only demand for steel occurs in China. We only allow conventional fossil steel production processes to occur in China, i.e., we do not consider the possibility of conventional iron or steel to be exported to China, as this is not something that happens today, and we are not investigating possible cost benefits of international trade in conventional iron or steel. All regions included are capable of producing and exporting green iron or steel. Details are summarised in Table 3.

TABLE 3. PRODUCTION AND DEMAND REGIONS CONSIDERED IN THE MODEL

Region	Conventional production processes included for this region	Green production processes included for this region	Demand included for this region	Using cost data as reported for CRU location
Australia	No	Yes	No	Port Kembla, NSW
Chile	No	Yes	No	Talcahuano
China North	Yes	Yes	Yes	Tangshan, Hebei
China South	Yes	Yes	Yes	Zhangjiagang, Jiangsu
China West	Yes	Yes	Yes	Jiuquan, Gansu
Brazil	No	Yes	No	Tubarao
Egypt	No	Yes	No	Alexandria
UAE	No	Yes	No	Musaffah

3.4 IRON ORE QUALITIES AND BENEFICIATION LEVELS CONSIDERED

The process models in this project consider the effect of a number of different qualities of the iron ore, specifically:

- Whether it is a hematite, goethite, or magnetite ore
- Its shape, either lump or fines, with lumps excluded from use in direct reduction in fluidised bed processes
- The Fe grade
- The silica content
- The alumina content
- The LOI (loss on ignition)

Where and how these qualities are considered in our process modelling is explained in each of the relevant subsection of section 3.6.

Other elements, including phosphorous (P) and sulphur (S), are ignored in current process models. Modelling P and S in steelmaking presents significant challenges due to their complex thermochemical behaviour and strong sensitivity to process conditions. Both elements undergo reactions that are highly dependent on temperature, slag composition, oxygen potential, and the presence of other alloying elements. Their distribution between metal, slag, and gas phases require detailed phase equilibrium and kinetic data that are often scarce or highly system-specific. Furthermore, their removal is influenced by non-equilibrium conditions that are difficult to capture in static or simplified models. These complexities make it challenging to model P and S in process simulations with high accuracy. The P and S content mostly affects steel quality and therefore its potential applications. In the current model, we do not

differentiate between demand for such different uses of steel, e.g., for automative or construction purposes, but rather consider a level of demand for all types of crude steel. Free moisture content too, is ignored, i.e., we consider all production as dry weight in megatonne (Mt), in the current model iteration. We may include P, S, and water content considerations in future iterations of the model.

For all ore, the input data on ore quality is taken from the CRU iron ore costing model. We include all 352 mines (or mine clusters) as reported by on by CRU. The mine clusters in the CRU data are summary data for mines within specific regions such as individual Chinese provinces, where CRU reports on total production volume, with average composition and average production costs, rather than for individual mines. The CRU dataset is stated to cover virtually all global production of iron ore. For the year 2024, it reports a total 2,349 Mt of iron ore production globally, versus circa 2,500 Mt reported by the US Geological Survey[31].

For each mine or mine cluster we define a node in the model that can supply the ore as mined after crushing and screening. This ore can be upgraded in beneficiation nodes or used directly in iron making processes in the blast furnace or in DRI making processes, either in the country of origin or in one of the regions listed in Table 3.

The model can choose to upgrade any ore (more in section 3.6.2) to a number of different levels, being:

- Every two per cent from 52% to 60%, i.e.,52%, 54%, 56%, 58%, 60% Fe
- Every per cent from 61 to 69%, i.e., 61%, 62%, 63%, 64%, 65%, 66%, 67%, 68%, 69% Fe.

There are technical limits to the maximum level of beneficiation possible for different ores, further discussed in the beneficiation process model section 3.6.1.

3.5 RESOURCES TRACKED

The model tracks the supply and transport of each of the as-mined and beneficiated ores to their iron making step, where it considers the composition of the ore to determine the energy inputs etc as described in our process models. The composition of the resulting iron is similarly considered in the steelmaking step.

The model tracks the transport of iron ore, iron (DRI, HBI, pig iron), scrap, and steel. Other resources required in processing, e.g., electricity, hydrogen, coke, flux, etc, are not tracked over the model's transport network. Rather they are supplied at each processing node as required. That is to say, we replicate real-world transport of iron ore and intermediate products from the location of production to the location of final demand. For energy and other materials required in processing, we consider these to be available in unlimited quantities from local suppliers.

FIGURE 1. PROCESS MODEL FLOWCHART

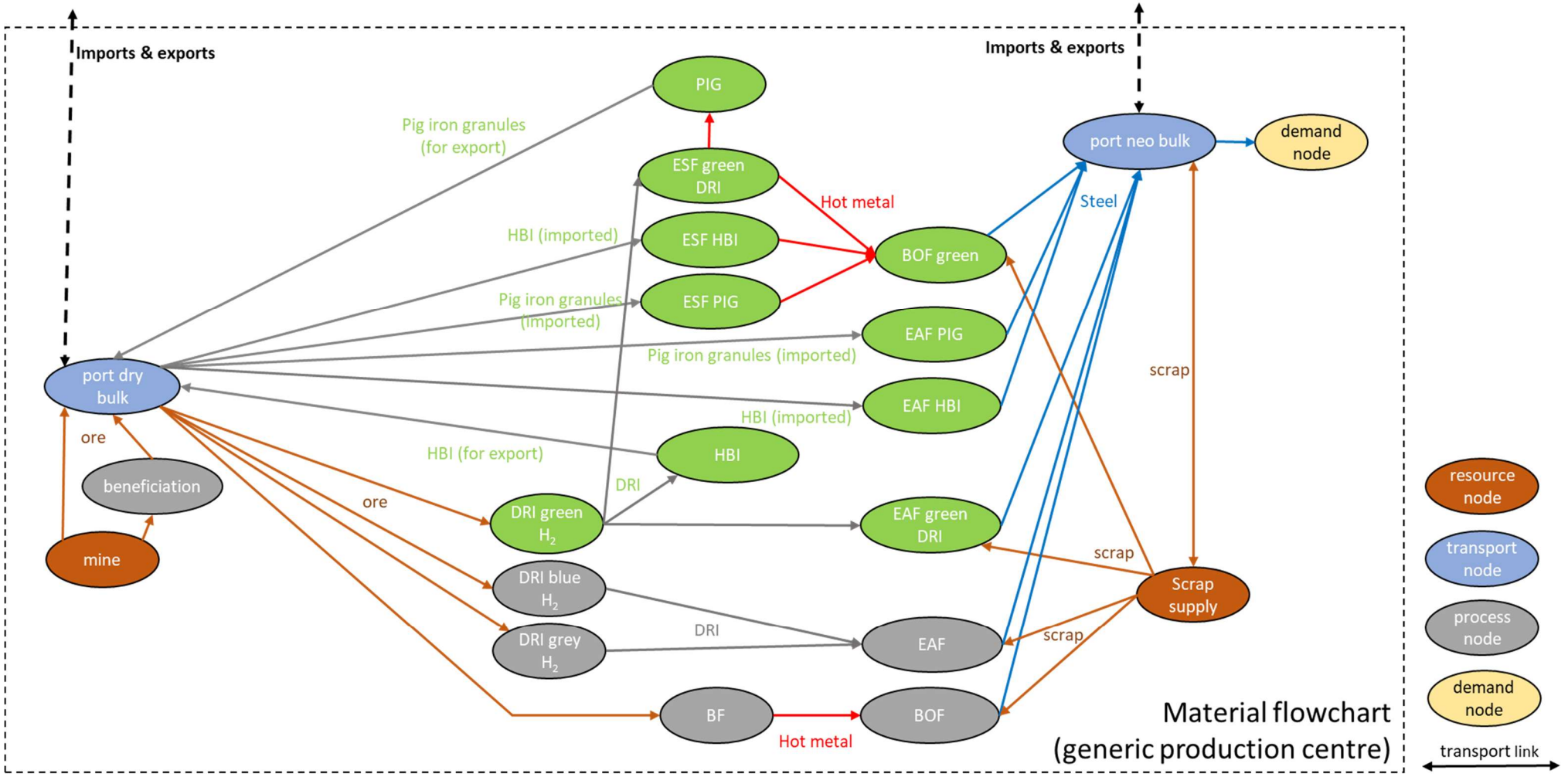

3.6 PROCESS MODELLING

3.6.1 Mining

For the mining process, we utilize the data from the CRU iron ore costing model directly. For each mine and year, we consider:

- Mine production capacity
- Production costs, here including mining, crushing and screening, site administration, finance, marketing, government royalties, and transportation to port, all as reported by CRU.
- Diesel and power consumption per ton of ore mined, including for crushing and screening
- Local diesel and power costs

The costs of port handling, and of transport to market are calculated separately by the model as resources are transported over the network.

We do not include CRU's value adjustment for different qualities of ore. This value adjustment is a price premium or penalty that reflects the additional cost in downstream processing, e.g., because of additional energy or flux requirement, due to the ore's composition (i.e., their iron, silica, and alumina content etc.). Given that we calculate the consumption levels of these inputs as dependent on ore composition with our detailed modelling of downstream processing, including this value adjustment would lead to double counting.

We do not include a capital charge in mining costs as it would not reflect the marginal production cost that steelmaking plants would see in real world markets.

3.6.2 Beneficiation (concentration)

Beneficiation yields are a critical variable in the end-to-end process. Table 4 lists all the inputs and outputs of the beneficiation model, along with the equations used to calculate each component.

TABLE 4. INPUTS AND OUTPUTS OF THE BENEFICIATION MODEL, ALONG WITH THE EQUATIONS USED TO CALCULATE EACH COMPONENT.

Input	
$\dot{m}_{\mathrm{O_{in}}}$	Amount of Fe_2O_3 in the ore (t/h)
$\dot{m}_{\mathrm{S_{in}}}$	Amount of SiO_2 in the ore (t/h)
$\dot{m}_{\mathrm{A_{in}}}$	Amount of Al_2O_3 in the ore (t/h)
$\dot{m}_{\mathrm{LOI_{in}}}$	Amount of LOI in the ore (t/h)
$\dot{m}_{\mathrm{in}}$	Amount of ore before beneficiation (t/h)
E_{ben}	Amount of electricity required (kWh/t)
Output	
W	Weight recovery (%)
Fe	Fe grade post beneficiation (%)
$\dot{m}_{\mathrm{out}}$	Amount of ore post beneficiation (t/h)
$\dot{m}_{\mathrm{O}}$	Amount of Fe_2O_3 post beneficiation (t/h)
$\dot{m}_{\mathrm{S}}$	Amount of SiO_2 post beneficiation (t/h)
$\dot{m}_{\mathrm{A}}$	Amount of Al_2O_3 post beneficiation (t/h)
$\dot{m}_{\mathrm{LOI}}$	Amount of LOI post beneficiation (t/h)

Equations
W from CRU data
Fe post beneficiation is predefined
$\dot{m}_{\mathrm{out}} = \dot{m}_{\mathrm{in}} \frac{W}{100}$
$\dot{m}_{\mathrm{O}} = \left(\frac{Fe}{100}\right) \dot{m}_{\mathrm{out}} \frac{\mathrm{M(Fe_2O_3)}}{\mathrm{2M(Fe)}}$
$\dot{m}_{\mathrm{S}} = \frac{\dot{m}_{\mathrm{S_{in}}}}{\dot{m}_{\mathrm{S_{in}}} + \dot{m}_{\mathrm{A_{in}}} + \dot{m}_{\mathrm{LOI_{in}}}} (\dot{m}_{\mathrm{out}} - \dot{m}_{\mathrm{O}})$
$\dot{m}_{\mathrm{A}} = \frac{\dot{m}_{\mathrm{A_{in}}}}{\dot{m}_{\mathrm{S_{in}}} + \dot{m}_{\mathrm{A_{in}}} + \dot{m}_{\mathrm{LOI_{in}}}} (\dot{m}_{\mathrm{out}} - \dot{m}_{\mathrm{O}})$
$\dot{m}_{\mathrm{LOI}} = \frac{\dot{m}_{\mathrm{LOI_{in}}}}{\dot{m}_{\mathrm{S_{in}}} + \dot{m}_{\mathrm{A_{in}}} + \dot{m}_{\mathrm{LOI_{in}}}} (\dot{m}_{\mathrm{out}} - \dot{m}_{\mathrm{O}})$
E_{ben} from CRU data

Data on energy consumption in the beneficiation process (electricity and diesel), as well as OpEx and CapEx data are taken from the CRU data, which reports these numbers for each individual mine (or mine cluster). This data is calibrated to volumes of ore input into the concentrator, i.e., scales linearly with the weight of natural ore processed, not with the weight of product produced. CRU does not provide any information on which of a range of possible technical processes are used in the beneficiation plants that they provide data on, but we presume that distinct processes will be used for hematite and magnetite ores, and we calibrate energy consumption and weight recovery separately for those ore types.

We use the energy consumption data as reported by CRU for each individual mine. For mines where CRU does not report any beneficiation, we use country-level average energy consumption for the same ore type (either hematite or magnetite). For OpEx and CapEx we use country-level averages for all mines as the cost data for the beneficiation nodes within each region.

For weight recovery, or yield, from the concentration process, we know that initial and final ore Fe grades are a good predictor. We also know that this yield is highly dependent on the type of ore (hematite or magnetite) and on the way the iron and gangue components are mixed, which largely depends on the local geology of the ore deposit.

In order to determine beneficiation yields for each of the mines in our dataset, and for a wide range of beneficiation levels, we presume that for comparable ores, e.g. different hematite deposits in the Pilbara, iron weight recovery will be the same for similar levels of beneficiation. Different ores, however, have different starting grades (Fe grade in situ) and also different theoretical maximum Fe grades. The different maximum ore grade is because most if not all hematite ores are actually a mix of hematite and goethite. Pure hematite ores would have a theoretical maximum grade of 69.9% Fe, pure goethite ores 62.9%. We calculate maximum ore grade for each individual ore by assuming the reported LOI is entirely bound water, i.e., that this LOI is due entirely to the level of goethite in the ore, and calculate the mix of hematite and goethite in each ore on the basis of this LOI.

We then define an index, the fraction of gangue removed (FGR), which represents the fraction of the gangue elements originally present in the natural ore that have been removed. We define this FGR as 0 for natural ores; no beneficiation has occurred, and none of the gangue has been removed. We define this FGR as 1 for ores which have been beneficiated to a degree where no gangue remains at all, i.e., at the theoretical maximum ore grade, where the product is pure iron oxide, whether in the form of hematite, goethite, or magnetite. We then presume that different ores will have the same yield (iron weight recovery) at the same point along this scale, e.g., that three ores with a:

- natural ore grade of 54% Fe (0 FGR), theoretical maximum Fe grade of 64% (1 FGR), at 59% Fe post-beneficiation;
- natural ore grade of 58% Fe (0 FGR) and a theoretical maximum Fe grade of 68% (1 FGR), at 63% Fe post-beneficiation;
- natural ore grade of 54% Fe (0 FGR) and a theoretical maximum Fe grade of 68% (1 FGR), at 61% Fe post-beneficiation;

will all have the same Fe weight recovery, as they are all exactly hallway between their natural ore grade and their theoretical maximum Fe grade, i.e., they are at 0.5 FGR, with half of the gangue originally present in the ore as-mined having been removed.

CRU reports the weight recovery for a single level of beneficiation for mines where beneficiation occurs. We use this CRU data to fit a curve (with equation $y = (1-x)^a$) to identify theoretical yields. For those mines where CRU reports a level of beneficiation and corresponding yield, we use this formula to derive the parameter *a* for each of these individual mines. This is equivalent to fitting a curve (as in Figure 2) that passes exactly through the data point for this mine. We use that parameter (or curve) to extrapolate weight recovery rates at different levels of beneficiation for ore from that specific mine. For mines where the CRU data does not report on benefits or weight recovery rates, we fit a curve through the collection of data points for mines with the same ore type and in the same country or country group (Figure 3), and use that curve to identify likely weight recovery rates at every possible level of beneficiation.

Whilst the method described above provides a metric for comparison of weight recovery rates across a range of ores with different natural Fe ore grades, the resulting plots as in Figure 3 are different from the weight recovery curves typically used in the iron ore industry. Such weight recovery curves would plot weight recovery versus the Fe grade of the final product out of the concentrator. To visualise how our method translates to such weight recovery curves, these are plotted for a number of selected mines producing hematite ores (Cloudbreak, Christmas Creek, Kings, and Roy Hill in the Pilbara, WA; Francis Creek in NT; Algeria in Brazil), in Figure 3.

FIGURE 2. CALIBRATION OF WEIGHT RECOVERY IN BENEFICATION, BY ORE TYPE AND COUNTRY GROUP

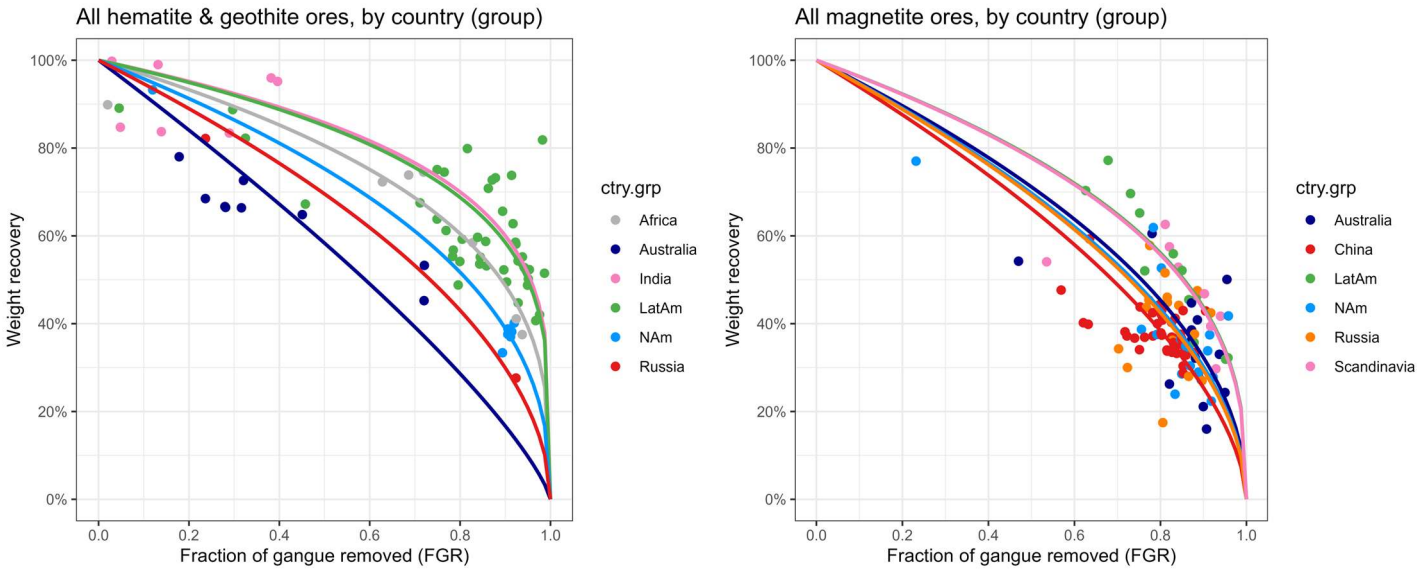

FIGURE 3. BENEFICIATION YIELD DERIVED IN OUR MODEL BACK-CALCULATED TO WEIGHT RECOVERY CURVES FOR SELECTED MINES

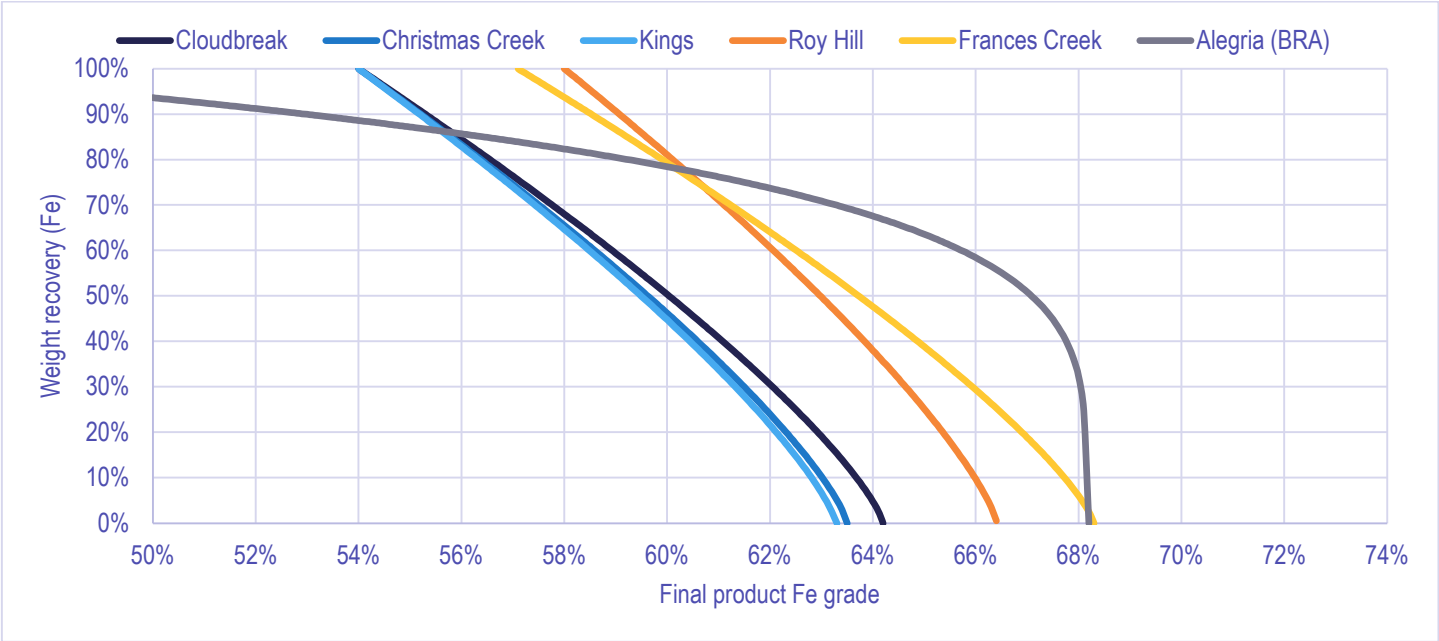

3.6.3 Agglomeration

There are two potential front-runners for H_2DRI, based on the type of ore, i.e., shaft furnace for lump ore and pellets and fluidised bed for fine ore. A key difference between the two pathways is the inclusion of an additional pelletisation step in the shaft furnace route, which is responsible for ~15% of total emissions from the steel industry and depends heavily on fossil fuel firing at very high temperatures. In the current model, we have only focused on the fluidised bed H_2DRI of iron ores and have not included the pelletisation or sintering step in this iteration. We ignore the cost and energy consumption associated with agglomeration for the blast furnace route in the current model iteration.

3.6.4 Hydrogen DRI making

The direct reduction of haematite to metallic iron using hydrogen (H_2DRI) is a multi-step process which depends on temperature. At temperatures below 570°C, the haematite is first reduced to magnetite, which is further reduced to metallic Fe, as shown in Eqs. (1)–(2). At higher temperatures an additional intermediate oxide becomes stable: wüstite ($Fe_{1-x}O$), where x represents the vacancies in the iron lattice. Consequently, the reaction proceeds in three steps as shown in Eqs. (3)–(5):

Two-step reaction:

$$3Fe_2O_3 + H_2 \rightleftharpoons 2Fe_2O_3 + H_2O \qquad \Delta\bar{h}^\circ = -1\ \text{kJ/mol} \qquad (1)$$

$$Fe_2O_3 + 4H_2 \rightleftharpoons 3Fe + 4H_2O \qquad \Delta\bar{h}^\circ = 50.4\ \text{kJ/mol} \qquad (2)$$

Three-step reaction:

$$3Fe_2O_3 + H_2 \rightleftharpoons 2Fe_2O_3 + H_2O \qquad \Delta\bar{h}^\circ = -1\ \text{kJ/mol} \qquad (3)$$

$$(1-x)Fe_3O_4 + (1-4x)H_2 \rightleftharpoons 3Fe_{1-x}O + (1-4x)H_2O \qquad \Delta\bar{h}^\circ = 24.9\ \text{kJ/mol} \qquad (4)$$

$$Fe_{1-x}O + H_2 \rightleftharpoons (1-x)Fe + H_2O \qquad \Delta\bar{h}^\circ = 25.4\ \text{kJ/mol} \qquad (5)$$

The stoichiometric amount of hydrogen required to completely reduce hematite to metallic iron is 0.054 tH_2/tFe ($Fe_2O_3 + 3H_2 \rightleftharpoons 2Fe + 3H_2O$). However, excess hydrogen is needed in the reactor to shift the equilibrium in favour of the final reduction step.

In HILT research projects RP1.004 *Impact of Hydrogen DRI on Melting in an Electric Furnace*, and RP2.005 *Hydrogen Ironmaking: fluidised bed H_2DRI with Australian focus*, we developed a process flow diagram of a three-stage fluidised bed H_2DRI process in HSC Sim software, which is used in this current project to model the DRI process. The basic process steps are described below.

Fine iron ore is preheated and sequentially reduced in a counter-current arrangement with hydrogen gas. The simulation integrates mineral processing, thermodynamic equilibrium calculations, and heat exchanger networks to optimise energy use. The heat exchangers network was implemented to capture the sensible heat from the high-temperature off-gas (unreacted hydrogen and steam) and preheat the iron ore and hydrogen feed stream into a three-stage fluidised bed reactor. An important consideration is that the off-gas from the last reactor and preheated hydrogen gas are heated in two heaters to ensure the adiabatic operation of the fluidised bed reactors. The final 100% metallised DRI is directed to the downstream steelmaking processes.

Table 5 lists all the inputs and outputs of the reduction model, along with the equations used to calculate each component.

TABLE 5. INPUTS AND OUTPUTS OF THE HYDROGEN DRI MODEL, ALONG WITH THE EQUATIONS USED TO CALCULATE EACH COMPONENT.

Input	
Fe	Fe grade post beneficiation (%)
$\dot{m}_{\text{out}}$	Amount of ore post beneficiation (t/h)
$\dot{m}_{\text{O}}$	Amount of Fe_2O_3 post beneficiation (t/h)
$\dot{m}_{\text{S}}$	Amount of SiO_2 post beneficiation (t/h)
$\dot{m}_{\text{A}}$	Amount of Al_2O_3 post beneficiation (t/h)
$\dot{m}_{\text{H}_2}$	Amount of hydrogen consumed (t/h)
$\dot{Q}$	Amount of heat required (MW)
Output	
$\dot{m}_{\text{Fe}_{\text{DRI}}}$	Amount of iron in the DRI (t/h)
$\dot{m}_{\text{S}}$	Amount of SiO_2 in the DRI (t/h)
$\dot{m}_{\text{A}}$	Amount of Al_2O_3 in the DRI (t/h)
$\dot{m}_{\text{DRI}}$	Amount of DRI (t/h)

Equations
$\dot{m}_{\text{Fe}_{\text{DRI}}} = \dot{m}_{\text{O}} \frac{2\text{M(Fe)}}{\text{M}(Fe_2O_3)}$
No change in the SiO_2 content
No change in the Al_2O_3 content
$\dot{m}_{\text{DRI}} = \dot{m}_{\text{Fe}_{\text{DRI}}} + \dot{m}_{\text{S}} + \dot{m}_{\text{A}}$
$\dot{m}_{\text{H}_2} = 3\dot{m}_{\text{O}} \frac{\text{M}(H_2)}{\text{M}(Fe_2O_3)}$
$\dot{Q} = -0.33Fe + 96.3$

3.6.5 Natural gas DRI making

We us the same process model for natural gas DRI making as for green hydrogen DRI making. We effectively consider that the syngas produced from natural gas is fully converted into hydrogen before entering the DRI plant. The syngas produced in a steam methane reforming (SMR) plant is typically a mixture of hydrogen and carbon monoxide, however, the amount of natural gas required to reduce the iron oxide is the same whatever the ratio of hydrogen and carbon monoxide in the syngas out of the SMR is.

We use CRU's reported values for grey hydrogen cost as a proxy for the natural gas and SMR process costs, whilst we assume the same CapEx and Opex for the shaft furnace typically used in natural gas DRI plants as for the fluidised bed CapEx and Opex that will be used for the green hydrogen DRI making process described in section 3.6.4.

3.6.6 HBI making

The process of making hot briquetted iron has not yet been fully implemented in the current version of the model. Energy consumption and CapEx, OpEx, for this process step are included with (small) place holder values. The contributions of this process to overall costs are presumed to be very marginal, and therefore this simplification is not considered to influence final results much. Earlier work on the comparison of costs of HBI produced via different processes or in different locations has typically ignored the costs of this specific process step[32,33].

We include the process of HBI making as the product is more amenable to shipping. Turning DRI into HBI briquettes compacts it and reduces porosity, which helps reduce reactivity. For HBI that is compacted to a density of at least 5 t/m^3, limited safety requirements apply for maritime shipping of the product[34]. For HBI with a density below this limit, the same strict safety requirements as associated with shipping DRI apply, in particular the use of a blanket of inert gas in cargo holds to reduce fire risks[34,35]. Shipping of DRI with such precautions has been done for several decades, for volumes of several dozen Mtpa, into and within the US in particular[36–38]. This is therefore not a novel technology, though it does add to shipping costs. Meeting this density requirement is typically not achievable for iron made with ores with more than 3% acid gangue content, though this depends on other factors including the carbon content[39].

3.6.7 Electric Smelter Furnace

The smelter process is modelled using a Gibbs energy minimization in HSC Sim, with feeds of hot or cold DRI, carbon, CaO, and electricity for heating or melting the DRI and outputs of hot metal, slag, and off gas[40]. The phases and species considered in the output stream of this unit include the following: (1) liquid metal: Fe, Mn, Al, Si, P, S, C, Ti, V, and Ni; (2) slag: FeO, CaO, MgO, SiO_2, MnO, Al_2O_3, P_2O_5, TiO_2, V_2O_5, and NiO; and (3) off gas: CO_2, CO, H_2O, and N_2. The temperature of hot/cold DRI with 100% metallization degree is assumed to be 600°C/25°C, while CaO and carbon are injected at 25°C. The melting temperature is set at 1,400°C, and the liquid metal, slag, and off gas are assumed to leave at the same temperature without any heat recovery. There are no downstream casting, rolling, or secondary (ladle) processes considered in this research. The following assumptions are taken into account for modelling the smelter in HSC Sim:

- The carbon addition is adjusted to yield 3.5% C in the liquid steel[41]. The maximum carbon content in the liquid metal is ~4%, beyond which carbon is not dissolved in the hot metal. HSC Sim does not capture the dissolution of carbon and models it as a molten product. However, dissolving carbon requires less energy, compared with melting carbon. To accommodate this, carbon is represented as a solid phase in the liquid metal.
- The reduction of SiO_2 in smelters is much lower than in BFs. The main difference between the two processes lies in the reduction mechanism. In the BF, reduction predominantly occurs in the gas phase, whereas in the smelter process, reduction takes place through the interaction of carbon with slag. The operating temperature of the BF is higher than that of the smelter, which facilitates the efficient reduction of SiO_2 and higher silicon content in the hot metal[42]. To account for this, the activity content of silicon content in the hot metal is adjusted to 0.4% using a controller in HSC Sim. This is based on FactSage modelling results and insights gained from expert industrial partners through personal communication.
- The CaO level is adjusted to provide a slag basicity ($CaO:SiO_2$ mass ratio) of 1.1[41]. This level of slag basicity is selected to make suitable slag for the cement industry after granulation[43].
- Heat losses are assumed to be negligible in the smelter.

Table 6 lists all the inputs and outputs of the smelter model, along with the equations used to calculate each component.

TABLE 6. INPUTS AND OUTPUTS OF THE SMELTER MODEL, ALONG WITH THE EQUATIONS USED TO CALCULATE EACH COMPONENT.

Input	
$\dot{m}_{\mathrm{Fe_{DRI}}}$	Amount of iron in the DRI (t/h)
$\dot{m}_{\mathrm{S}}$	Amount of SiO_2 in the DRI (t/h)
$\dot{m}_{\mathrm{A}}$	Amount of Al_2O_3 in the DRI (t/h)
$\dot{m}_{\mathrm{DRI}}$	Amount of DRI (t/h)
$\dot{m}_{\mathrm{CaO_{smelter}}}$	Amount of CaO required (t/h)
$\dot{m}_{\mathrm{c}}$	Amount of carbon required (t/h)
$E_{\mathrm{HDRI_{smelter}}}$	Amount of electricity required in the case of hot DRI in the smelter (kWh/tHM)
$E_{\mathrm{CDRI_{smelter}}}$	Amount of electricity required in the case of cold DRI in the smelter (kWh/tHM)
b	Basicity
s	Si fraction in hot metal
c	Carbon fraction in hot metal
Output	
$\dot{m}_{\mathrm{s_{HM}}}$	Amount of Si in the hot metal (t/h)
$\dot{m}_{\mathrm{slag_{smelter}}}$	Amount of slag produced (t/h)
$\dot{m}_{\mathrm{HM}}$	Amount of hot metal produced (t/h)

Equations
$\dot{m}_{\mathrm{CaO}} = b\left(\dot{m}_{\mathrm{S}} - \dot{m}_{\mathrm{s_{melt}}}\frac{\mathrm{M(SiO_2)}}{\mathrm{M(Si)}}\right)$
$\dot{m}_{\mathrm{HM}} = \frac{\dot{m}_{\mathrm{Fe_{DRI}}}}{(1-s-c)}$
$\dot{m}_{\mathrm{c}} = \dot{m}_{\mathrm{HM}}\, c$
$\dot{m}_{\mathrm{s_{HM}}} = \dot{m}_{\mathrm{HM}}\, s$
$\dot{m}_{\mathrm{slag_{smelter}}} = (b+1)\left(\dot{m}_{\mathrm{S}} - \dot{m}_{\mathrm{s_{melt}}}\frac{\mathrm{M(SiO_2)}}{\mathrm{M(Si)}}\right) + \dot{m}_{\mathrm{A}}$
$E_{\mathrm{HDRI_{smelter}}} = -10.59Fe + 1010.25$
$E_{\mathrm{CDRI_{smelter}}} = -12.84Fe + 1254.93$

3.6.8 Blast furnace

The consumption of flux (burnt lime) and the production of slag in the blast furnace is calculated in the same way as for the electric smelter furnace.

Our process modelling found no clear relationship between iron ore grade and required fuel rates, nor was one found in the CRU data (Figure 4). For the consumption of coke and PCI[1] in the blast furnace, we presume that there are large differences in fuel rates between different plants, based on furnace size, age, and other factors. We also presume that the coke:PCI ratio is strongly driven by local operator considerations.

It is however well established that the use of lower grade ores will result in higher fuel rates. To represent this relationship, we use the CRU data on fuel rates to determine relative efficiency and coke:PCI ratios used in different locations. We then consider that the amount of material fed into the blast furnace and presume coke and PCI rates at each location, in the case of using different ore grades, would scale linearly with differing amounts of material fed into the blast furnace. Future iterations of the model will investigate this relationship in more detail.

Further, it is well established that the use of lower ore grades reduces the potential annual output of a blast furnace. This is likely a key economic driver for the use of beneficiated ores, as the opportunity costs of the resulting lost revenue associated with the use lower quality ores appear to greatly exceed the additional costs incurred by the higher use of energy and flux associated with the use lower quality ores (more in Appendix 1).

To represent this relationship, we use a fixed factor of 1.7 as the presumed ratio between the material feed rate (iron ore fed into the furnace) and production capacity (hot metal produced by the furnace), calibrated on the average quality (59.4% Fe) of material currently fed through blast furnace according to the CRU data. We presume that it is the material feed rate of the blast furnace that is fixed, i.e., that no matter the grade of ore the total mass of ore fed into the furnace is restricted at a fixed capacity, and therefore that the production capacity (of hot metal) of the furnace scales linearly with the iron content of the ore fed into it. This too is likely a

[1] Pulverized Coal Injection (PCI), a process used in blast furnaces to reduce coke consumption by injecting finely ground coal into the furnace. The coal used for this process is also referred to as PCI.

simplification of real-world operational characteristics of the blast furnace and will be investigated in more detail in future iterations of this model.

FIGURE 4. RELATION BETWEEN FE GRADE AND FUEL RATE AS PER CRU DATA

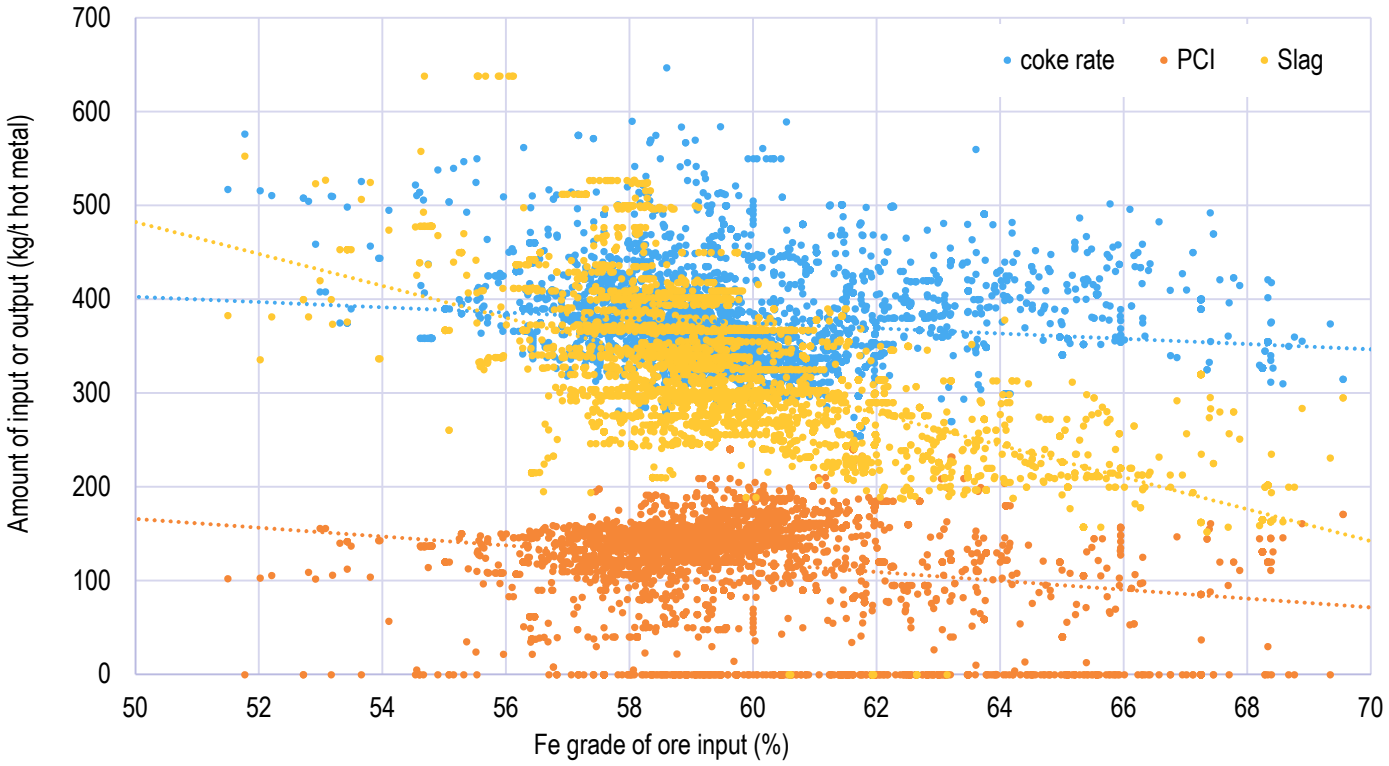

3.6.9 Pig iron granule making

The process of making pig iron granules from hot metal out of the ESF has not yet been fully implemented in the current version of the model. Energy consumption and CapEx, OpEx, for this process step are included with (small) place holder values. We presume the CapEx, OpEx and input costs associated with this process to be fairly marginal, see also our explanation with the modelling of HBI making in section 3.6.6.

Granulated pig iron is likely an attractive form of iron to ship internationally as the International maritime solid bulk cargoes (ISMBC) code considers it to pose no particular hazards and allows it to be shipped without particular precautions[35].

3.6.10 Basic Oxygen Furnace

The BOF process is modelled using a Gibbs energy minimization in the HSC Sim, with feeds of hot metal, MgO, CaO, oxygen, and scrap, and outputs of liquid metal, slag, and off gas[44]. Scrap is modelled as solid Fe in this research. The hot metal charged into the BOF is typically composed of ~96% Fe, ~3.5% C, ~0.4% Si, and the secondary remaining gangue components including P, S, Mn, Ti, and V. The phases and species considered in this unit are similar to those discussed in the smelter process. The temperature of hot metal is assumed to be 1,400°C, while MgO, CaO, oxygen, and scrap are injected at 25°C. The BOF temperature is set at 1,650°C[45], and the liquid metal, slag, and off gas are assumed to leave at the same temperature without any heat recovery. The following assumptions are taken into account for modelling BOF in HSC Sim:

- The CaO level is adjusted to provide a slag basicity of 3.5, which is consistent with a value reported by Primetals Technologies[41]. This value depends on the operating conditions, product requirement, scrap quality, and the phosphorus content of the hot metal[46].
- Carbon in the liquid steel has been taken as 0.08% of the weight of the liquid steel. The activity coefficient has been adjusted to achieve this amount in HSC Sim. In reality, the actual behaviour of carbon is a function of temperature and metal composition.
- The MgO level in the BOF slag varies between 5% and 20%[45,47]. In this research, the MgO level is controlled to maintain 7% MgO in slag, similar to that of EAF model.

- The FeO content of BOF slag ranges from 10% to 30% on the mass basis[45,47]. The oxygen level is regulated to achieve 20% FeO in the slag phase in the present model as a reasonable typical value.
- The amount of scrap added to the BOF process is regulated to ensure an adiabatic reactor condition. The scrap composition is taken as 100% Fe.
- The heat loss in the BOF process is assumed to be 5% of the total heat input[46].

Table 7 lists all the inputs and outputs of the BOF model, along with the equations used to calculate each component.

TABLE 7. INPUTS AND OUTPUTS OF THE BOF MODEL, ALONG WITH THE EQUATIONS USED TO CALCULATE EACH COMPONENT.

Input	
$\dot{m}_{\mathrm{HM}}$	Amount of hot metal produced (t/h)
$\dot{m}_{\mathrm{c}}$	Amount of carbon in hot metal (t/h)
$\dot{m}_{\mathrm{s_{HM}}}$	Amount of Si in the hot metal (t/h)
$\dot{m}_{\mathrm{CaO_{BOF}}}$	Amount of CaO required in BOF (t/h)
$\dot{m}_{\mathrm{MgO}}$	Amount of MgO required (t/h)
$\dot{m}_{\mathrm{scrap}}$	Amount of scrap required (t/h)
b	Basicity
f	FeO fraction in slag
m	MgO fraction in slag
c	Carbon fraction in liquid steel
sc	Scrap fraction
Output	
$\dot{m}_{\mathrm{slag_{BOF}}}$	Amount of slag produced (t/h)
$\dot{m}_{\mathrm{LS}}$	Amount of liquid steel produced (t/h)

Equations
$\dot{m}_{\mathrm{CaO}} = b\,\dot{m}_{\mathrm{s_{HM}}}\frac{\mathrm{M(SiO_2)}}{\mathrm{M(Si)}}$
$\dot{m}_{\mathrm{slag_{BOF}}} = \frac{\dot{m}_{\mathrm{CaO}} + \dot{m}_{\mathrm{s_{melt}}}\frac{\mathrm{M(SiO_2)}}{\mathrm{M(Si)}}}{(1-f-m)}$
$\dot{m}_{\mathrm{MgO}} = \dot{m}_{\mathrm{slag_{BOF}}}\,m$
$\dot{m}_{\mathrm{scrap}} = \dot{m}_{\mathrm{HM}}sc$
$\dot{m}_{\mathrm{LS}} = \dot{m}_{\mathrm{Fe_{DRI}}} + \dot{m}_{\mathrm{scrap}} - \dot{m}_{\mathrm{slag_{BOF}}}f$

3.6.11 Electric Arc Furnace

The EAF process is modelled using a Gibbs energy minimization in the HSC Sim, with feeds of hot DRI, flux (CaO, MgO), oxygen, air (by leakage), and methane[44]. The proposed model for the EAF process is not intended to capture the detailed thermodynamics of complex reactions in steelmaking such as dephosphorization. The phases and species considered in this unit are similar to those discussed in the smelter process. The temperature of hot DRI with 100% metallization degree is assumed to be 600°C, while CaO, MgO, CH_4, O_2, and air are injected at 25°C. The EAF temperature is taken to be 1,600°C[48], and the liquid metal, slag, and off gas are assumed to leave at a temperature of 1,600°C without any heat recovery. In the EAF process, controlling the slag basicity, MgO saturation, and FeO levels in the slag are important parameters to avoid unnecessary high Fe losses with the slag and to achieve the maximum metal yield. The chemical composition of EAF slag typically consists of FeO (10%–40%), SiO_2 (6%–34%), CaO (22%–60%), MgO (3%–13%), and Al_2O_3 (3%–14%)[49]. The following settings are applied in the end-to-end model:

- The CaO flux charge is adjusted to provide a slag basicity (CaO:SiO_2 mass ratio) of 2. This level of slag basicity is selected to facilitate impurity removal, ensure slag fluidity, promote oxidation reactions, and achieve desired steel quality.
- The MgO flux charge is adjusted to ensure that the resulting slag contains 7% MgO. MgO is added to the steelmaking process as a flux or slag conditioner to modify the properties of the slag and protect the refractories[50].
- The rate of oxygen addition is regulated to achieve a specific mass fraction of 20% FeO in the slag phase. The optimum level of FeO in the slag is found to be 20%–25%, beyond which there is a subsequent increase in the electricity consumption in the EAF process and reduction in the slag viscosity[51]. This value was chosen as a reasonable typical value.
- CH_4 is introduced at the rate of 4 kg/tLS based on the mass and energy balance model developed by Pfeifer and Kirschen[52]. The CH_4 injection into an EAF process (1) increases arc voltage at constant arc length and current and (2) accelerates nitrogen removal[53].
- Air infiltration in the form of extra nitrogen is assumed at the level of 100 kg/tLS[52] as the EAF is open and not sealed. Air infiltration into EAF results in (1) decreased energy efficiency, (2) increased oxidation of molten metal, and (3) reduced temperature control. We have assumed that air does not participate in the reaction; however, it imposes a heating penalty on the reactor.
- The EAF process is subjected to heat loss mainly from the roof, sidewalls, and other miscellaneous ways. Heat loss at the rate of 49 kWh/tLS is assumed in this research[54].

We ignore the effect of different input DRI resulting in different slag composition and corresponding value, and instead use a single average value for the price of slag. Table 8 lists all the inputs and outputs of the EAF model, along with the equations used to calculate each component.

TABLE 8. INPUTS AND OUTPUTS OF THE EAF MODEL, ALONG WITH THE EQUATIONS USED TO CALCULATE EACH COMPONENT.

Input	
$\dot{m}_{\mathrm{Fe_{DRI}}}$	Amount of iron in the DRI (t/h)
$\dot{m}_{\mathrm{S}}$	Amount of SiO_2 in the DRI (t/h)
$\dot{m}_{\mathrm{A}}$	Amount of Al_2O_3 in the DRI (t/h)
$\dot{m}_{\mathrm{DRI}}$	Amount of DRI (t/h)
$\dot{m}_{\mathrm{CaO}}$	Amount of CaO required (t/h)
$\dot{m}_{\mathrm{MgO}}$	Amount of MgO required (t/h)
E_{EAF}	Amount of electricity required (kWh/t)
b	basicity
f	FeO fraction in slag
m	MgO fraction in slag
Output	
$\dot{m}_{\mathrm{slag}}$	Amount of slag produced (t/h)
$\dot{m}_{\mathrm{LS}}$	Amount of liquid steel produced (t/h)

Equations
$\dot{m}_{\mathrm{CaO}} = b\,\dot{m}_{\mathrm{S}}$
$\dot{m}_{\mathrm{slag}} = \frac{\dot{m}_{\mathrm{A}}+(b+1)\dot{m}_{\mathrm{S}}}{(1-f-m)}$
$\dot{m}_{\mathrm{MgO}} = \dot{m}_{\mathrm{slag}}\,m$
$\dot{m}_{\mathrm{LS}} = \dot{m}_{\mathrm{Fe_{DRI}}} - \dot{m}_{\mathrm{slag}} f \frac{\mathrm{M(Fe)}}{\mathrm{M(FeO)}}$
$E_{\mathrm{EAF}} = -16.59Fe + 1504.96$

3.7 OPTIMISATION MODEL

The model optimises (minimizes) total system cost, which consists of the sum of all:

- cost of mining
- cost of transport
- cost of all consumables, i.e., energy, flux, slag, scrap, etc, used in all processing steps
- cost of all OpEx for all processes, exclusive of consumables
- cost of all CapEx for all processes

This is subject to the following constraints:

- Mass balance constraint: flows of any resource out of a node cannot exceed the flow of that resource into the node plus the supply of the resource by the node itself.
- Supply constraint: a node cannot supply more of any resource than its production capacity. For example, iron ore in mining nodes, or steel from EAF or BOF nodes. Supply cannot be negative.
- Process feed rate constraint: for the blast furnace and electric smelter furnace nodes, production capacity is not limited in output, but in feed rates. This effectively represents the notion that these furnaces' output is a function of ore quality, with lower grade ores resulting in reduced output of hot metal. This constraint is implemented by limiting the amount of iron ore (blast furnace) or the sum of DRI, HBI, and pig iron (electric smelter furnace).
- Process requirement constraint: no processing node can supply a resource unless the resources required to produce it are consumed in this node. For example, a blast furnace node may not supply any hot metal unless it receives or supplies sufficient iron ore, coke, PCI, and flux, and produces the required amount of slag. These 'recipes' are pre-calculated for every different quality of iron ore fed into the blast furnace, or iron into the smelter furnace, etc.
- Transport capacity constraint: total flows of resources across any link cannot exceed its transport capacity. Flows cannot be negative.
- Port capacity constraint: total handling of resources through any port node cannot exceed its handling capacity.
- Demand constraint: all demand must be met, separately for total steel demand for green steel demand.

3.8 REPRESENTATION OF PROCESS MODELS IN THE OPTIMISATION MODEL

The core of the optimisation model is a node-and-link network that represents global production facilities (mines, beneficiation plants, iron and steelmaking steps) and the transport links between them. This is an implementation of a source-and-sink multi-commodity network flow problem, one of the archetypical problems analysed in linear programming[55].

These problems can feasibly be used to track a limited or at least finite number of resources over the network. The process models as described above define required energy or other raw material inputs, slag outputs and iron losses to slag as functions of ore composition, and are capable of representing an unlimited combination of inputs and corresponding outputs.

To address this issue, and keep the problem workable, these process model functions are not themselves represented in the optimisation model. Rather, we pre-calculate a discrete set of possible inputs and corresponding outputs. We do so by starting with the complete set of ore qualities included in the CRU iron ore cost model[9], which covers 340 mines, many of which produce a combination of lump, fines, and pellet feed, each with a specific ore composition. The fines and pellet feed fractions of these ores can be upgraded in the beneficiation nodes, to a finite number of final ore grades, roughly every integer value within the range of usually traded Fe grades (see section 3.4). This set of natural grade and beneficiated ores can then be processed in iron making and steel making nodes, with each step producing a new, large but finite, set of new resources.

The calculation of the energy and other inputs, as well slag production, iron losses to slag, and final product output are all pre-calculated (in R) and used to build spreadsheet with 'recipes' of required inputs and outputs for each individual resource processed in a specific process node. In the optimisation model itself, constraints are imposed that state that the processing node cannot supply any resource (e.g., iron or steel) unless the prerequisite set of energy and raw material inputs is consumed, corresponding volumes of slag are produced, etc. The constraint is defined such that the sum of energy and raw materials consumed in a processing node must equal the sum-product of all resources flowing out of the node multiplied with their corresponding required inputs. For example, any steel making node can produce any mix of different qualities of steel as long as the sum of all inputs required for the sum of all qualities of steel flowing out of that node are supplied to it or by it.

3.9 COST ASSUMPTIONS

All CapEx, OpEx, and raw material cost numbers are taken from the CRU iron ore and steel costing models[8,9], with some adjustments.

For the CapEx, we use overnight construction cost as reported by CRU but multiply these with a factor of 3 for high wage countries, and a factor of 2 for all other countries, on advice of industry partners that these appear to be strong underestimates. Of the regions considered in our model, only Australia is considered a high wage country (see Table 3). We calculate a capital charge per ton of steel produced by using the WACC as reported by CRU for each producer region and presuming a 40 year plant lifetime and a 10 year payback period. The multiplication of the CRU reported overnight construction cost would seem a very substantial adjustment but these equate to only about $17 of total capital charges, or 6.9% of a total production cost of $245 per ton of liquid steel in the BF-BOF pathway (cheapest possible ton of liquid steel) or $38 of total capital charges, or 6.1% of a total production cost of $621 per ton of liquid steel in the H_2DRI-ESF-BOF pathway, after applying this correction. We have run the model without this correction, and overall results, in terms of the location where iron and steel occurs most cost-competitively, are not affected by this correction.

There are two exceptions to this approach for calibrating CapEx costs. First, blast furnace and electric smelting furnace CapEx are not calibrated on production capacity (ton of hot metal produced) but on feed rate (ton of ore or iron fed into the furnaces); see also note on economic drivers for beneficiation in Appendix 1.

Second, the CRU data is very scarce on cost data for ESF plants. It contains cost data for:

- A 1 Mtpa submerged arc furnace (SAF) in Duisburg, Germany
- A 2 Mtpa submerged arc furnace in Dunkerque, France
- A 0.7 Mtpa submerged arc furnace in Glenbrook, New Zealand
- A 0.7 Mtpa scrap melting process (SMP) plant in Hirohata, Japan

These have substantially different associated CapEx. We select the data for the largest SAF plant, in Dunkerque, and set all ESF costs globally to this level. The exception is for the ESF plants utilising imported pig iron: re-melting of this material requires a much simpler plant, and we use the much lower CapEx costs of the Hirohata SMP plant as the best cost proxy for this process, again undifferentiated globally. While energy costs remain a much bigger driver of relative competitiveness in any H_2DRI-ESF pathway, this deserves further investigation in a future iteration of the model.

For the OpEx, we again use the CRU iron ore and steel costing models[8,9] as the basis. We subtract all energy and raw material costs that are separately modelled in our process models from total reported OpEx.

The levels of consumption of energy and raw material inputs, as well as slag production, are determined by our process models. These levels of consumption are multiplied with CRU reported energy and raw material cost. Cost for key inputs such as the hydrogen price are varied in different scenarios.

For scrap costs, we cannot readily use CRU data, which reports scrap prices paid by steel producers, not production costs. This matters as this price is a function of steel demand, with scrap prices typically tracking steel prices, representing a discount versus the costs of inputs paid for primary steelmaking. Rather than endogenizing the modelling of scrap costs we choose to use the lowest spot price in Chinese scrap markets over the period 2006-2025[56] as a proxy, presuming that these represent a cost at which Chinese scrap suppliers are still willing to supply to the steelmaking industry.

3.10 DATA SOURCES

An overview of our data sources is provided in Table 9. CRU models steel cost data through to 2035, and iron ore cost data through to 2040. In order to extrapolate through to 2050 we have used linear trends in CapEx and OpEx cost, in in real 2025 dollar values, for the last five years of data in either data set. For iron ore mine production capacity we simply copy the 2040 data for the year 2050. The 2050 results presented here should therefore be interpreted as based on 2040 data, with 2050 levels of demand and scrap supply.

TABLE 9. LIST OF KEY MODEL DATA SOURCES

Data point	Data source	Notes
Steel demand	Steel Sector Transition Strategy Model (ST-STSM)[57]	Historical data and forecast of steel demand through to 2050. We presume Chinese production levels are equal to domestic demand plus 6% exports, an average level seen over 2020-2024. Green steel demand is set as simple scenarios, with the baseline scenario seeing increasing shares of total demand as green steel, working to 100% by 2060. Two alternative scenarios, with 100% green steel and 0% green steel are also included.
Scrap supply levels	Steel Sector Transition Strategy Model (ST-STSM)[57]	Historical data and forecast of steel demand through to 2050.
Production capacity	CRU iron ore costing model[9] GEM steel plant tracker[58] GEM blast furnace tracker[59]	Production capacity for individual mines and years as reported by CRU. Historical production capacity of blast furnaces and EAF as reported by Global Energy Monitor (GEM). We do not forecast changes to future Chinese BF or EAF production capacity, i.e., these can be varied with simple scenario settings; baseline scenario settings assume no future changes to these capacities. The production capacity of green production routes is not limited.
Process CapEx	CRU steel costing model[8] CRU iron ore costing model[9]	CapEx levels are determined as overnight construction costs and WACC as provided by CRU, calculated as a per ton of product capital charge assuming a 30 year plant life time and a 30 year payback period. For all processes CapEx are calculated as $/t of output, apart from the blast furnace, the electric smelter furnace and the beneficiation plant, for which CapEx are calculated as $/t of input. We do not consider CapEx for mines.
Process OpEx	CRU steel costing model[8] CRU iron ore costing model[9]	OpEx levels are determined from the CRU steel costing data by considering total production cost minus the cost of consumables that we model in our process models (energy, reductant, flux, slag) For all processes OpEx are calculated as $/t of output, apart from the beneficiation plant, for which OpEx are calculated as $/t of input.
Raw material cost	CRU steel costing model[8] CRU iron ore costing model[9]	Cost data used for consumables considered in our process models, specifically renewable and grid electricity, green, grey and blue hydrogen, diesel, coke, PCI, burnt lime, burnt dolo, BF, BOF, EAF, and ESF slag, water, and steel scrap
USD inflator	CRU steel costing model[8]	CRU steel cost model. Historical data plus 2% inflation for all future years. All cost data in this model is recalculated to real 2025 dollar values.
Process modelling recipes	HILT RP1.004/5	The method of determining the consumption of energy, flux, the production of slag and the losses of iron in different processes, for different iron ore qualities, is explained in section 3.5

4. RESULTS

Below we provide analysis on a number of different outcomes from our model, with forecasts for the years 2035 and 2050 in a number of different scenarios. First, we analyse where different processing steps would take place, in particular where iron and steel production would occur if China were to shift to decarbonised steelmaking (section 4.1) Secondly, what countries would be supplying the ore going into these steelmaking supply chains (section 4.2). And third, what processes are used for different grades of iron ore, from different national suppliers (section 4.3).

We run the model with a combination of model settings, being:

- Different points in time, specifically the years 2025, 2035, and 2050;
- Different levels of demand for green steel, with a baseline scenario assuming 15% of steel demand is met with green steel in 2035 and 80% in 2050, corresponding to a linear trajectory to fully decarbonised Chinese steel demand by 2060, the year China targets in its net-zero emissions plans. We include alternative scenarios with either 100% or 0% of steel demand met with green steel, to compare how very different levels of decarbonisation may affect Australian exports of iron ore and iron;
- Different Chinese EAF capacity and acid gangue limits. For 2025, EAF capacity is set to 150 Mt, roughly equal to currently installed Chinese EAF capacity[58]. Chinese policy dictates a gradual increase in EAF use, from 15% of steel production to be produced through EAFs in 2025 and 20% by 2030, up from around 10% of production in 2023[60]. Longer term targets are unclear but likely to keep rising with growing scrap availability. For the baseline scenario, we presume Chinese installed EAF capacity to grow to 300 Mt by 2035 and 450 Mt by 2050. In the 'high EAF' scenario, we presume Chinese EAF capacity to grow to 450 Mt by 2035 and 900 Mt by 2050, or more than total demand forecast for 2050[57]. As such these are not forecasts of EAF capacity but represent a range of possible futures with either steady or very rapid build-out of Chinese EAF capacity. For acid gangue limits of material processed via the EAF pathway, we use a value of 3% for all years in the baseline, corresponding with what is currently considered 'DR grade' iron ore, i.e., what is generally accepted by EAF operators[16]. In an alternative 'high EAF' scenario we set Chinese installed EAF capacity to 450 Mt in 2035 and 900 Mt in 2050, and a maximum 7% acid gangue limit, assuming that future EAF operating procedures may change under increased pressure to produce green steel from poorer ore grades.

Beyond different levels of demand and EAF capacity and gangue limits, we investigate a number of further model sensitivities, specifically different relative hydrogen production costs in Australia versus China (section 4.4) and different levels of Electric Smelter Furnace (ESF) capacity (section 4.5).

Lastly, we provide a comparison of the supply cost of the cheapest ton of steel delivered to South China, with the production of green iron occurring in each of the different production locations (see section 3.3 for an overview of these locations) included in our model (section 4.6). This exercise ranks production costs in different locations, and quantifies the gap in relative costs between different locations considered.

In all scenarios discussed below, an Australian Hydrogen Production Tax Incentive (HPTI) of A$2/kg green hydrogen has been included.

4.1 LOCATION OF PROCESSING STEPS

Below we present a series of plots that visualise where each of the processing steps would optimally occur according to the model, from mining through to steel making (Figure 5, 7-10). Note that, for the results presented for mining and beneficiation, the country group 'Rest of World' includes all other countries with operating iron ore mines, whereas for the results for the iron and steel making steps, the country group 'Rest of World' only includes all other iron or steel producing nodes in our model, specifically Chile, Egypt, and the UAE (see also section 3.3., Table 3).

We start with a now-cast of the year 2025 (Figure 5), to check that the model produces reasonable estimates of current real-world conditions, which it does so fairly well. This gives optimism about the quality of its forecasts for the future years.

Specifically, iron ore supplies roughly match observed trade patterns (Figure 6). The data in Figure 6 is presented as product post-beneficiation, as this is typically the manner in which ore production and trade is reported in other sources. Note that this is different from data on output from mines in Figure 5, 7-10, which present run-of-mine ore production, and therefore cannot be directly compared with data in Figure 6. We should also add that comparison of iron ore volumes between different data sources and/or results from our model is always somewhat limited by a lack of data on iron grade of the ore produced or traded, making it less clear what volumes of iron content are produced or traded. The largest difference in the predicted and observed origin of iron ore consumed in China is a much smaller share of Chinese iron ore in our model results than observed in reality (Figure 6). This could be explained by a Chinese preference for domestic iron ores, based on considerations beyond cost alone, for example for purposes of supply chain securitisation or domestic industry support. The resulting shortfall in iron ore supply in our model is made up with a higher amount of iron ore imports from Australia than is observed in the real world (Figure 6). The relevance of this difference is further discussed in section 4.2, where we compare the supply of ore from different countries to China in different model scenario settings.

Our model results for 2025 further predict that 921 Mt of steel production in China would be met via the BF-BOF pathway, and about 128 Mt, or about 12.2% of total production, from scrap recycling via the EAF. This is a close approximation to the 10.2% of steel produced via the EAF pathway reported for 2024 by the World Steel Association[61]. Our model also predicts that all available steel scrap would be consumed, in line with the current understanding that steel from recycled scrap is a more cost-effective production route than primary steel produced with iron ore and coking coal, and the observation that scrap steel has very high recycling rates[62].

A number of results from model forecasts plotted in Figures 7-10 deserve particular attention.

First, in all scenarios, all production of steel, whether via the EAF of BOF, occurs in China. There is no transport of steel between different countries, or between different Chinese regions. The models cost settings suggest that transport of steel products is prohibitively expensive and that the additional cost incurred for such transport exceed cost savings for locating steelmaking steps in low-cost regions. The production of iron via the blast furnace also always occurs in China, as our model only considers use of the hot metal in local BOF and does not consider the possibility of exporting pig iron from the blast furnace.

Second, a large share of green steel demand may be met with recycled steel scrap. In our scenarios with baseline green steel demand levels for 2035, where 15% of all steel demand must be met with green steel, there is no production of DRI with green hydrogen (Figure 7 & 9, top panels). The production of green steel from scrap recycling, with renewable electricity powering the EAF, is much cheaper than H_2DRI-EAF or H_2DRI-ESF-BOF production, and the model chooses to produce as much steel from recycled scrap as the supply of scrap or the installed EAF capacity allows. For 2050, where baseline demand for green steel is 80% of all steel demand, well over two-thirds of green steel demand may be met with scrap-based steel (Figure 8, top panel), and possibly even almost all of green steel demand may be met with scrap-based steel in a scenario where Chinese EAF capacities are very large (Figure 10, top panel). Demand for steel made via the green hydrogen DRI route may therefore be quite limited if and when steel demand and scrap supply converge as is forecast, and China builds the EAF required to process all this scrap. In scenarios for 2050 with 0% green steel production, available scrap supply and EAF capacity are not always completely exhausted (compare scrap supply in bottom panels in Figures 8 & 10 with other panels in the same figures), suggesting that some BF-BOF production may be cheaper than scrap-EAF steel. Future scrap supply, prices, and suitability to replace all types of steel demand is further discussed in section 5.

Third, in scenarios where there is production of DRI with green hydrogen, this is forecast to occur largely or entirely in China for baseline cost settings. Only in the scenarios for 2035, where 100% of demand is met with green steel, does any production of green iron occur outside of China. In these scenarios, roughly a quarter of H_2-DRI production is forecast to occur in Brazil and Chile, with the remainder three quarters produced in China (Figures 7 & 9). In these scenarios, the DRI is briquetted in those origin countries and shipped to China in the form of HBI. In no scenario does any DRI production occur in Australia, which can be largely attributed to assumptions on relative hydrogen production cost; this is discussed further in section 4.4, on Australian hydrogen production cost gaps required to support Australian green iron production. The production of green iron in Brazil and Chile in the scenario with 100% of demand met with green steel in 2035, but not in 2050, can similarly be explained by developments in relative hydrogen production cost; this is further discussed in section 4.8, on key model sensitivities.

Fourth, our model suggests that the use of beneficiation will drop off in most future scenarios. Only in the scenarios for 2035, where 100% of steel demand is met with green steel (Figures 7 & 9, middle panels), do we see levels of beneficiation similar to those seen today (Figure 5). These are the scenarios that see the largest production of green iron, with processing via the H_2DRI-EAF pathway requiring highly upgraded ore, and processing of Chinese and Brazilian ores via the H_2DRI-ESF-BOF pathway more economical with highly upgraded ores. Further discussion is provided in section 4.3 on processes used for different ore grades and national suppliers.

Whilst the model suggests about 650 Mt ore as-mined to be beneficiated before being consumed in a blast furnace currently (Figure 5), the model forecasts almost no ore will be beneficiated before being consumed in Chinese blast furnaces in 2035 or 2050. The key economic driver for beneficiation, optimal metal output out of a limited blast furnace capacity (see Appendix 1), will be much reduced by then, as steel demand starts to fall whilst blast furnace capacity remains high. We should note that the model forecasts very limited beneficiation of Australian ores. This likely has to do with the relatively steep losses of material in the beneficiation process of low grade Pilbara ores, when compared with beneficiation of Brazilian, Chinese, Indian, or other ores (see section 3.6.2 on beneficiation), with our model concluding that beneficiation of these ores does not provide a cost advantage versus processing these as ore as-mined. Calibrating these beneficiation curves is something that can be investigated again in future iterations of the model. The fact that there are only very marginal difference in the final cost of steel produced with Pilbara ores beneficiated to either low to medium levels (Appendix 1) gives confidence that this will not greatly influence downstream model results.

FIGURE 5. PROCESS LOCATIONS IN THE BASELINE SCENARIO, 2025

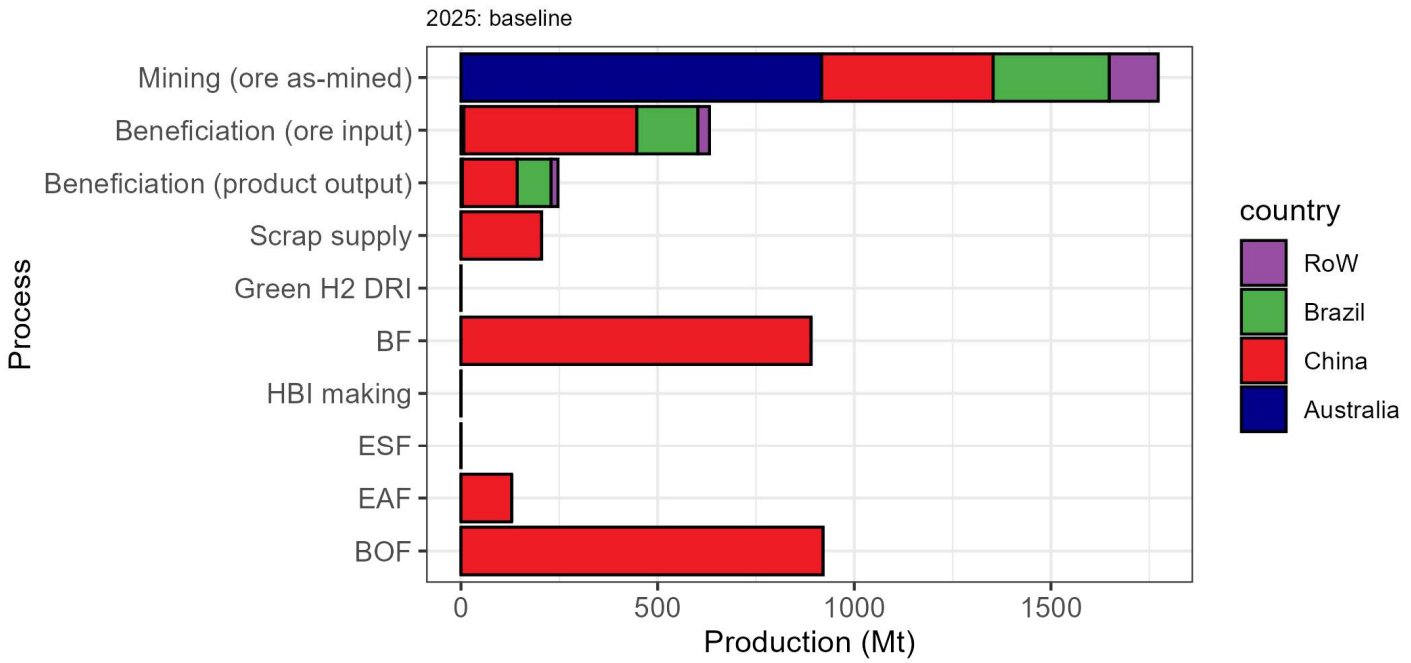

Scenario settings: Chinese BF capacity of 884 Mt, EAF capacity of 150 Mt, unlimited ESF capacity, 3% max acid gangue through the EAF pathway, 0% green steel demand.

FIGURE 6. BENCHMARKING MODEL PREDICTION VS OBSERVED SUPPLIERS OF IRON ORE CONSUMED IN CHINA

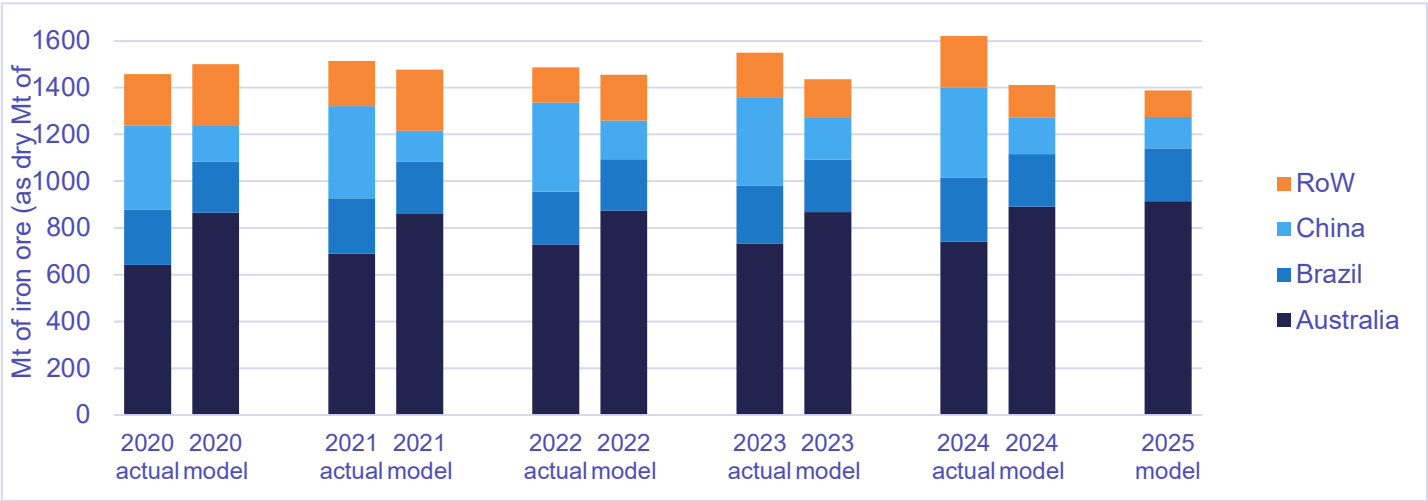

Source: 2020-2024 data: UN Comtrade[63] for Chinese imports, US Geological Survey[31] for Chinese production. Note all data here is presented as product post-beneficiation, and can therefore not be directly compared with mine output in Figure 5, 7-10, which present ore as-mined production.

FIGURE 7. PROCESS LOCATIONS BY SCENARIO, 2035

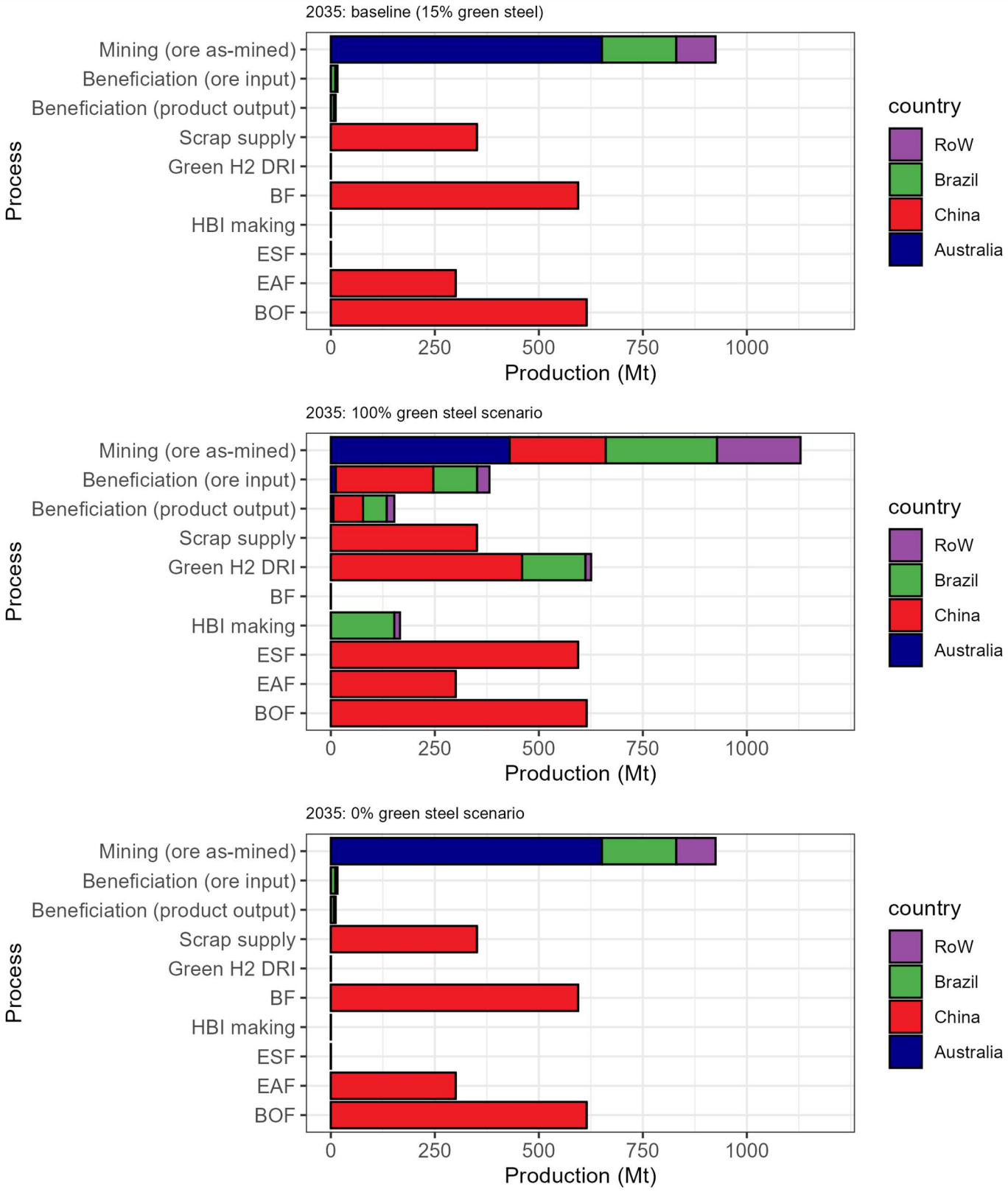

Scenario settings: Chinese BF capacity of 884 Mt, EAF capacity of 150 Mt, unlimited ESF capacity, 3% max acid gangue through the EAF pathway. Steel from recycled scrap counted as green. Australian green hydrogen production cost reduced by a Hydrogen Production Tax Incentive (HPTI) of A$2/kg.

FIGURE 8. PROCESS LOCATIONS BY SCENARIO, 2050

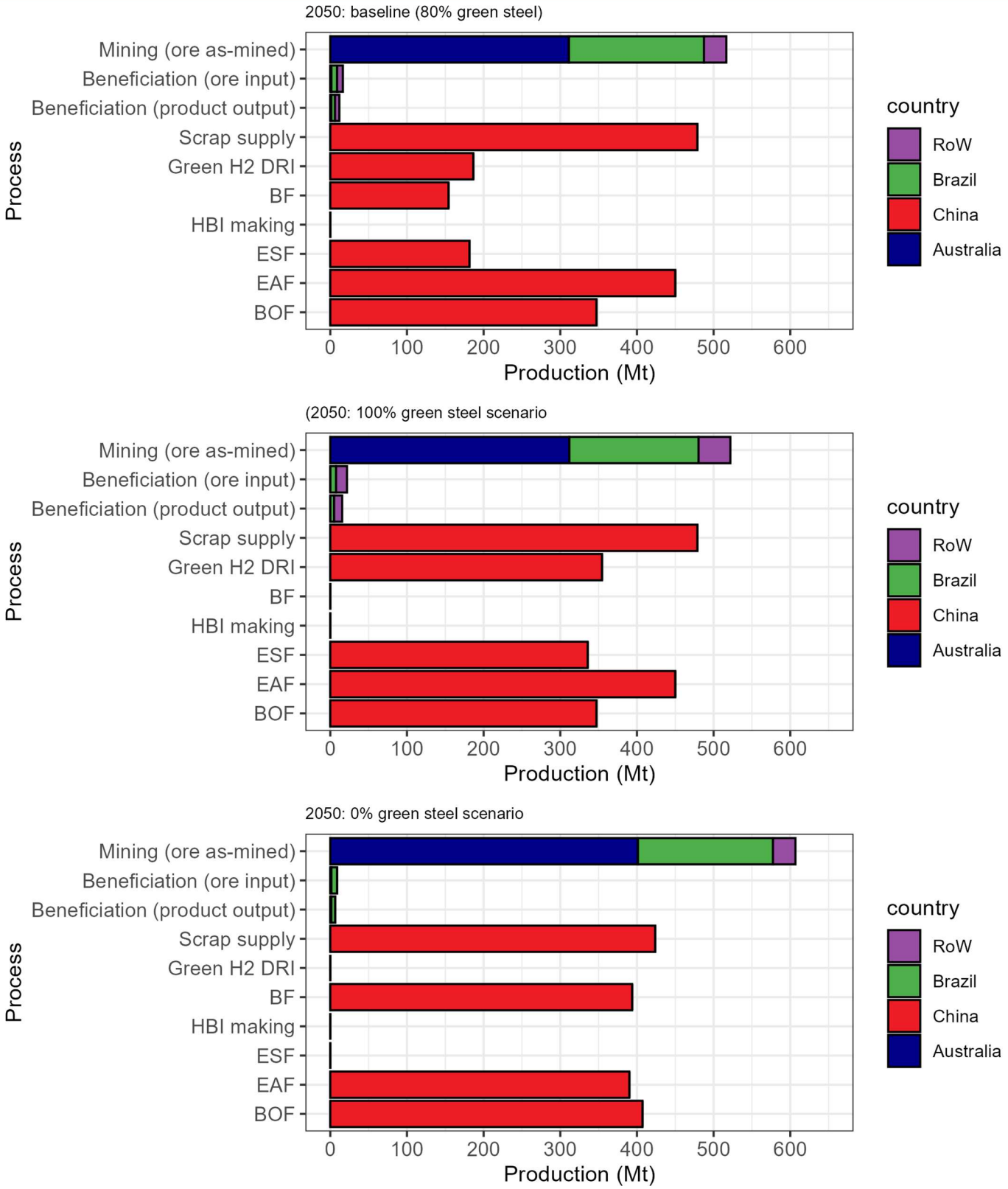

Scenario settings: Chinese BF capacity of 884 Mt, EAF capacity of 150 Mt, unlimited ESF capacity. 3% max acid gangue through the EAF pathway. Steel from recycled scrap counted as green. Australian green hydrogen production cost reduced by a Hydrogen Production Tax Incentive (HPTI) of A$2/kg.

FIGURE 9. PROCESS LOCATIONS BY SCENARIO, 2035, HIGH EAF SCENARIO

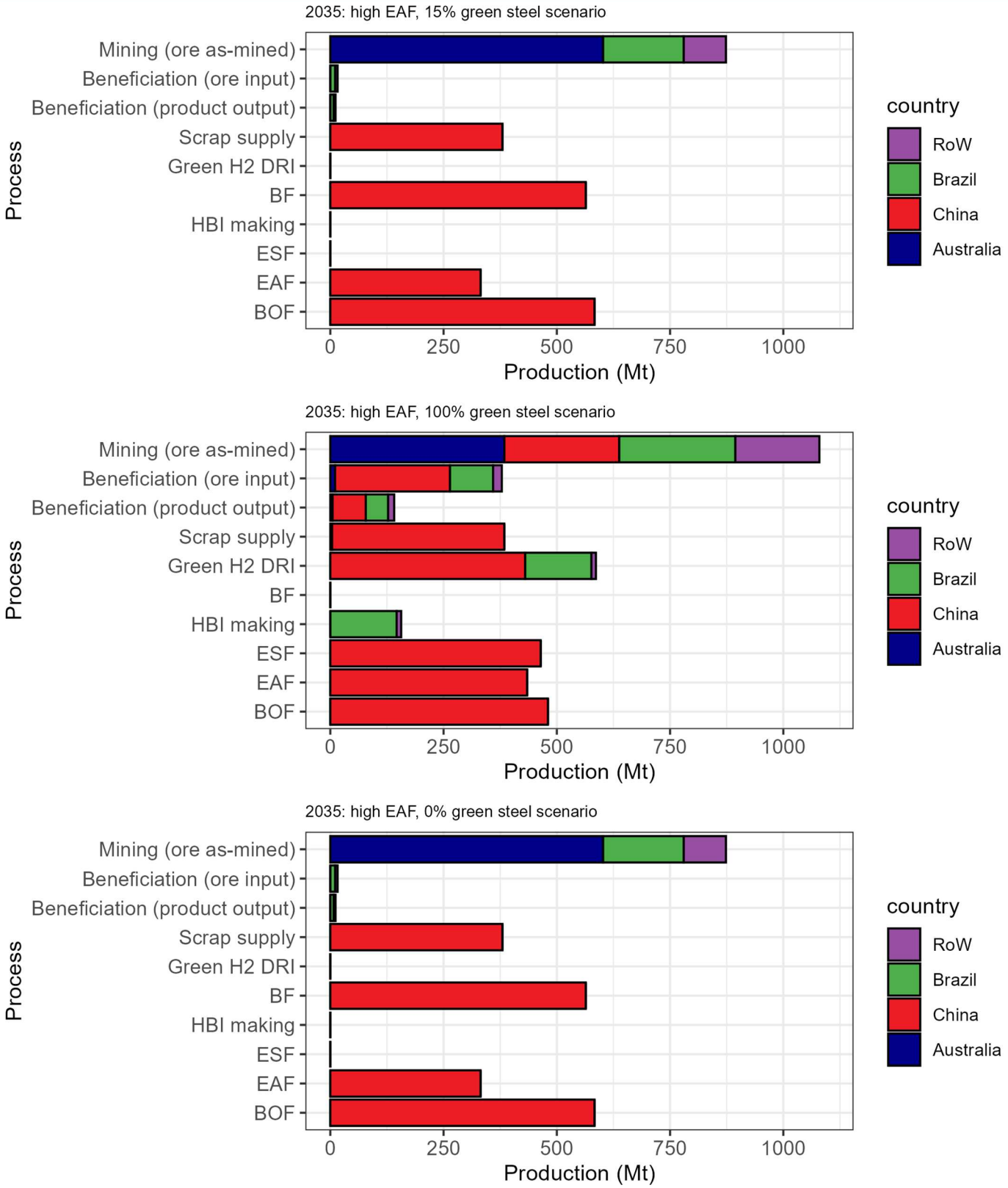

Scenario settings: Chinese BF capacity of 884 Mt, EAF capacity of 450 Mt, unlimited ESF capacity. 7% max acid gangue through the EAF pathway. Steel from recycled scrap counted as green. Australian green hydrogen production cost reduced by a Hydrogen Production Tax Incentive (HPTI) of A$2/kg.

FIGURE 10. PROCESS LOCATIONS BY SCENARIO, 2050, HIGH EAF SCENARIO

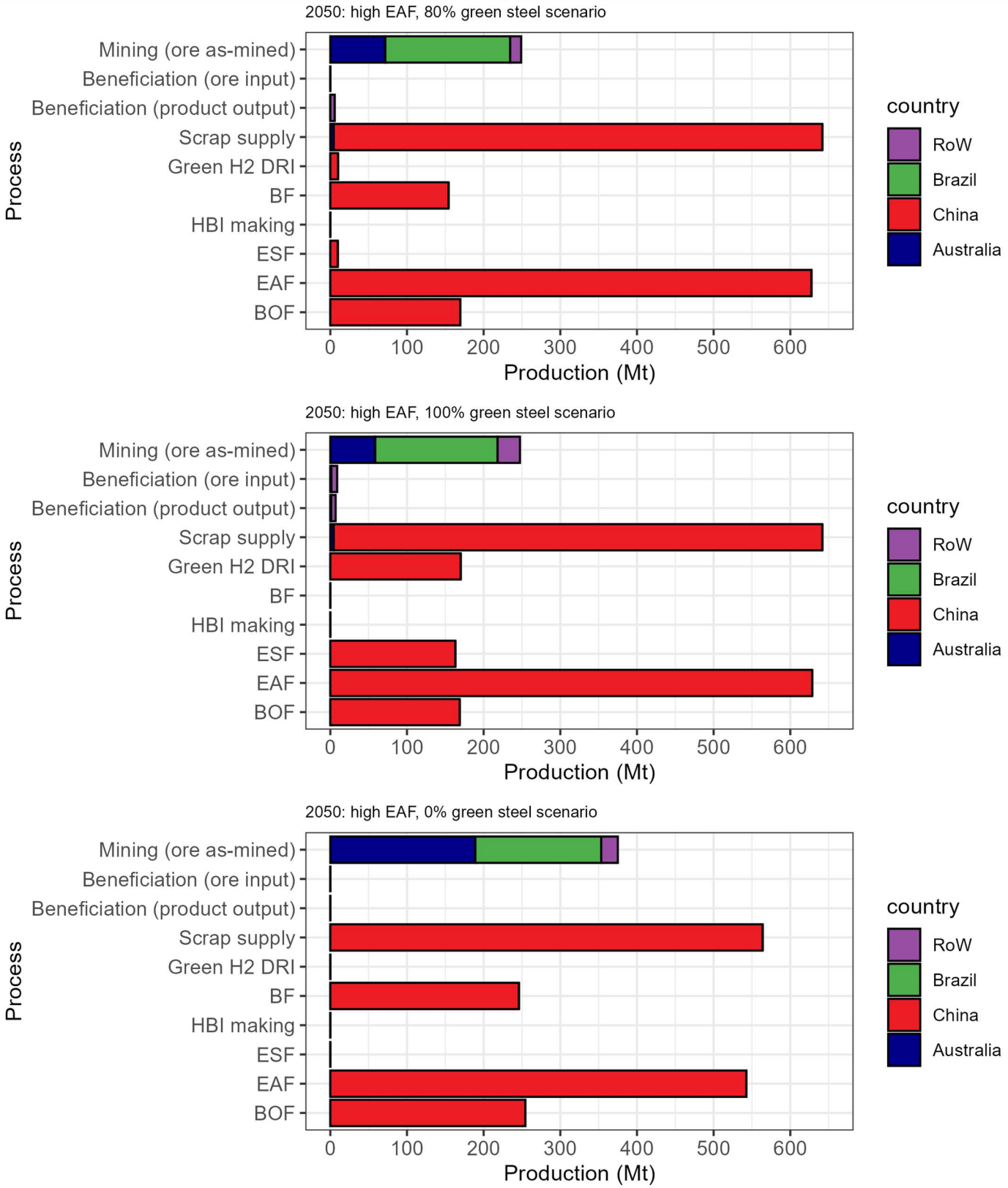

Scenario settings: Chinese BF capacity of 884 Mt, EAF capacity of 900 Mt, unlimited ESF capacity. 7% max acid gangue through the EAF pathway. Steel from recycled scrap counted as green. Australian green hydrogen production cost reduced by a Hydrogen Production Tax Incentive (HPTI) of A$2/kg.

4.2 SUPPLY AND SUPPLIERS OF IRON ORE

The figures 7-10 provided an overview of locations where all processes in the steelmaking value chain might occur in futures with different ambition levels for decarbonisation and different installed capacities of specific technological pathways. Here we zoom in on the supply of iron ore across the same set of scenarios. This helps provide an understanding of effects on expected future Australian iron ore production, regardless of whether that is processed into iron or steel in Australia or in other locations.

The iron ore production in each of these scenarios is summarised in Figure 11. Note that results in this figure are reported as Mt of product (i.e., post-beneficiation), making these more easily comparable with other data sources, as this is the more usual way in which iron ore production or trade is reported. This does mean these numbers are not directly comparable with numbers reported in the columns for 'Mining' in Figures 5 and 7-10, as those report in Mt of ore as-mined, i.e., pre-beneficiation. There are a number of key trends that appear from these results plotted in Figure 11.

First, Chinese consumption of iron ore is expected to fall to about 800-900 Mt by 2035, and to as little as 250-600 Mt by 2050, compared to about 1,400 Mt today. This is due to combined trends of falling demand for steel and increased supply of scrap, which will reduce demand for primary steel production. In scenarios with high EAF capacity, demand for iron ore further falls as more of the available scrap supply is consumed in the scrap-EAF pathway. The likelihood of such a scenario is further discussed in section 4.7 on key model sensitivities.

Second, the model logic also suggests that demand for Australian ores is most strongly affected by the ambition level for green steel as a percentage of total demand, and by the availability of EAF capacity (Figure 11). The effect of a push for green steel leading to reduced demand for Australian ores is explained in large part by reduced production via the BF-BOF route, where Australian ores appear more competitive vs supplies from other countries.

Third, in green steel production routes, large shares of demand are met with ore from Brazil and other countries, mostly Guinea, Liberia, Gabon, and some from India and Peru. In scenarios with very high green iron demand, production via the H_2DRI-ESF-BOF route uses a mix of Australian, Brazilian, and other ores; in scenarios with smaller amounts of green iron production, it is mostly Brazilian and less Australian ores that get processes via this route (more in section 4.3 on processes used for different iron ore types). In scenarios with high green iron demand and high EAF capacity, some production occurs via the H_2DRI-EAF pathway, and it is predominantly Brazilian and Guinean iron ores that get consumed via this pathway (more on this in section 4.3). The overall result is that Brazilian iron ore demand appears most resilient due its flexibility in both conventional and green production pathways, whereas demand for Australian ores appear most sensitive to such changes in production processes. We should note that the model forecasts no consumption of Chinese ore in almost all scenarios, an issue also identified in section 4.1 on model calibration versus observed patterns. Should Chinese consumers or policy value the supply of domestic ores even if these are not strictly the most cost-competitive, this could result in a further reduction for Australian ore demand beyond what is plotted in Figure 11.

FIGURE 11. CONSUMPTION OF ORE BY SUPPLIER: COMPARISON OVER THE DIFFERENT SCENARIOS

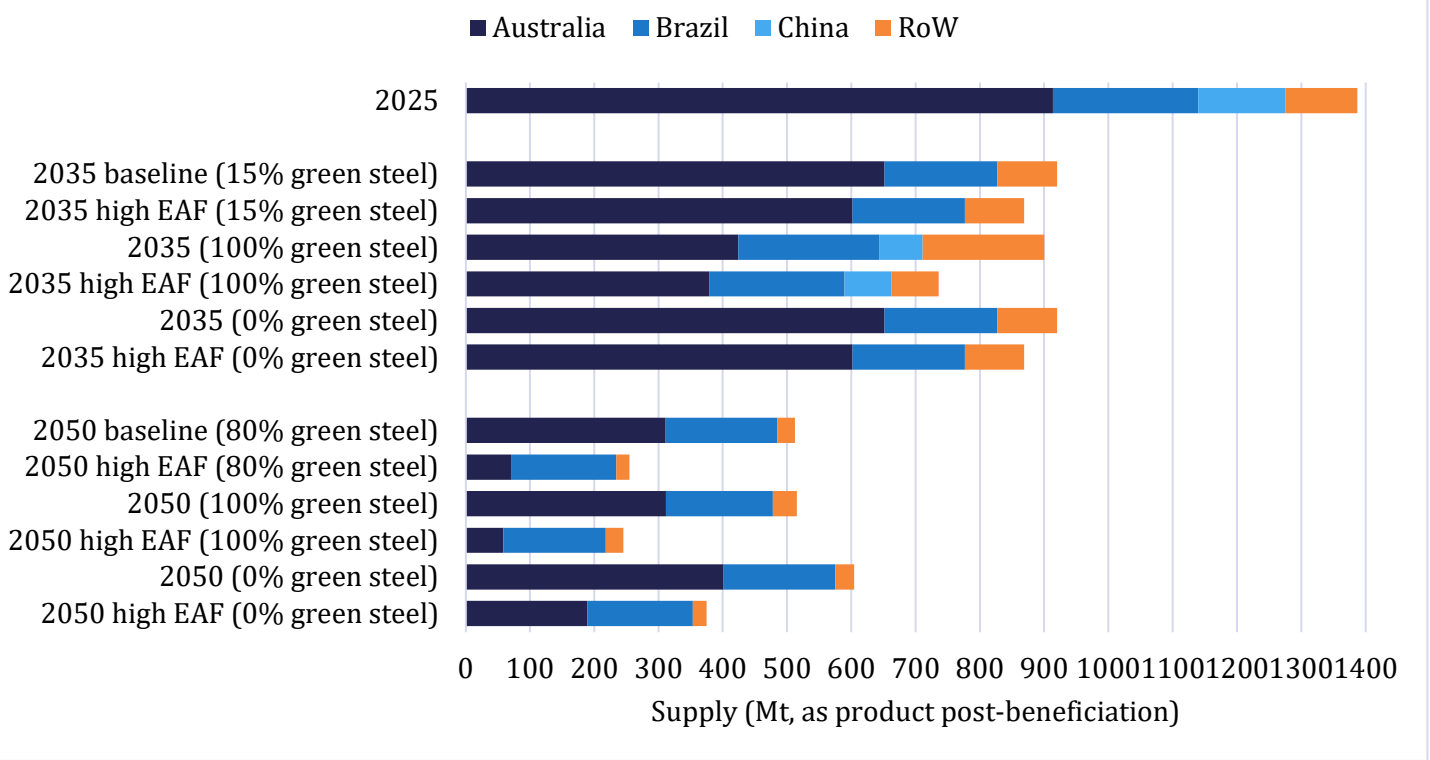

4.3 PROCESSES USED FOR DIFFERENT IRON ORE GRADES AND ORIGINS

Here we analyse the same set of model results, but focus on the grades and national origin of iron ore used in different processes in different scenarios (Figures 12-16).

In section 4.1, it was found that the key economic driver for beneficiation in the BF-BOF route, the maximisation of metal output from a given blast furnace capacity, would be reduced in scenarios with less demand for steel from the BF-BOF pathway. The results in Figures 12-16, for the 0% green steel scenarios (bottom panels in each figure) similarly shows a reduced use of beneficiation, but with some nuance: with falling demand for steel from the BF-BOF pathway, we see less very high grade (> 65% Fe), but simultaneously also less low grade (<60%) ores processed via the blast furnace. The further the demand for steel from the BF-BOF pathway is reduced in these scenarios, the more the demand for ore seems to be concentrated on the 60-65% Fe grades. This reduced demand for high-grade ores impacts mostly high-grade Chinese magnetite ores; the reduced demand for low-grade ores impacts Australian hematite ores. Overall, consumption of low-grade ores sees stronger reductions than that of very high-grade ores.

A very similar pattern can be seen in consumption of material consumed through the ESF-BOF pathway (middle panels in each of the Figures 13-16). In scenarios with high demand for steel from this pathway (e.g., Figure 13, middle panel), ores with a very wide range, of between 55 and 70% Fe grades, including beneficiated Chinese magnetite and Brazilian hematite ores, are consumed. In scenarios with lower demand for this steel from this pathway, the range of ores consumed again narrows to a band between 60-65% Fe grades, with similar reductions of very high-grade Chinese magnetite and low-grade Australian hematite.

We assume this trend towards the middle is because very high levels of beneficiation will always lead to some reductions in weight recovery (see section 3.6.2), and increase end-to-end cost because it increases the amount of material that needs to be mined to produce a tonne of steel, whilst lower grade ores tend to require higher inputs of energy and fluxing materials in subsequent processing steps (sections 3.6.7 and 3.6.8). Demand for Brazilian hematite ores, much of which has very high Fe grades as-mined, appears to be most resilient to these trends, as it can be consumed in both BF-BOF and ESF-BOF pathways, and falls within that band of between 60-65% Fe grades.

In our selection only the 2035 scenario where 100% of steel demand is met with green steel shows demand for steel from the H2DRI-EAF pathway, (Figure 15, middle panel). In this case, we see consumption of only very high grades (65% Fe or more) of ore, due to limitations set on acid gangue contents through this pathway. This would benefit the consumption of high-grade Chinese magnetite ores, and again Brazilian hematite ores, which have both high Fe grades in ore as-mined and are very amenable to further beneficiation (see also section 3.6.2).

FIGURE 12. CONSUMPTION OF ORE BY PROCESS, SUPPLIER, AND ORE GRADE: 2025

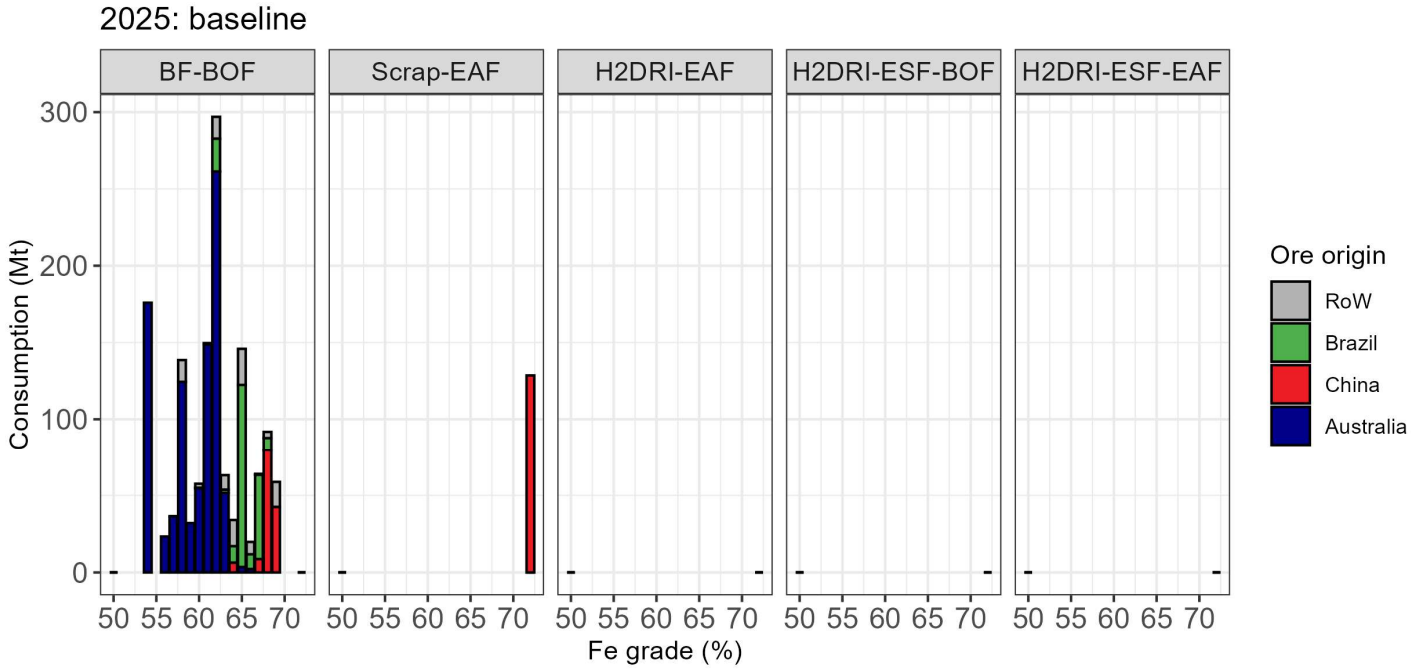

Scenario settings: Chinese BF capacity of 884 Mt, EAF capacity of 150 Mt, unlimited ESF capacity. 3% max acid gangue through the EAF pathway. Steel from recycled scrap counted as green as long as this is produced with renewable electricity. Scrap via the EAF pathway here plotted at 72% Fe to limit x-axis range. Australian green hydrogen production cost reduced by a Hydrogen Production Tax Incentive (HPTI) of A$2/kg.

FIGURE 13. CONSUMPTION OF ORE BY PROCESS, SUPPLIER, AND ORE GRADE: 2035

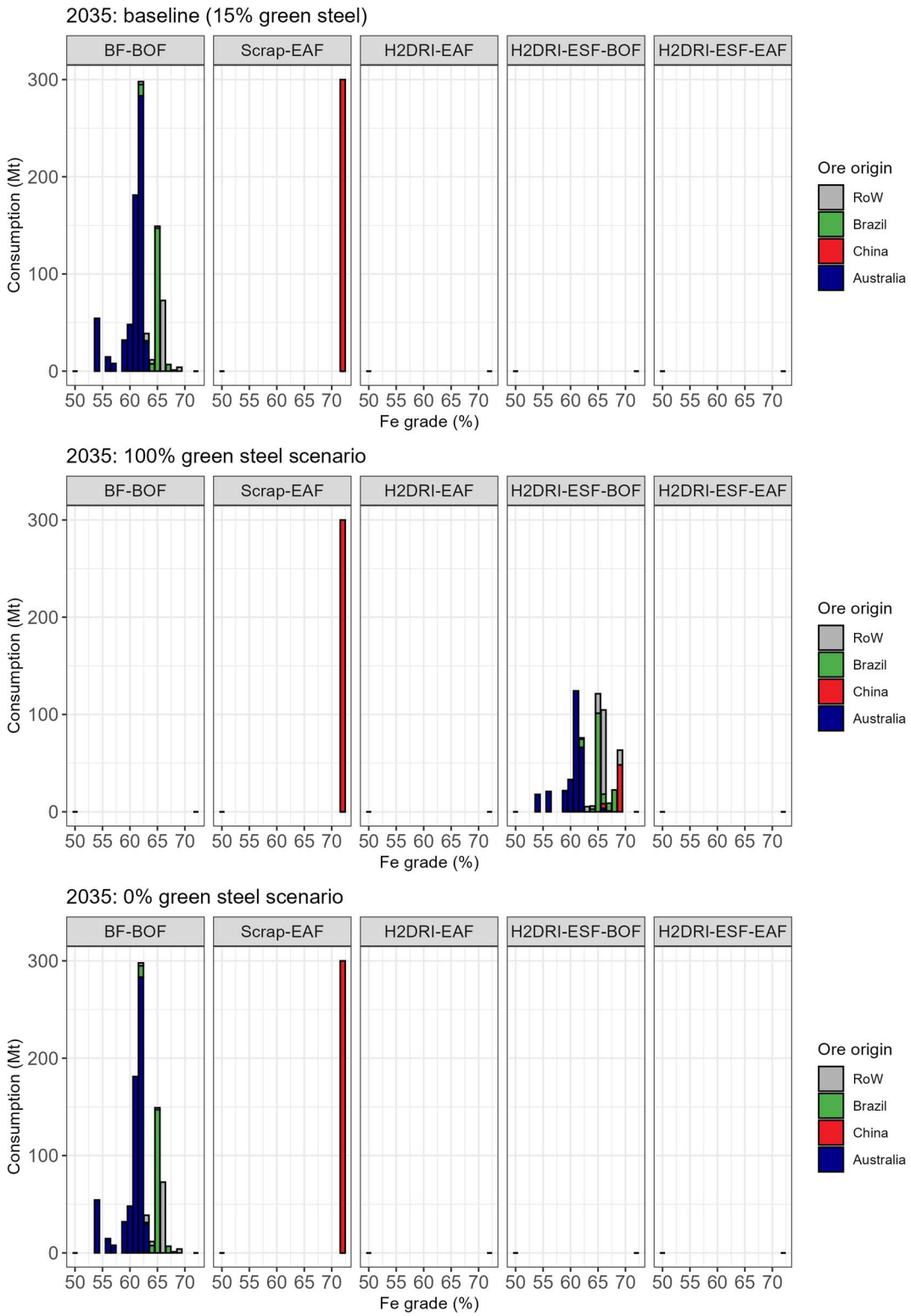

Scenario settings: Chinese BF capacity of 884 Mt, EAF capacity of 300 Mt, unlimited ESF capacity. 3% max acid gangue through the EAF pathway. Steel from recycled scrap counted as green as long as this is produced with renewable electricity. Scrap via the EAF pathway here plotted at 72% Fe to limit x-axis range. Australian green hydrogen production cost reduced by a Hydrogen Production Tax Incentive (HPTI) of A$2/kg.

FIGURE 14. CONSUMPTION OF ORE BY PROCESS, SUPPLIER, AND ORE GRADE: 2050

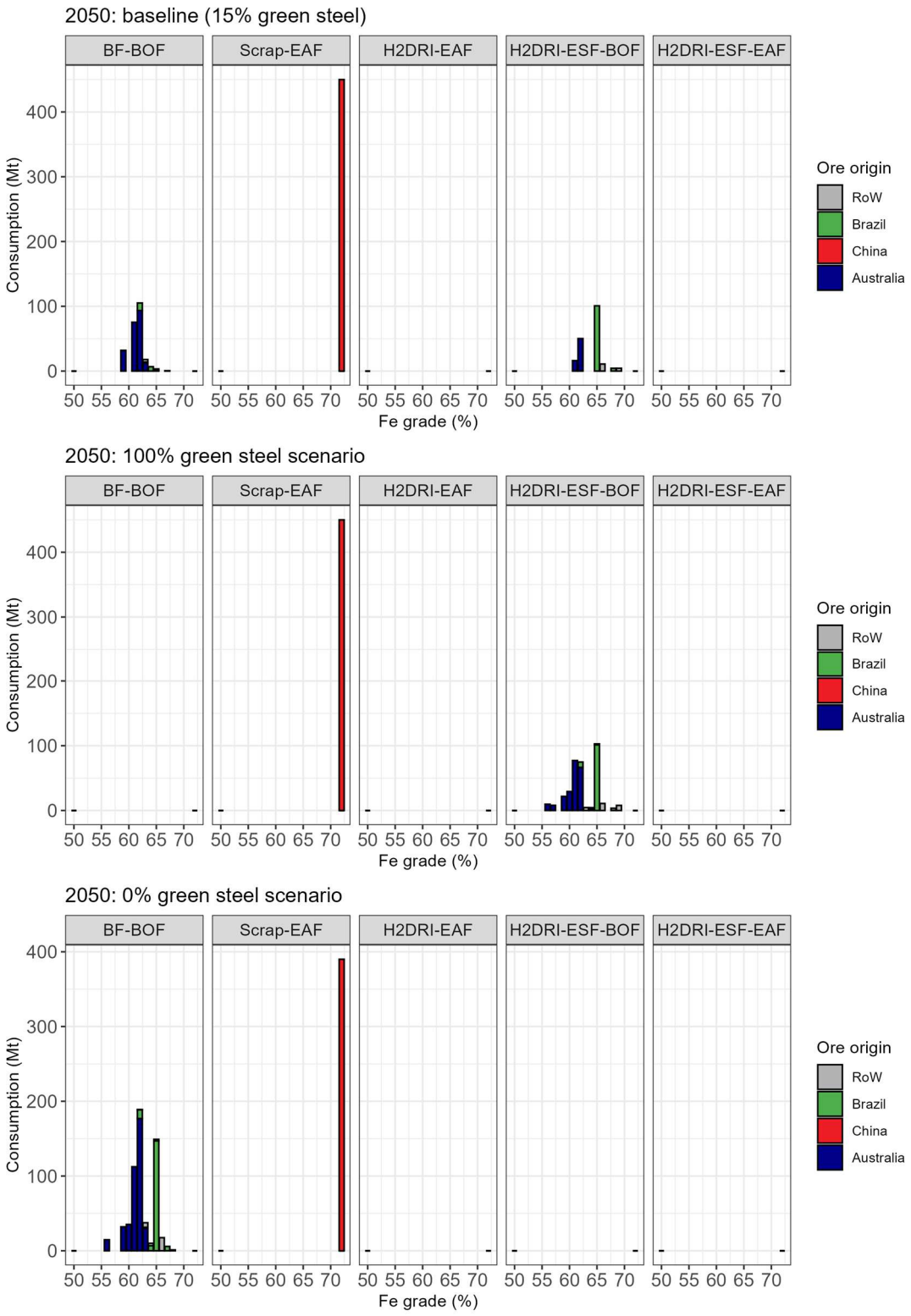

Scenario settings: Chinese BF capacity of 884 Mt, EAF capacity of 450 Mt, unlimited ESF capacity. 3% max acid gangue through the EAF pathway. Steel from recycled scrap counted as green as long as this is produced with renewable electricity. Scrap via the EAF pathway here plotted at 72% Fe to limit x-axis range. Australian green hydrogen production cost reduced by a Hydrogen Production Tax Incentive (HPTI) of A$2/kg.

FIGURE 15. CONSUMPTION OF ORE BY PROCESS, SUPPLIER, AND ORE GRADE: 2035, HIGH EAF SCENARIO

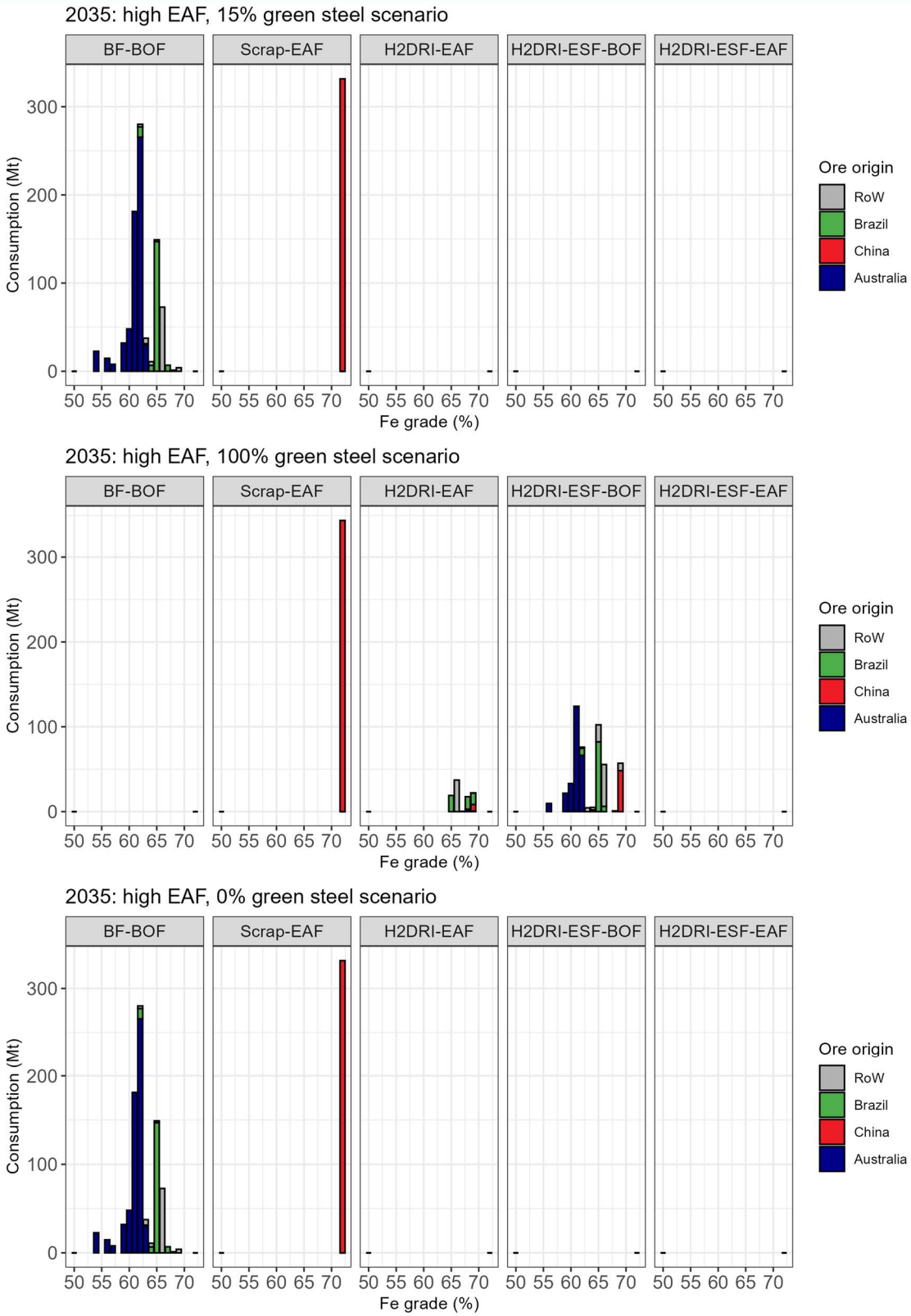

Scenario settings: Chinese BF capacity of 884 Mt, EAF capacity of 450 Mt, unlimited ESF capacity. 7% max acid gangue through the EAF pathway. Steel from recycled scrap counted as green as long as this is produced with renewable electricity. Scrap via the EAF pathway here plotted at 72% Fe to limit x-axis range. Australian green hydrogen production cost reduced by a Hydrogen Production Tax Incentive (HPTI) of A$2/kg.

FIGURE 16. CONSUMPTION OF ORE BY PROCESS, SUPPLIER, AND ORE GRADE: 2050, HIGH EAF SCENARIO

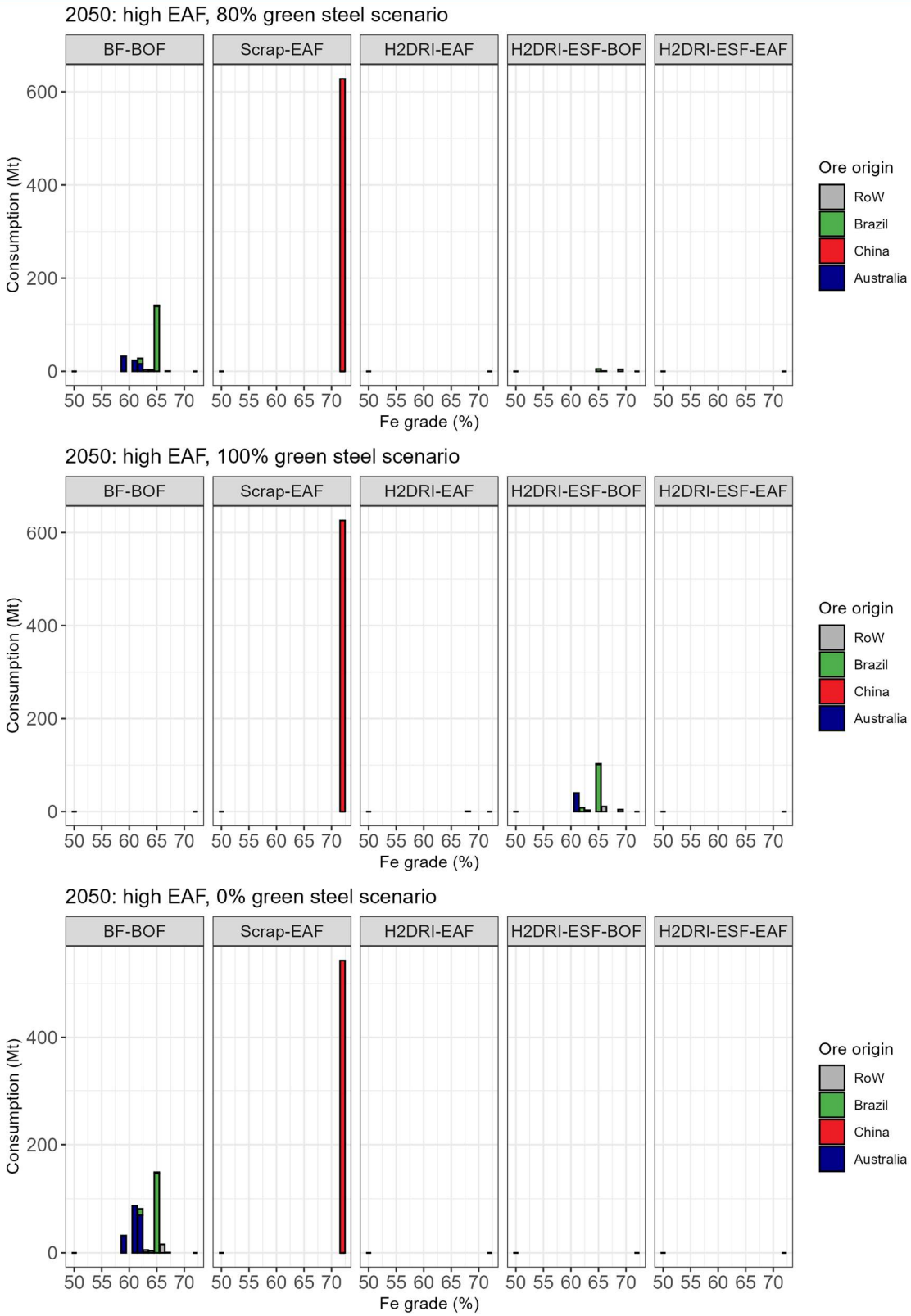

Scenario settings: Chinese BF capacity of 884 Mt, EAF capacity of 900 Mt, unlimited ESF capacity. 7% max acid gangue through the EAF pathway. Steel from recycled scrap counted as green as long as this is produced with renewable electricity. Scrap via the EAF pathway here plotted at 72% Fe to limit x-axis range. Australian green hydrogen production cost reduced by a Hydrogen Production Tax Incentive (HPTI) of A$2/kg.

4.4 HYDROGEN PRODUCTION COST DIFFERENCES AND AUSTRALIAN IRON PRODUCTION LEVELS

There is a strong variation in estimates of current and forecasts of future green hydrogen costs[64]. National strategies and even the IEA Global hydrogen review have near-term forecasts that presume very steep reductions in costs over the next few years versus prices quoted in auctions or forward contracts today[65], whilst the IEA has updated their forecasts for green hydrogen costs upwards in each of the annual Global hydrogen reviews to date[66–70]. In this report we use the green hydrogen cost forecasts as provided by CRU, which are on the conservative side.

Regardless of what future hydrogen costs turn out to be, we can investigate the hydrogen production cost differential required to competitively produce green iron in Australia. This is effectively the same determining the cost gap in remaining cost items, mostly OpEx, CapEx, and conventional energy and raw material expenses, that needs to be closed by hydrogen costs differences.

For this exercise we use the baseline cost settings as provided by CRU, for everything apart from the green hydrogen costs. We further presume all hydrogen production costs in all regions apart from Australia are as listed in Table 10. We consider 2035 levels of steel demand, scrap supply, and cost estimates, and consider that all Chinese demand for steel has to be met with green steel. For this exercise we use an unlimited EAF capacity model setting; as we vary ESF capacity, remaining green steel demand must be met via the H_2DRI-EAF pathway, and therefore we must make sure sufficient EAF capacity exists in order to meet steel demand. We then vary Australian hydrogen production costs to determine the level of green iron production occurring in Australia. Given that we are concerned with Chinese steel demand, we vary the difference between Australian hydrogen production costs and the Chinese hydrogen production costs, given in Australian dollars.

This analysis indicates that no production of iron would occur in Australia if Australian hydrogen production costs are at parity or above Chinese hydrogen production costs (Figure 17). However, if Australian producers could bring hydrogen costs down to as little as A$0.50/kg H_2 (or US$0.32/kg H_2) below Chinese production costs, substantial levels of iron production would be competitive in Australia (Figure 17). Note again that this is regardless of absolute hydrogen costs in either country; these results hold as long as the difference in green hydrogen production cost between China and Australia is about A$0.50/kg H_2.

At that level, about 300 Mt of iron would be produced in Australia, equivalent to about 48% of total Chinese demand for iron in 2035. This level of iron production in Australia would ramp up to about 430 Mt, or about 67% of total Chinese demand for iron in 2035 in a scenario where Australia could produce green hydrogen at a discount of A$1.25/kg green hydrogen.

Australian iron production ramps up very slowly with further increases in in the hydrogen production cost gap beyond this. This is because additional Australian ores are relatively expensive to mine and/or beneficiate to required levels for processing. Brazilian and a small fraction of Chilean iron production are resilient in any of these scenarios; their costs remain below that of Chinese domestic iron production. In summary the Australian competition over market share for supplying the Chinese market with green iron is mostly with Chinese domestic production of iron.

Note that in the model results described up until this point, we have assumed that HBI of any density may be shipped internationally with only limited technical hurdles or additional costs (see also section 3.6.6). Should the future prove these hurdles or costs prove to be prohibitive, this would affect the feasibility of shipping HBI made with high gangue content ores, which could affect the competitiveness of Australian Pilbara ores. The export of these ores as green iron could then still occur in the form of pig iron, but this would appear to be a more costly value chain option. The resulting exports of iron from Australia would be reduced to zero in such a scenario, unless Australian hydrogen production cost could be achieved at a discount of A$2/kg H_2 or more versus Chinese hydrogen production cost (Figure 18). Shipments of iron from Brazil and Chile are also reduced in such a scenario, though only very marginally, as most ores from these countries may be processed into HBI that meets the density requirements for safe shipping without particular safety precautions. The model suggests that processing of Australian high-gangue ores will be cheapest via the H_2DRI-ESF-BOF route, with ore shipped to China, followed by the H_2DRI-HBI-ESF-BOF route, with HBI shipped to China including possibly fairly costly maritime transport, followed by the H_2DRI- ESF-EAF route, with pig iron shipped to China.

FIGURE 17. AUSTRALIAN IRON PRODUCTION AS A FUNCTION OF HYDROGEN PRODUCTON COST DIFFERENCE WITH CHINA

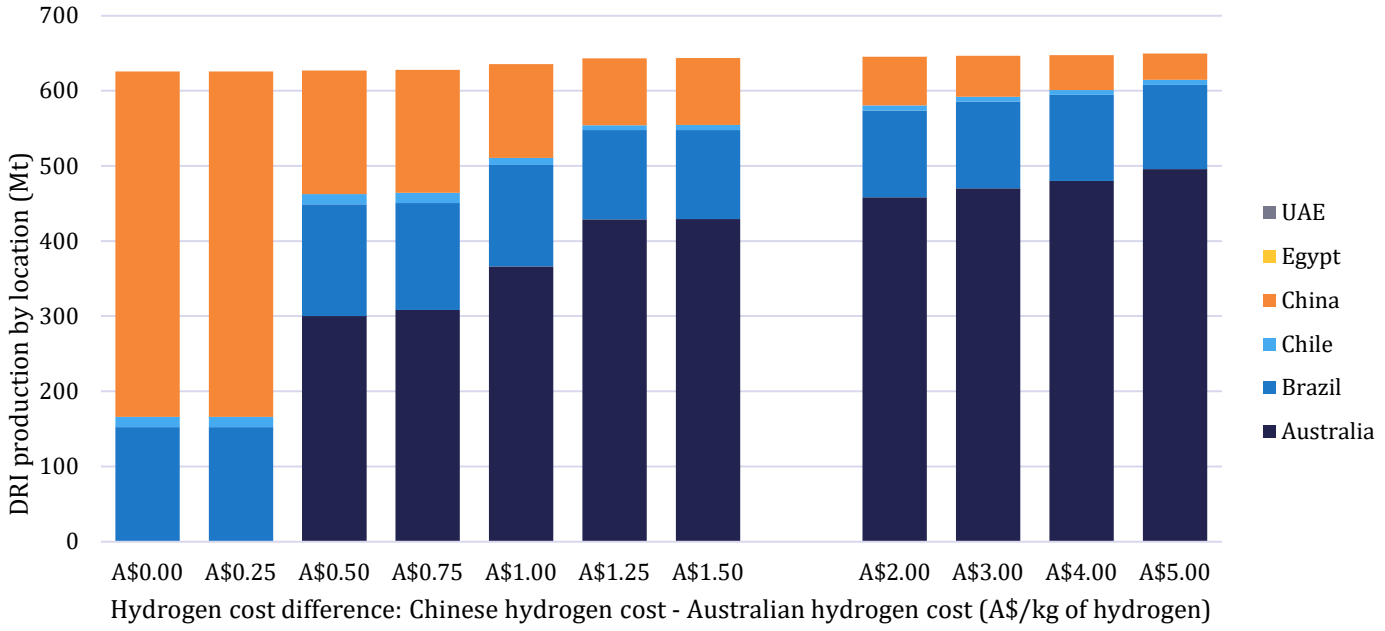

Note: outcomes for a scenario where we presume HBI, including with a density < 5 t/m^3, can be shipped without major technical or cost hurdles. Results for 2035, with 100% green steel demand, and baseline settings for EAF and ESF capacity, etc. Australian hydrogen costs is the only cost varied versus baseline settings.

FIGURE 18. AUSTRALIAN IRON PRODUCTION AS A FUNCTION OF HYDROGEN PRODUCTON COST DIFFERENCE WITH CHINA

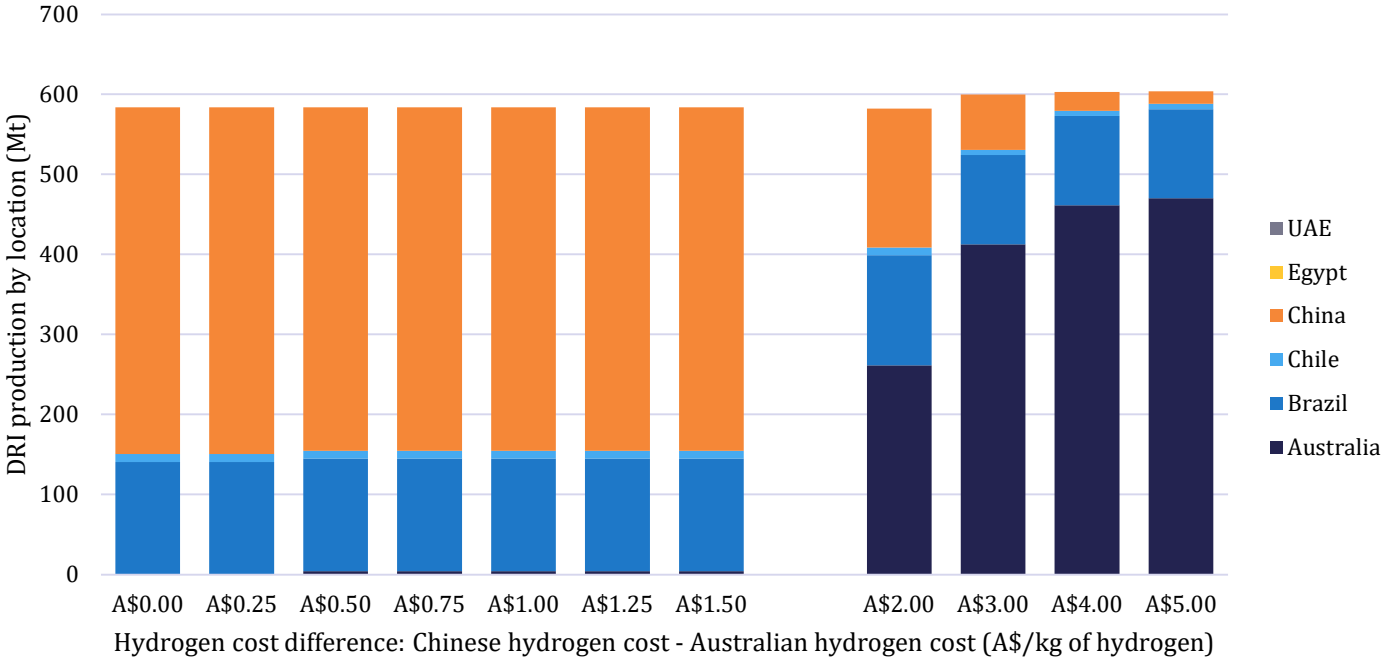

Note: outcomes for a scenario where we presume major technical or cost hurdles with the shipping of HBI with a density <5 t/m^3. In this scenario the only iron products shipped internationally are HBI with a density >5t/m^3 and pig iron. Results for 2035, with 100% green steel demand. Australian hydrogen costs is the only cost varied versus baseline settings. We use unlimited EAF and ESF capacity for this exercise as the pig iron exports route largely depends on the availability EAF capacity; this additional EAF capacity also causes a slightly higher scrap consumption versus results in Figure 17, resulting in a slight drop in total DRI production (compare bars at the $A0,00 scenario).

4.5 RELEVANCE OF THE ELECTRIC SMELTER FURNACE FOR AUSTRALIAN IRON ORE EXPORTS

In previously reported results, EAF capacity was assumed fixed, at either 300 Mt in 2035 and 450 Mt in 2050 for the baseline scenario, or alternatively 450 Mt in 2035 and 900 Mt in 2050 in the high EAF scenario. ESF capacity was unrestricted in any of these scenarios.

This matters because Australian high gangue iron ores are more economical to process via the ESF pathway. This is most clear in Figure 15, where it is only Brazilian, Chinese and other ores that are processed via the EAF pathway, whilst all Australian ores are processed via the ESF or BF pathway. This has to do with the limited recovery rates of Australian hematite ores in the beneficiation process (see also section 3.6.2), which means that in order to produce a ton of product at a given Fe grade, relatively high volumes of Australian ore need to be fed into the concentrator. The same amount of product would require fewer tons of e.g., Brazilian ore to be fed through the same concentrator process, resulting in lower overall cost. Furthermore, many Australian ores are so highly goethititic (and have such low theoretical maximum Fe grades) that they would never achieve the final Fe grade required for processing via the EAF pathway.

This in turn implies that in a world with increasing demand for green steel, demand for Australian ore will depend on the total available ESF processing capacity. This relation is visualised in Figure 19. In scenarios with ESF capacity of 300 Mt or above, demand for Australian ores is about 380 Mt, or about 45% of total Chinese demand for iron ore. Note again that this is considerably less than in today's market, or in a 2035 market with much less demand for green steel, and more for conventional steel (Figure 11).

Results in Figure 19 also make clear that ore from new mines in Guinea are very competitive in a world with Chinese demand for green steel and are estimated to provide approximately 108 Mt of iron ore to the Chinese market by 2035. Note that Guinean mines produce high Fe grade hematite ores, and demand for this product is similar in scenarios with demand for conventional steel only.

At ESF capacities above 400 Mt, demand for Australian ores does not change any further. Below that level, total Australian ore demand scales almost linearly with total available ESF processing capacity. Note again that this is different from results in Figure 11 where EAF capacity was capped, and ESF capacity was unrestricted.

Promoting the development of the ESF technology, and its deployment either in Australia or in China, is therefore likely of great relevance to future demand for Australian ores in decarbonising global steelmaking value chains.

FIGURE 19. DEMAND FOR ORE BY COUNTRY OF ORIGIN, AS A FUNCTION OF CHINESE ESF CAPACITY

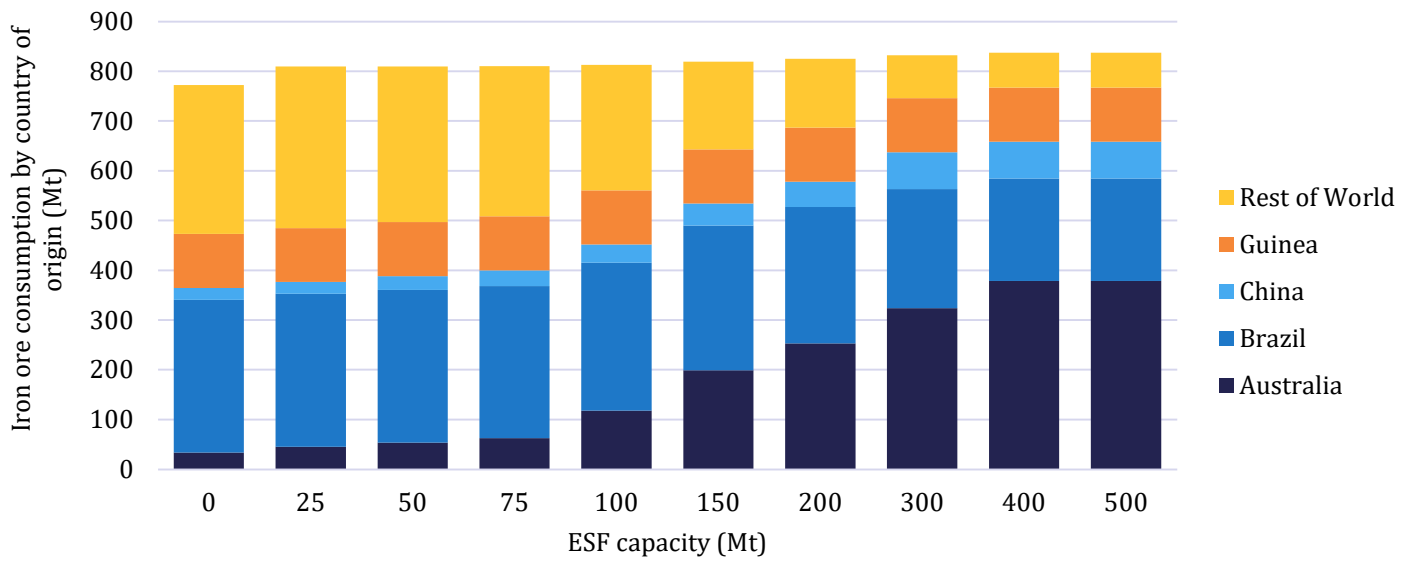

Note: Iron ore consumption as Mt of product (post-beneficiation) into green iron making processes. Scenario settings: results for 2035, with 100% of steel demand met with green steel; unlimited EAF capacity, 3% max acid gangue through the EAF pathway. All ESF capacity in China. Australian green hydrogen production cost reduced by a Hydrogen Production Tax Incentive (HPTI) of A$2/kg.

4.6 LEAST COST SUPPLY OF GREEN STEEL TO CHINA FROM KEY GLOBAL IRON & STEEL SUPPLIERS

Here we compare the cost competitiveness of the different iron producer regions included on our model (Table 3). Specifically, we compare the production costs of the cheapest ton of steel, for delivery to Southern China, for scenarios where iron production (or alternatively both iron and steel production) occurs in each of these regions (Figure 20). This is distinct from the scenarios presented in section 4.1. For this exercise, Chinese demand is set to a single ton of green steel, and ESF and EAF capacity is unrestricted. The values in Figure 20 therefore do not represent the average production costs, nor costs for the typical quality of ore from each of these regions, but the cheapest single ton of steel that can be produced from iron produced in each of these regions, for supply to Southern China. This gives some indication of where these regions sit on global supply curves, how large the relative cost difference between them is, and what cost elements explain the cost differences.

For each of the regions included in Figure 20, the least costly option was to export HBI for processing into steel in Southern China. Production of steel in any of the locations, with steel exported to Southern China, was a more costly pathway because of the high costs associated with the transportation of finished steel products versus a bulk product like HBI.

The largest cost differences are driven by relative hydrogen production costs, as well as mining costs. The results for Chile, Egypt and the UAE, with relatively higher mining and beneficiation costs, are all using Peruvian magnetite ore, upgraded to 69% Fe grade before being processed into DRI. Brazilian and Australian results are with locally mined ores, and results for all three Chinese regions are with Indian hematite ores.

At baseline cost settings, Australia is the highest cost producer (Figure 20). The Hydrogen Production Tax Incentive (HPTI) of A$2/kg of green hydrogen improves this, though model results do suggest that production of iron in Latin American or in China would be cheaper than in Australia. Note that these baseline settings use CRU data on green hydrogen costs.

Comparison of these results with earlier work (for example the studies listed in Table 1) is not necessarily straightforward as differences exist in the year of different forecasts, their consideration of iron ore quality and production cost, and their method of hydrogen production costing, and other choices in method, scope, or reporting. The MRIWA[26] and TSI[71] reports compare green iron production costs across different regions in Australia, but not with production in China or other potential supplier countries. The WWF report[27] sees Australian production costs marginally above US and marginally below those in MENA but does not include comparison with Chinese or Latin-American production. Like our results, the Mandala report[30] similarly considers production costs of green iron in Australia to be higher than in China, and lower than in MENA, but unlike our results, sees Brazil as a more costly location than Australia. RMI's green iron corridor report[6] sees Brazil as one of the cheapest locations and has Chile roughly on par with Australian production costs, but does not report costs in China or the MENA region. Both the Mandala and RMI reports do not consider any differences in iron ore quality or production costs between these regions, however.

We note that the CRU cost estimates are rather conservative, i.e., on the higher side versus other reports listed in Table 1, for both Australia and other regions. We choose to use the CRU values on advice of our HILT CRC industry partners, who expressed concern that lower values in other reports were overly optimistic and not in line with current or near-term costs in real world markets.

The CRU data is also limited in geographic specificity as cost estimates are the same for entire continents or regions. Sub-national estimates, e.g., for different Australia and States and Chinese provinces, would be required to reveal more nuanced views on relative competitiveness in green iron production between the two countries. The development of more realistic estimates is planned for a future expansion of the modeling presented here, building on the region-specific hydrogen cost modeling developed under HILT CRC project RP2.006, which will be expanded to relevant countries and sub-national regions across the globe.

FIGURE 20. CHEAPEST SUPPLY OF STEEL TO SOUTH CHINA WITH IRON PRODUCTION IN DIFFERENT LOCATIONS

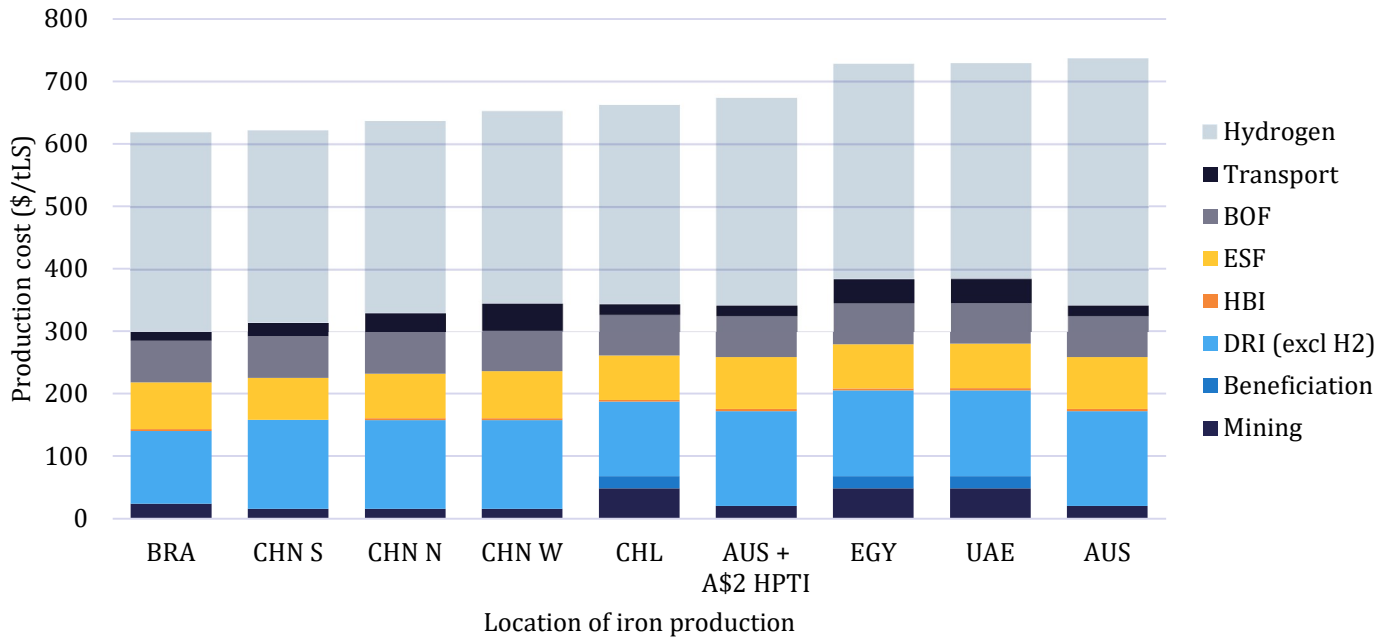

Note: Results for the year 2035, and using CRU's original hydrogen cost estimate for Australia (right-most bar) and with a A$2.00 HPTI included.

5. DISCUSSION

The model results presented in this report are sensitive to data input or scenario settings and some shortcomings in our modelling methodology. Some of these key variables have been explicitly addressed in sections 4.1 through 4.6 and are summarised here.

First, the relative competitiveness of different countries or regions in the production of green iron are clearly most strongly driven by relative hydrogen production, as these make up the largest portion of total green iron cost (Figure 20). It is also clear that small differences in relative hydrogen production cost may substantially change the level of green iron trade (Figure 17).

That means the quality of model results would benefit from improved hydrogen cost modelling. Our approach in the current iteration has been to use the CRU suggested values for green hydrogen production costs, as is the approach for most of the other costs data we use. We have compared these costs with other values reported in the literature, and whilst these CRU values are conservative, they are not outside of the range found in other sources. Most importantly, however, we have little clarity on how these costs were derived. In discussions with CRU on the issue they have shared some of the logic used in modelling these costs, but were not willing to share values to derive final hydrogen production cost numbers, leaving limited room for us to calibrate or adjust specific cost items, either against other sources or in cost development scenarios. HILT project RP2.001 and RP2.006 developed detailed hydrogen cost modelling and this will be integrated into the model developed under this project in future iterations.

Relatedly, the CRU data as well as many other sources of hydrogen production cost estimates are of very limited geographic granularity, typically single values for individual countries[72], whilst it is well established that these are subject to strong regional variation[69,73]. HILT project RP2.006 identified cost differences of a factor two between different regions of Australia, for example[74]. The model derived from that work will be expanded to cover relevant potential future green iron production locations in future iterations of the model presented in this report. The same model will also be used to help differentiate hydrogen production costs and help assess the potential for green iron production in different regions of Australia, including the Pilbara, Geraldton, and Kwinana in Western Australia, and regions in South Australia, Tasmania, and elsewhere. There are also studies that suggest that there are limits to the availability of low-cost renewable energy in China, i.e., that the cost-curve for renewable energy will have a fairly steep slope at the higher levels of demand for renewable energy required to transition the entire Chinese economy to net-zero emissions[75]. The higher cost for renewables in such scenarios may improve competitiveness of Australian green iron exports to China; this too requires further investigation.

Simultaneously, it would be possible to close this relative cost gap in other cost components, although the potential for large changes may be more limited in some cases. Capital costs, for example, were determined to make up only US$38/t (of final liquid steel produced) for production based in China and US$47/t in Australia, or about 6 to 7% of total steel production cost in the H_2DRI-ESF-BOF pathway. While forecasts of technological costs, e.g., for the Electric Smelter Furnace, may be subject to substantial uncertainty, any development is unlikely to substantially impact the relative competitiveness between the two countries given the minor share in total production costs and assuming that costs come down at similar rates in both countries. Costs for other, more material inputs such as flux would seem unlikely to see drastic cost changes in the future.

Substantial changes that could shift relative competitiveness are more likely to be found in relative labour costs, and therefore innovations that reduce labour inputs could benefit Australian production. Exchange rates developments too, could have meaningful impacts. Stimulus policies including a range of different possible tax incentives, early investment in green iron production in Australia or key competitor countries, etc, could change the balance in relative competitiveness in iron production as well.

Technological developments including those investigated in HILT CRC projects, such as improved smelter furnace operation (RP1.014), flash iron smelting (RP1.009), novel beneficiation technologies (RP1.008), or magnetite processing (RP1.018), may do much to improve the outlook for the demand for Australian iron ores in green steelmaking value chains, but will not necessarily affect the relative competitiveness of Australia as a producer of green iron, as any of these technologies may be used in either China or Australia. This is similar to the findings on the relevance of the Electric Smelter Furnace capacity development in section 4.5; this will impact the demand for Australian ores, even if this processing capacity is based in China, but is not guaranteed to impact of green iron production in Australia.

Forecasts of Chinese steel demand, scrap availability and suitability for recycling, are subject to considerable uncertainty and may impact demand for green iron, including levels of demand for Australian green iron. The current model builds on an open-source forecast produced by the Mission Possible Partnership[57], which forecasts combined trends of falling demand for steel and an increasing supply of scrap. The current model logic presumes that any ton of scrap can be recycled into a ton of new steel, which then leads to a rapidly falling Chinese demand for primary steel. Both the steel demand and scrap supply forecasts are of course subject to considerable variability. There are also limits on how much of this scrap can be utilised for recycled steel production, and there may be limits to the types of steel products that could be produced from recycled scrap, as shown in HILT project RP3.005. We also use the lowest spot price identified over the period 2006-2025 as a proxy for scrap costs. Even at this low level we find that the model still leaves some small shares of scrap supply unutilised and selects to produce primary steel in a 2050 scenario with no green steel demand (see section 4.1 for more). These items all require further investigation in a future iteration of the model.

As noted, the development of the capacity of Electric Arc Furnace and Electric Smelter Furnaces will substantially influence the demand for ores of different Fe grades and therefore the country that may supply these ores. The future capacity development of both

technological pathways is of course subject to substantial uncertainty, in particular as the ESF technology is still at a limited level of technological development.

In our modelling, we have presumed that maritime transport of any type of HBI, regardless of density, as well as any type of pig iron, is feasible. The current reality is that the shipping of HBI with a density lower than 5 t/m^3 is subject to the same strict safety precautions as those that apply to the shipping of DRI products, primarily a blanket of an inert gas over the cargo[34,35]. This limit can likely only be met with ores with less than 3% gangue content[76], with some variation for other such as carbon content[39]. While this creates additional requirements on the storage and transport of the product, there is existing experience with applying these techniques in the shipping of DRI[36,37]. Industry partners have suggested that the additional cost of these safety measures may roughly double transport costs, from about US$16/t to US$32/t for a trip from port Hedland to Bohai Bay, or an additional 2.5-3% on total cost of about US$600-700 for a ton of liquid green steel (see also Figure 20). It should also be mentioned that there is ongoing research on methods to achieve the HBI density limit with low-grade Pilbara ores, as well as on other techniques including coatings that may reduce the cost of passivation of low density HBI. There is also ongoing inquiry into whether the chosen limit of 5 t/m3 really is the right limit, i.e., whether HBI with lower density may still be safely shipped even without the current strict safety precautions[39]. Our current model does not differentiate the cost of transport for HBI that does or does not meet the 5 t/m^3 density requirement. Whether this transport cost difference is a significant driver of cost competitiveness between low-grade ores typically mined in the Pilbara and high-grade ores typically found in e.g., Brazil or Guinea, is something that will be researched in a future iteration of this model.

Our model suggests that such a strict limit on future shipping of HBI would negatively impact the cost-competitiveness of green iron production in Australia, as the H_2DRI- ESF-EAF route, with pig iron shipped to China, appears less cost-competitive than the H_2DRI-HBI-ESF-BOF route, with HBI shipped to China. The majority of results presented in this report, on the location of iron production and other processing steps (section 4.1), on the suppliers of iron ore (section 4.2), processes used (section 4.3), and the impact of Chinese ESF capacity on consumption of ore from Australia and elsewhere would not be impacted by an assumption that low-density HBI would be technically impossible or carry prohibitive cost in the future, as these results currently forecast no international transport of low-density HBI.

Lastly, this research project focused on the Australia-China relationship in (green) steel value chains, and that is what has been reported on in above results section. The lack of iron production in Australia in the baseline results as presented here (though note the previous discussion of hydrogen cost settings) says nothing about the cost-competitiveness of Australian green iron production for supply into the Japanese, Korean, Indian, Taiwanese, European, or other markets. The same is true for iron ore supplies: results for the Chinese market do not mean to say the same would be true for supplies into green steel value chains elsewhere. Each of these markets has their own characteristics in terms of future steel demand, growth of scrap supply, and renewable energy and hydrogen production costs and capacity. An expansion to global demand markets as well as broader coverage of potential future suppliers of green iron is planned for a future iteration of the model.

With future version of this model, that include hydrogen cost assumptions that are calibrated to regional renewable resource and labour and other cost conditions, as well as a broader set of global demand and production locations, there are further questions that may be answered on the development of global green steel value chains and Australia's role in it. That includes for example at what point in time or at what level of demand Australian iron ores first become in demand for processing in green steel production; for example it may or may not be the case that Latin-American or African ores would sit lower on the global cost curve. Such a model could also help identify the relative cost-competitiveness of green iron production in South Australia or Tasmania versus the Pilbara.

6. CONCLUSIONS AND RECOMMENDATIONS

Our model results suggest that Chinese demand for Australian iron ore will decline, if forecasted reductions in steel demand and increases in suitable scrap supply materialise.

Regarding the relevance of Australian iron ore in current and future Chinese markets, our model suggests Chinese demand for Australian iron ore of about 910 Mt in 2025, and forecasts this to fall to about 650 Mt by 2035, with bigger reductions if China implements very ambitious green steel targets and especially if EAF capacity is ramped up. By 2050, Chinese demand for iron ore is forecast to fall significantly, following sharp reductions in primary steel production, to between 600 and as little as 250 Mt total demand for iron ore, with demand for Australian iron ore falling to between 400 and 50 Mt.

These numeric forecasts strongly depend on increases in scrap supply materialising, and the possibility that all or most steel demand can be met with steel from recycled scrap. However, overall trends suggest that demand for iron ore in the Chinese market will fall, depending on the rate that the supply of scrap, and the capacity of EAF to process this scrap, can fulfill demand for new steel.

Demand for Brazilian iron ore is more resilient to such changes, seeing much smaller relative reductions than Australian ores due to their flexibility for use in both conventional and green production routes. In scenarios with very high levels of green steel demand in particular, demand for Brazilian iron ore is more robust than that for Australian iron ore, with Brazil supplying about 160 Mt, and Australia supplying about 60 Mt of the total 245 Mt of remaining demand for iron ore.

In terms of the relevance of Australian green iron production into future Chinese green steel value chains, our model suggests that Brazil or Chile may be cost-competitive producers of green iron for the Chinese market in scenarios with high green steel demand, with up to a quarter of all iron consumed in China imported from these locations at baseline cost assumption settings. The remainder of the iron would be produced domestically, including from Australian ores. Australia or countries in the MENA region would not produce any green iron for export to China under baseline cost settings.

The cost-competitiveness of different countries or sub-national regions in the production of green iron is most strongly driven by the local production cost of green hydrogen. The hydrogen production costs in the baseline scenario are values suggested by CRU[8] and these values are both known to be conservative and provide a single value for all of Australia, ignoring substantial production cost differences between different locations within Australia[74]. These local hydrogen production cost differences require further investigation, which is planned or a future iteration of the model, utilising modelling methodology developed for Australia under the HILT CRC RP2.006 project[74].

Even without good estimates of hydrogen production cost in either location, we can still ask what hydrogen costs would be required for Australian green iron production to be competitive. This effectively means determining the hydrogen production cost differential required to close the gap in all other production costs, including the relative CapEx and labour costs in Australia and China. Our model suggests at hydrogen cost parity between Australia and China, the production of green iron would still occur entirely in China. At a cost differential of just A$0.50/kg H_2, our model suggests Australia may produce as much as 300 Mt of green iron for export to China. This number climbs to about 430 Mt if the cost differential is as large as A$1.25/kg H_2. Future development of the model presented here, which will include integration with HILT CRC developed hydrogen cost modelling, will help establish whether such a production cost differential is likely to materialise. That means we cannot comment on the required level of the Hydrogen Production Tax Incentive in order to make Australia a competitive green iron producer, beyond noting that the hydrogen production cost is a key driver of competitive green iron production, that costs other than hydrogen appear to put Australia at a slight disadvantage versus production in China, and that a Hydrogen Production Tax Incentive can help close that gap. The planned model expansion will allow more specific comments on the required level of this incentive.

Lastly, our model results show that the Electric Smelter Furnace will be of key importance to the cost-competitiveness of Australian iron ore in future green steel markets in China. In the 2035 Chinese market, if there were an ESF capacity of 400 Mt, Australian ores would make up to 380 Mt of a total 850 Mt of iron ore consumption. At 150 Mt of ESF capacity, this number would fall to just under 200 Mt, and in scenarios where there would be no or very limited ESF capacity, Australian ores would supply less than 50 Mt of Chinese demand. Australian ores are not suited for, or not competitive in, the H_2-DRI-EAF pathway, and scenarios where EAF processing capacity is relatively large compared to ESF processing capacity, market shares of other ores, mostly from Brazil, Russia, Ukraine, and Sweden, would grow at the expense of Australian supplies of ore. It is therefore imperative that Australian industry and government work to stimulate the technological development of the ESF, which is currently still in the demonstration stage, and help support their industrial-scale rollout. This may mean developing ESF processing capacity domestically, or convincing customers in China or other key markets that investments in ESF capacity are worthwhile.

7. REFERENCES

(1) Zhou, T.; Gosens, J.; Xu, H.; Jotzo, F. *China's Green Steel Plans: Near-Term Policy Challenges & Australia-China Links in Decarbonization. ANU Policy Brief.*; 2022.

(2) DISER. *Resources and Energy Quarterly Q1 2022*; Canberra, Australia, 2022.

(3) Rumsa, M.; John, M.; Biswas, W. Global Steel Decarbonisation Roadmaps: Near-Zero by 2050. *Environmental Impact Assessment Review* **2025**, *112*, 107807. https://doi.org/10.1016/j.eiar.2025.107807.

(4) Venkataraman, M.; Csereklyei, Z.; Aisbett, E.; Rahbari, A.; Jotzo, F.; Lord, M.; Pye, J. Zero-Carbon Steel Production: The Opportunities and Role for Australia. *Energy Policy* **2022**, *163*, 112811. https://doi.org/10.1016/J.ENPOL.2022.112811.

(5) Rahbari, A.; Shahabuddin, M.; Sabah, S.; Brooks, G.; Pye, J. Production of Green Steel from Low-Grade Ores: An End-to-End Techno-Economic Assessment. *Cell Reports Sustainability* **2025**, *2* (1). https://doi.org/10.1016/j.crsus.2024.100301.

(6) Rachel Wilmoth, Quailan Homann, Chathurika Gamage, Lachlan Wright, Kaitlyn Ramirez, Sascha Flesch, Thanh Ha, Joaquin Rosas, Natalie Janzow. *Green Iron Corridors: Transforming Steel Supply Chains for a Sustainable Future*; RMI. https://rmi.org/insight/green-iron-corridors/.

(7) Rasul, M. G.; Hazrat, M. A.; Sattar, M. A.; Jahirul, M. I.; Shearer, M. J. The Future of Hydrogen: Challenges on Production, Storage and Applications. *Energy Conversion and Management* **2022**, *272*, 116326. https://doi.org/10.1016/j.enconman.2022.116326.

(8) CRU. *Steel Cost Model*; CRU, 2022.

(9) CRU. *Iron Ore Cost Model*; CRU, 2022.

(10) Rhee, Y.; O'Neill, K.; Al Ghafri, S. Z. S.; May, E. F.; Johns, M. L. Effect of Location on Green Steel Production Using Australian Resources. *International Journal of Hydrogen Energy* **2024**, *90*, 827–841. https://doi.org/10.1016/j.ijhydene.2024.09.370.

(11) Wang, C.; Walsh, S. D. C.; Weng, Z.; Haynes, M. W.; Summerfield, D.; Feitz, A. Green Steel: Synergies between the Australian Iron Ore Industry and the Production of Green Hydrogen. *International Journal of Hydrogen Energy* **2023**, *48* (83), 32277–32293. https://doi.org/10.1016/j.ijhydene.2023.05.041.

(12) Wang, F.; Swinbourn, R.; Li, C. Shipping Australian Sunshine: Liquid Renewable Green Fuel Export. *International Journal of Hydrogen Energy* **2023**, *48* (39), 14763–14784. https://doi.org/10.1016/j.ijhydene.2022.12.326.

(13) Makepeace, R. W.; Tabandeh, A.; Hossain, M. J.; Asaduz-Zaman, Md. Techno-Economic Analysis of Green Hydrogen Export. *International Journal of Hydrogen Energy* **2024**, *56*, 1183–1192. https://doi.org/10.1016/j.ijhydene.2023.12.212.

(14) Curtis, A. J.; McLellan, B. C. Potential Domestic Energy System Vulnerabilities from Major Exports of Green Hydrogen: A Case Study of Australia. *Energies* **2023**, *16* (16), 5881. https://doi.org/10.3390/en16165881.

(15) Fastmarkets. *Understanding the High-Grade Iron Ore Market*; 2021. https://pearlgulliron.com.au/wp-content/uploads/2021/09/Understanding_the_high-grade_iron_ore_market_Fastmarkets.pdf.

(16) IEEFA. *Iron Ore Quality a Potential Headwind to Green Steelmaking*; 2022. https://ieefa.org/resources/iron-ore-quality-potential-headwind-green-steelmaking-technology-and-mining-options-are.

(17) Klaveness Research. *2021 Dry Bulk Outlook - Will Iron Ore Export Be Able to Meet Demand?*; 2021. https://www.klaveness.com/news/2020/10/30/2021-dry-bulk-outlook-will-iron-ore-export-be-able-to-meet-demand.

(18) Pustov, A.; Malanichev, A.; Khobotilov, I. Long-Term Iron Ore Price Modeling: Marginal Costs vs. Incentive Price. *Resources Policy* **2013**, *38* (4), 558–567. https://doi.org/10.1016/j.resourpol.2013.09.003.

(19) Bulayani, M. M.; Raghupatruni, P.; Mamvura, T.; Danha, G. Exploring Low-Grade Iron Ore Beneficiation Techniques: A Comprehensive Review. *Minerals* **2024**, *14* (8), 796. https://doi.org/10.3390/min14080796.

(20) Quast, K.; Skinner, W. Influence of Matrix Type on WHIMS Performance in the Magnetic Processing of Iron Ores. *Minerals Engineering* **2020**, *152*, 106346. https://doi.org/10.1016/j.mineng.2020.106346.

(21) Kukkala, P. C.; Kumar, S.; Nirala, A.; Khan, M. A.; Alkahtani, M. Q.; Islam, S. Beneficiation of Low-Grade Hematite Iron Ore Fines by Magnetizing Roasting and Magnetic Separation. *ACS Omega* **2024**, *9* (7), 7634–7642. https://doi.org/10.1021/acsomega.3c06802.

(22) Bilici, S.; Holtz, G.; Jülich, A.; König, R.; Li, Z.; Trollip, H.; Call, B. M.; Tönjes, A.; Vishwanathan, S. S.; Zelt, O.; Lechtenböhmer, S.; Kronshage, S.; Meurer, A. Global Trade of Green Iron as a Game Changer for a Near-Zero Global Steel Industry? - A

Scenario-Based Assessment of Regionalized Impacts. *Energy and Climate Change* **2024**, *5*, 100161. https://doi.org/10.1016/j.egycc.2024.100161.

(23) Ellersdorfer, P.; Wang, C.; Saydam, S.; Canbulat, I.; MacGill, I.; Daiyan, R. Unlocking New Export Opportunities: An Open-Source Framework for Assessing Green Iron and Steel Supply Chains. *International Journal of Hydrogen Energy* **2024**, *92*, 1366–1374. https://doi.org/10.1016/j.ijhydene.2024.10.163.

(24) Devlin, A.; Kossen, J.; Goldie-Jones, H.; Yang, A. Global Green Hydrogen-Based Steel Opportunities Surrounding High Quality Renewable Energy and Iron Ore Deposits. *Nat Commun* **2023**, *14* (1), 2578. https://doi.org/10.1038/s41467-023-38123-2.

(25) Cao, T.; Sugiyama, M.; Ju, Y. Prospects of Regional Supply Chain Relocation for Iron & Steel Industry Decarbonization: A Case Study of Japan and Australia. *Resources, Conservation and Recycling* **2024**, *209*, 107804. https://doi.org/10.1016/j.resconrec.2024.107804.

(26) Minerals Research Institute of Western Australia. *Western Australia's Green Steel Opportunity, MRIWA Project M10471*; 2023. https://www.mriwa.wa.gov.au/minerals-research-advancing-western-australia/focus-areas/green-steel/.

(27) WWF & Deloitte. *Forging Futures: Changing the Nature of Iron and Steel Production*; 2025. https://assets.wwf.org.au/image/upload/f_pdf/WWF_Green_Steel_Forging_Futures_Report_2025.

(28) Chris Bataille, Seton Stiebert, Francis Li. *Facility Level Global Net-Zero Pathways under Varying Trade and Geopolitical Scenarios: Final Technical & Policy Report for the Net-Zero Steel Project, Part II*; 2024. https://netzeroindustry.org/wp-content/uploads/pdf/net_zero_steel_report_ii.pdf.

(29) Mission Possible Partnership. *Making Net-Zero Steel Possible: An Industry-Backed, 1.5°C-Aligned Transition Strategy*; 2022. https://www.missionpossiblepartnership.org/action-sectors/steel/.

(30) Mandala. *Growing Australia's Iron Advantage*; 2024. https://mandalapartners.com/reports/growing-australias-iron-advantage.

(31) US department of the interior. *Mineral Commodity Summaries 2024: Iron Ore*. https://www.usgs.gov/centers/national-minerals-information-center/iron-ore-statistics-and-information.

(32) Rhee, Y.; O'Neill, K.; Al Ghafri, S. Z. S.; May, E. F.; Johns, M. L. Effect of Location on Green Steel Production Using Australian Resources. *International Journal of Hydrogen Energy* **2024**, *90*, 827–841. https://doi.org/10.1016/j.ijhydene.2024.09.370.

(33) Weiss, R.; Ikäheimo, J. Flexible Industrial Power-to-X Production Enabling Large-Scale Wind Power Integration: A Case Study of Future Hydrogen Direct Reduction Iron Production in Finland. *Applied Energy* **2024**, *365*, 123230. https://doi.org/10.1016/j.apenergy.2024.123230.

(34) International Iron Metallics Association. *Hot Briquetted Iron (HBI): A Guide to Shipping, Handling & Storage*. https://www.westpandi.com/getmedia/70a46f8c-e574-47b1-b038-ff99db724105/hbi_guide_amendment1may20.pdf.

(35) International Maritime Organization (IMO). *International Maritime Solid Bulk Cargoes (ISMBC) Code, Amendment 07-23*; 2023. https://puc.overheid.nl/nsi/doc/PUC_756966_14/.

(36) Midrex. *Shipping of DRI "The Nu-Iron Experience";* 2014. https://www.midrex.com/case-study/shipping-of-dri-the-nu-iron-experience/.

(37) Yazir, D.; Sahin, B.; Alkac, M. Selection of an Inert Gas System for the Transportation of Direct Reduced Iron. *Mathematical Problems in Engineering* **2021**, *2021* (1), 8529724. https://doi.org/10.1155/2021/8529724.

(38) Midrex. *2023 World Direct Reduction Statistics*; 2024. https://www.midrex.com/wp-content/uploads/MidrexSTATSBook2023.Final_.pdf.

(39) Midrex. *HBI: Steel Most Versatile Metallic in the Transition to the Hydrogen Economy*; 2021. https://www.midrex.com/wp-content/uploads/Midrex-DFM-3rdQtr2021-Final-1.pdf.

(40) Shahabuddin, M.; Rahbari, A.; Sabah, S.; Brooks, G.; Pye, J.; Rhamdhani, M. A. The Performance and Charge Behaviour in Melter/Smelter for the Production of Hot Metal in Hydrogen DRI-Based Steelmaking. *Ironmaking & Steelmaking* **2024**, 03019233241265179. https://doi.org/10.1177/03019233241265179.

(41) Wimmer, G.; Rosner, J.; Fleischanderl, A.; Apfel, J. Smelter Technology for Transforming Integrated Steelmaking towards Net-Zero Carbon. *The Iron and Steel Institute of Japan (ISIJ), Bulletin Ferrum: Tokyo, Japan* **2022**, *27*.

(42) Gustavsson, J.; Andersson, M. A. T.; Jönsson, P. G. Comparison of Calculated Equilibrium and Operation Data for Blast Furnace with Focus on Silicon. *Ironmaking & Steelmaking* **2009**, *36* (5), 341–353. https://doi.org/10.1179/174328109X401596.

(43) Wimmer, G.; Rosner, J.; Fleischanderl, A. Two Steps towards Net Zero Carbon? *Steel Times International* **2022**, *46* (3), 58–61.

(44) Sabah, S.; Shahabuddin, M.; Rahbari, A.; Brooks, G.; Pye, J.; Rhamdhani, M. A. Effect of Gangue on CO2 Emission for Different Decarbonisation Pathways. *Ironmaking & Steelmaking* **2024**, *51* (4), 356–368. https://doi.org/10.1177/03019233241242553.

(45) Madhavan, N.; Brooks, G. A.; Rhamdhani, M. A.; Rout, B. K.; Schrama, F. N. H.; Overbosch, A. General Mass Balance for Oxygen Steelmaking. *Ironmaking & Steelmaking* **2021**, *48* (1), 40–54. https://doi.org/10.1080/03019233.2020.1731252.

(46) Madhavan, N.; Brooks, G. A.; Rhamdhani, M. A.; Rout, B. K.; Overbosch, A. Application of Mass and Energy Balance in Oxygen Steelmaking. *Ironmaking & Steelmaking* **2021**, *48* (8), 995–1000. https://doi.org/10.1080/03019233.2020.1850170.

(47) Thomas, C.; Rosales, J.; Polanco, J. A.; Agrela, F. Steel Slags. In *New trends in eco-efficient and recycled concrete*; Elsevier, 2019; pp 169–190.

(48) Kho, T. S.; Swinbourne, D. R.; Blanpain, B.; Arnout, S.; Langberg, D. Understanding Stainless Steelmaking through Computational Thermodynamics Part 1: Electric Arc Furnace Melting. *Mineral Processing and Extractive Metallurgy* **2010**, *119* (1), 1–8. https://doi.org/10.1179/174328509X431454.

(49) Menad, N.-E.; Kana, N.; Seron, A.; Kanari, N. New EAF Slag Characterization Methodology for Strategic Metal Recovery. *Materials* **2021**, *14* (6), 1513. https://doi.org/10.3390/ma14061513.

(50) Kirschen, M. Visualization of Slag Data for Efficient Monitoring and Improvement of Steelmaking Slag Operation in Electric Arc Furnaces, with a Focus on MgO Saturation. *Metals* **2021**, *11* (1), 17. https://doi.org/10.3390/met11010017.

(51) Aminorroaya-Yamini, S.; Edris, H. The Effect of Foamy Slag in Electric Arc Furnaces on Electric Energy Consumption. **2002**.

(52) Pfeifer, H.; Kirschen, M. Thermodynamic Analysis of EAF Energy Efficiency and Comparison with a Statistical Model of Electric Energy Demand. In *7th European electric steelmaking conference*; 2002; Vol. 26, p 1.

(53) Neuschütz, D.; Spirin, D. Nitrogen Removal and Arc Voltage Increase in EAF Steelmaking by Methane Injection into the Arc. *steel research international* **2003**, *74* (1), 19–25. https://doi.org/10.1002/srin.200300156.

(54) Hornby, S.; Brooks, G. Impact of Hydrogen DRI on EAF Steelmaking. *Direct from MIDREX* **2021**.

(55) Trivella, A.; Corman, F.; Koza, D. F.; Pisinger, D. The Multi-Commodity Network Flow Problem with Soft Transit Time Constraints: Application to Liner Shipping. *Transportation Research Part E: Logistics and Transportation Review* **2021**, *150*, 102342. https://doi.org/10.1016/j.tre.2021.102342.

(56) MacroMicro. *China - Scrap Steel Spot Price*; 2025. https://en.macromicro.me/series/875/scrap-steel-spot.

(57) Mission Possible Partnership. *Steel Sector Transition Strategy Model*; 2023. https://github.com/missionpossiblepartnership/mpp-steel-model.

(58) Global Energy Monitor. *Global steel plant tracker*. https://globalenergymonitor.org/projects/global-steel-plant-tracker/.

(59) Blobal Energy Monitor. *Global Blast Frunace Tracker*; 2024. https://globalenergymonitor.org/projects/global-blast-furnace-tracker/.

(60) Transition Asia. *Will China Win the Green Steel Race? H2 -Dri-Eaf Market and Policy Development to 2030*; 2024. https://transitionasia.org/wp-content/uploads/2025/01/Will_China_Win_the_Green_Steel_Race_250124.pdf.

(61) World Steel Association. *World Steel in Figures 2025*; 2025. https://worldsteel.org/data/world-steel-in-figures/world-steel-in-figures-2025/.

(62) Bureau of International Recycling. *World Steel Recycling in Figures 2019 – 2023*. https://www.bir.org/images/uploads/publications/Ferrous_report_2019-2023.pdf.

(63) UN Trade Statistics Branch. UN Comtrade Database, 2021. https://comtrade.un.org/data/ (accessed 2021-08-19).

(64) Frieden, F.; Leker, J. Future Costs of Hydrogen: A Quantitative Review. *Sustainable Energy & Fuels* **2024**, *8* (9), 1806–1822. https://doi.org/10.1039/D4SE00137K.

(65) fgiacco. *Liebreich: Clean Hydrogen's Missing Trillions*. BloombergNEF. https://about.bnef.com/insights/clean-energy/liebreich-clean-hydrogens-missing-trillions/ (accessed 2025-06-13).

(66) International Energy Agency. *The Future of Hydrogen for G20*; 2019.

(67) *Global Hydrogen Review 2021 – Analysis*. IEA. https://www.iea.org/reports/global-hydrogen-review-2021 (accessed 2025-06-13).

(68) *Global Hydrogen Review 2022 – Analysis*. IEA. https://www.iea.org/reports/global-hydrogen-review-2022 (accessed 2025-06-13).

(69) IEA. *Global Hydrogen Review 2024*; 2024. https://www.iea.org/reports/global-hydrogen-review-2024.

(70) *Global Hydrogen Review 2023 – Analysis*. IEA. https://www.iea.org/reports/global-hydrogen-review-2023 (accessed 2025-06-13).

(71) The superpower institute. *A Green Iron Plan for Australia: Securing Prosperity in a Decarbonising World*. https://www.superpowerinstitute.com.au/work/green-iron-plan.

(72) Moritz, M.; Schönfisch, M.; Schulte, S. Estimating Global Production and Supply Costs for Green Hydrogen and Hydrogen-Based Green Energy Commodities. *International Journal of Hydrogen Energy* **2023**, *48* (25), 9139–9154. https://doi.org/10.1016/j.ijhydene.2022.12.046.

(73) Kan, X.; Reichenberg, L.; Hedenus, F.; Daniels, D. Renewable Export Cost Index as an Indicator of Global Renewable Energy Trade Potential. *Commun Earth Environ* **2025**, *6* (1), 1–12. https://doi.org/10.1038/s43247-025-02094-7.

(74) Tara Hosseini, Shuang Wang, Li Luo, Joe Coventry, Ahmad Mojiri, Alireza Salmachi, John Pye, Peter Ashman, Fiona Beck, Alireza Rahbari, Gus Nathan. *Hydrogen Supply within HILT Regional Hubs-H2 Cost and Synergistic Opportunities. HILT CRC RP2.006 Final Technical Report*; 2024. https://hiltcrc.com.au/projects/hydrogen-supply-within-hilt-regional-hubs-h2-cost-and-synergistic-opportunities/.

(75) Zhuo, Z.; Du, E.; Zhang, N.; Nielsen, C. P.; Lu, X.; Xiao, J.; Wu, J.; Kang, C. Cost Increase in the Electricity Supply to Achieve Carbon Neutrality in China. *Nat Commun* **2022**, *13* (1), 3172. https://doi.org/10.1038/s41467-022-30747-0.

(76) Midrex. *The IMSBC Code: Regulatory Framework for International Shipment of Solid Bulk Cargoes*; 2025. https://www.midrex.com/tech-article/the-imsbc-code-regulatory-framework-for-international-shipment-of-solid-bulk-cargoes/.

(77) Fan, J.; Hannah, P. *Understanding the High-Grade Iron Ore Market*; Fastmarkets, 2021; p 22.

(78) Zhou, D.; Cheng, S.; Wang, Y.; Jiang, X. Production and Development of Large Blast Furnaces from 2011 to 2014 in China. *ISIJ International* **2015**, *55* (12), 2519–2524. https://doi.org/10.2355/isijinternational.ISIJINT-2015-353.

(79) U.S. Geological Survey. *USGS Revision of Global Iron Ore Production Data—Clarification of the Reporting of Iron Ore Production in China and Application of a Uniform Comparison Methodology (2000-2015)*; 2022.

(80) Trading Economics. *Steel*. https://tradingeconomics.com/commodity/steel.

(81) Trading Economics. *Iron Ore*. https://tradingeconomics.com/commodity/iron-ore (accessed 2025-02-25).

8. APPENDIX 1 – ECONOMIC DRIVERS FOR BENEFICIATION

Here we provide some additional insight specifically into the economic drivers for beneficiation, and why we believe a future Chinese market, which will likely see lower rates of utilisation of the blast furnace, will see much reduced pressure to beneficiate.

The economic drivers for beneficiation include:

- Reduced cost of transport, as less gangue material is transported
- Reduced energy cost, as coke and PCI consumption in the blast furnace can be reduced with less material to melt
- Reduce cost of flux, as there is less gangue to remove
- Reduced CapEx cost, as smaller capacity blast furnaces are needed to handle ores with less gangue

We plot how these costs compare over a number of different levels of beneficiation in Figure A1. Note that results in this figure considers a fuel rate (coke and PCI consumption) that scales linearly with the amount of material fed into the blast furnace, as well a CapEx that scales linearly with the volume of ore fed into the blast furnace (rather than presuming a fixed CapEx per ton of hot metal). This plot shows that cost savings in transport and in the blast furnace process would not outweigh the additional cost of using higher levels of Fe grade product, given the additional cost associated with iron losses in beneficiation and resulting need to mine larger volumes of ore.

The result is an increase in end-to-end process costs with higher levels of beneficiation, with small cost increases at limited levels of beneficiation, but ramping up quickly at higher levels of beneficiation, when iron losses in the beneficiation process start to become very substantial (Figure A1). When considering these cost items, then, our model would hold that the most cost-optimal manner in which to process low grade ores would be without any beneficiation. Such a result is not in line with behaviour observed in current real-world markets, where we do see beneficiated material processed via the blast furnace.

This behaviour can be explained when we consider factors beyond the cost of the different line items for processing via the blast furnace itself. According to a report by Fastmarkets[77], the “most influential factor driving the high-grade premium” in iron ore markets is that blast furnace operators try to maximise profits by increasing hot metal production, which they can achieve with the use of ores with higher Fe grades. That is to say, an operator with a blast furnace with a given capacity may still improve hot metal output and therefore revenue, by using higher grades of iron ore.

Our model replicates this real-world market behaviour well, once we consider real-world blast furnace capacity in operation in China. With model settings at about 850 Mt of blast furnace capacity (and 150 Mt of EAF capacity), as currently exists in China, the model chooses levels of beneficiation that are very close to those seen in current global markets for individual ores from a number of key Pilbara mines (Figure A2 & Table A1). The same effect is also visible when we run the model with the full set of mines: stronger limits on blast furnace capacity result in the model pushing less low-grade ores and more high-grade ores through the blast furnace (Figure A3).

In our model, the explanation for this logic is that demand is fixed. If the model feeds lower grade ores through the blast furnace, this limits the output of hot metal via the blast furnace route, and demand has to be fulfilled via the more costly EAF production route. We can visualise the size of this effect, by assuming that any lost production when processing low grade ores via the bast furnace must instead be met with production via alternative routes, at marginal costs roughly equal to market prices, so approximately $500/t at 2024 levels. If we add this to the plot, the optimal model choice becomes a beneficiation level of about 60% for the representative Pilbara ore chosen for this exercise. Any higher would generate prohibitively high costs for mining and beneficiation, any lower would require large additional costs to supplement supply from more expensive production routes at marginal production cost. This matches reported average ore grades of ‘around 59%’[78] or ‘58% to 60%’[79] as consumed in Chinese blast furnaces.

In real-world markets, the opportunity cost penalty as calibrated in Figure A4 is equivalent to a reduced revenue that any blast furnace operator will consider, as their output of steel falls with the use of lower quality ores. Fan & Hannah [77] argue that the price premium for higher ore grades “tends to be well correlated with indicators of mill profitability – although these can be difficult to estimate with precision given business variabilities in the steel industry”. That said, the revenue penalty hat we calculate tracks very closely with CRU’s so-called ‘Value In Use’ penalty (or premium) for Fe grade (Figure A5), suggesting that we capture this dynamic at levels that are well calibrated versus real-world markets.

A factor that has not been represented very well in our (current) model is the large differences that may exist between blast furnaces within a specific region. It is quite feasible that in real-world markets, some older, less efficient plants may shut down, even as more efficient plants still try to optimise profits by using higher grade ores. In our current model, China is represented by 3 regional nodes with average fuel rates, CapEx and OpEx charges derived from the CRU steel costing model. A model with multiple blast furnace nodes in any region, with varying costs, may be better in replicating the real-world cost curve for that region.

FIGURE A1. COST FOR STEEL PRODUCED VIA THE BF-BOF ROUTE FOR A REPRESENTATIVE AUSTRALIAN ORE

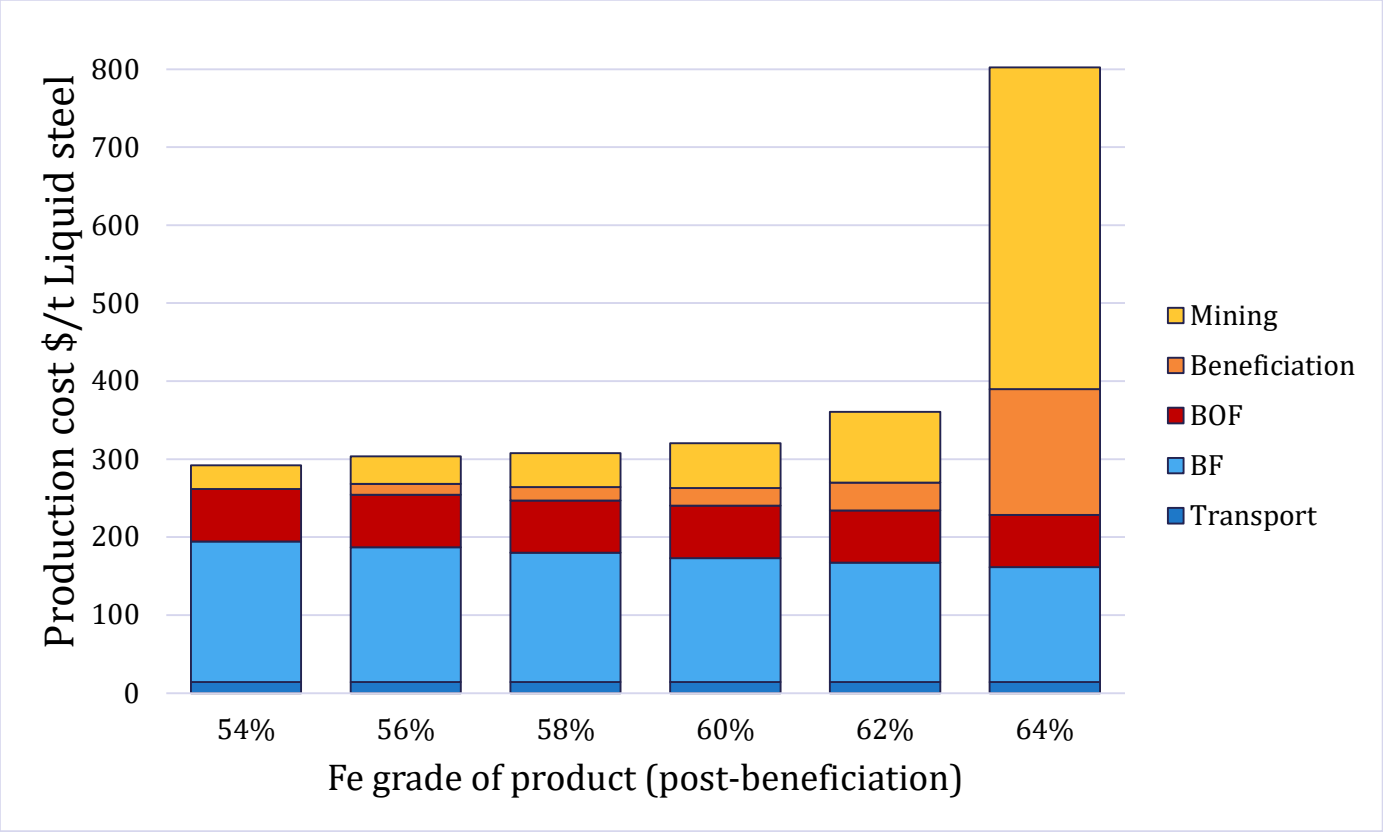

Note: y-axis is censored at $400/t; production costs at beneficiation to 64% Fe can be seen in table below.

Ton of ore mined	1.72	2.01	2.45	3.24	5.11	23.25
Ton of product	1.72	1.66	1.60	1.55	1.50	1.45
Fe grade of product	**54%**	**56%**	**58%**	**60%**	**62%**	**64%**
Mining	30.52	35.71	43.60	57.51	90.73	412.90
Beneficiation	0.00	13.94	17.01	22.44	35.41	161.12
BF	180.55	172.97	165.93	159.17	153.18	147.40
CapEx	11.92	11.38	10.89	10.41	9.97	9.57
OpEx	13.93	13.93	13.93	13.93	13.93	13.93
Coke	115.46	111.30	107.46	103.84	100.64	97.45
PCI	27.58	26.66	25.74	24.79	24.06	23.32
Burnt lime	14.98	12.46	10.17	7.97	5.90	4.04
BF slag	-3.32	-2.77	-2.26	-1.78	-1.33	-0.91
BOF	67.14	67.14	67.14	67.14	67.14	67.14
Transport	20.28	19.56	18.88	18.24	17.66	17.11
Total	**298.49**	**309.32**	**312.57**	**324.50**	**364.11**	**805.68**
Costs vs 60% bene level						
Mining + beneficiation	-49.43	-30.31	-19.34	0.00	46.18	494.08
BF	21.38	13.81	6.76	0.00	-5.99	-11.77

FIGURE A2. MODEL SELECTIONS OF BENEFICIATION LEVELS IN TEST SETTINGS

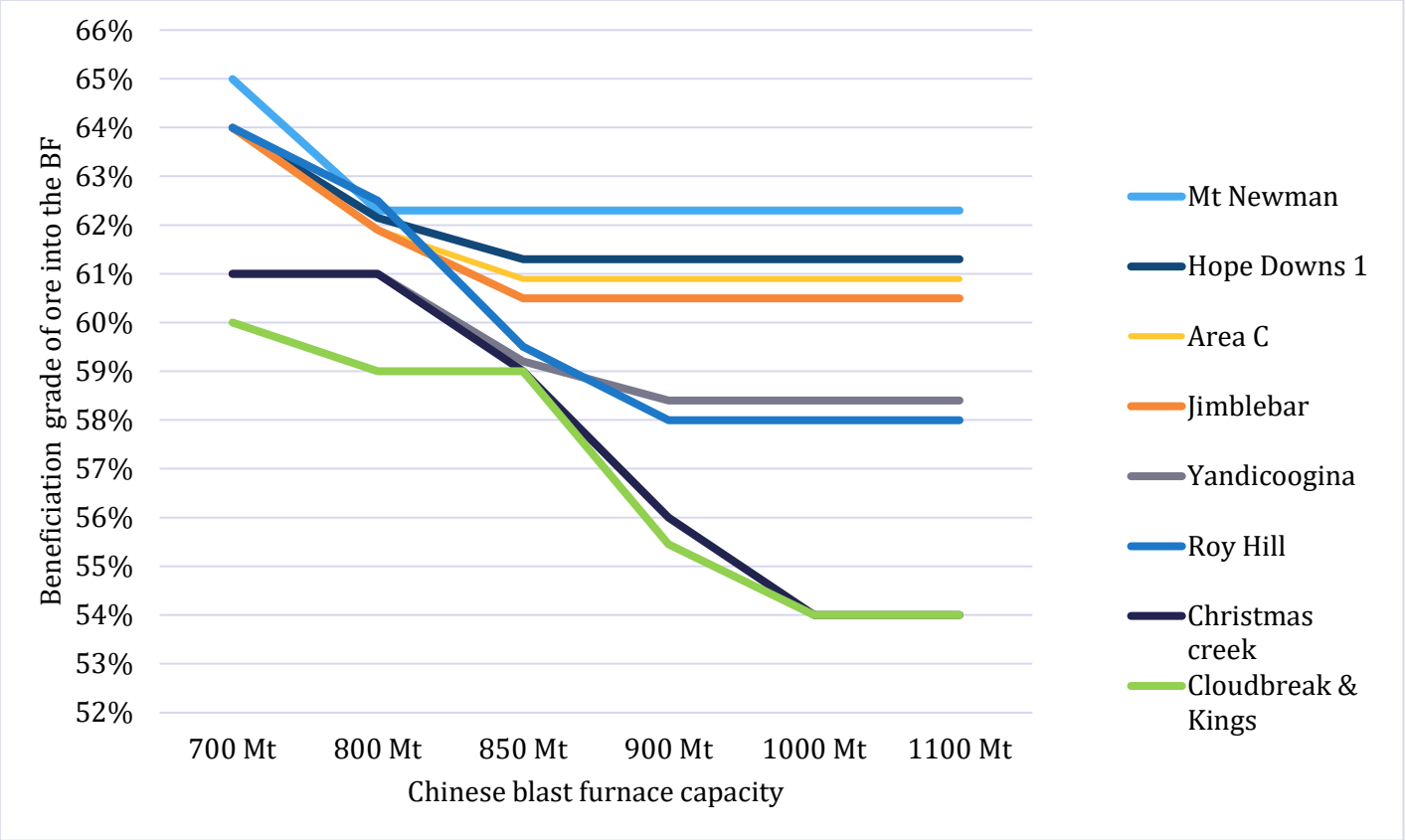

TABLE A1. MODEL SELECTIONS OF BENEFICIATION LEVELS IN TEST SETTINGS

Chinese blast furnace capacity	700 Mt	800 Mt	850 Mt	900 Mt	1000 Mt	1100 Mt
Christmas creek	61%	61%	58% & 60%	54%[1] & 58%	54%[1]	54%[1]
Roy Hill (lump & fines)	61.5%[1,2]	61.5%[1,2]	61.5%[1,2]	61.5%[1,2]	61.5%[1,2]	61.5%[1,2]
Roy Hill (fines only)	64%	62% & 63%	58%[1] & 61%	58%[1]	58%[1]	58%[1]
Mt Newman	65%	62.3%[1]	62.3%[1]	62.3%[1]	62.3%[1]	62.3%[1]
Jimblebar	64%	63% & 60.5%[1]	60.5%[1]	60.5%[1]	60.5%[1]	60.5%[1]
Area C (lump & fines)	62.6%[1,2]	62.6%[1,2]	62.6%[1,2]	62.6%[1,2]	62.6%[1,2]	62.6%[1,2]
Area C (fines only)	64%	63% & 60.9%[1]	60.9%[1]	60.9%[1]	60.9%[1]	60.9%[1]
Yandicoogina	61%	61%	60% & 58.4%[1]	58.4%[1]	58.4%[1]	58.4%[1]
Kings	60%	60% & 58%	60% & 58%	56.9% & 54%[1]	54%[1]	54%[1]
Cloudbreak	60%	60% & 58%	60% & 58%	56.8% & 54%[1]	54%[1]	54%[1]
Hope Downs 1	64%	63% & 61.3%[1]	61.3%[1]	61.3%[1]	61.3%[1]	61.3%[1]

Note: scenarios run with ore from a single mine only, in unlimited supply. In all scenarios demand is set at 1050 Mt, EAF capacity set at 150 Mt, ESF capacity unlimited but at very high OpEx. 1) Unbeneficiated ore; 2) lump ore.

FIGURE A3. MODEL SELECTIONS OF BENEFICIATION LEVELS AT DIFFERENT BF CAPACITY LEVELS

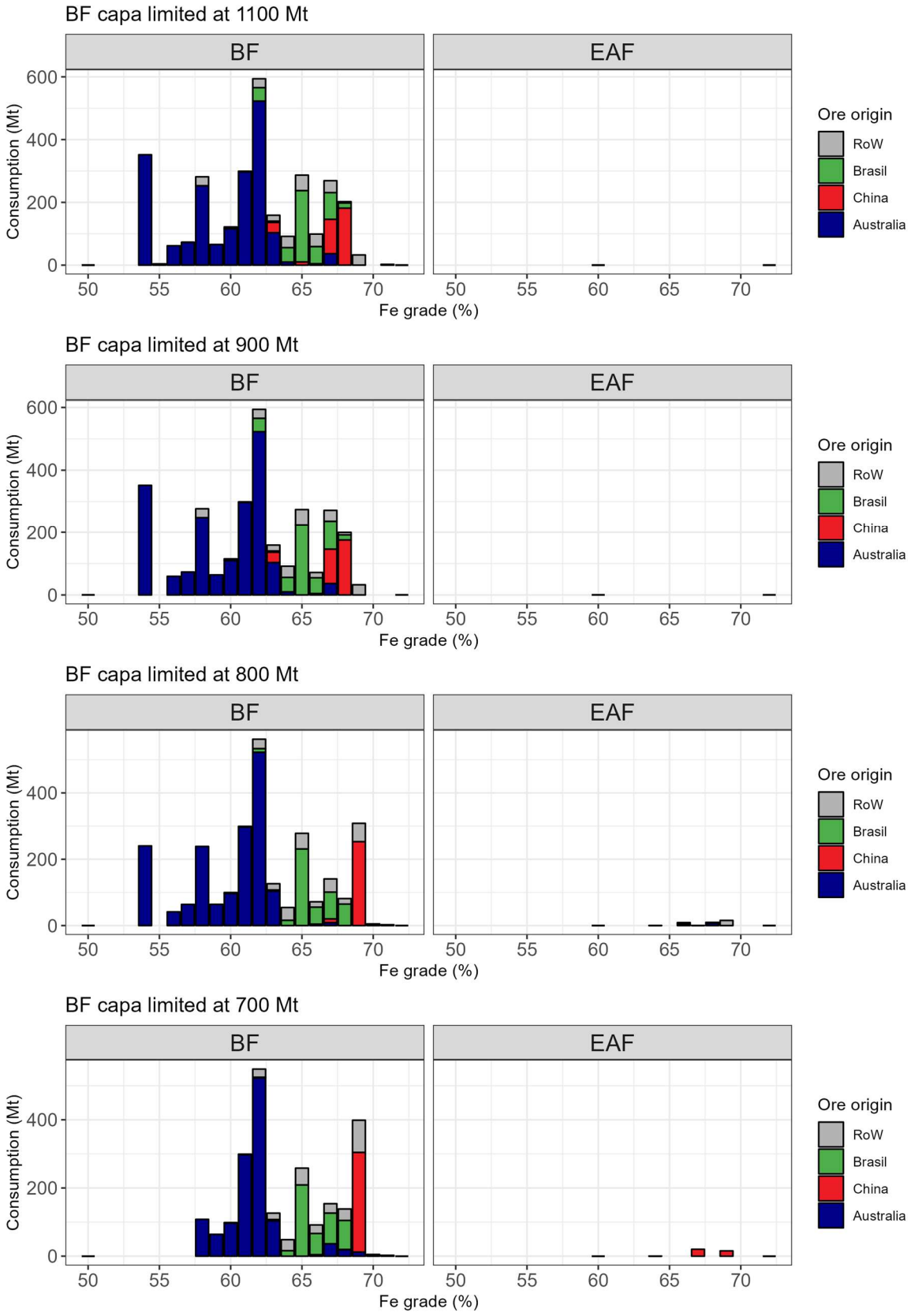

FIGURE A4. COST FOR STEEL PRODUCED VIA THE BF-BOF ROUTE FOR A REPRESENTATIVE AUSTRALIAN ORE, INCLUDING OPPORTUNITY COST PENALTY

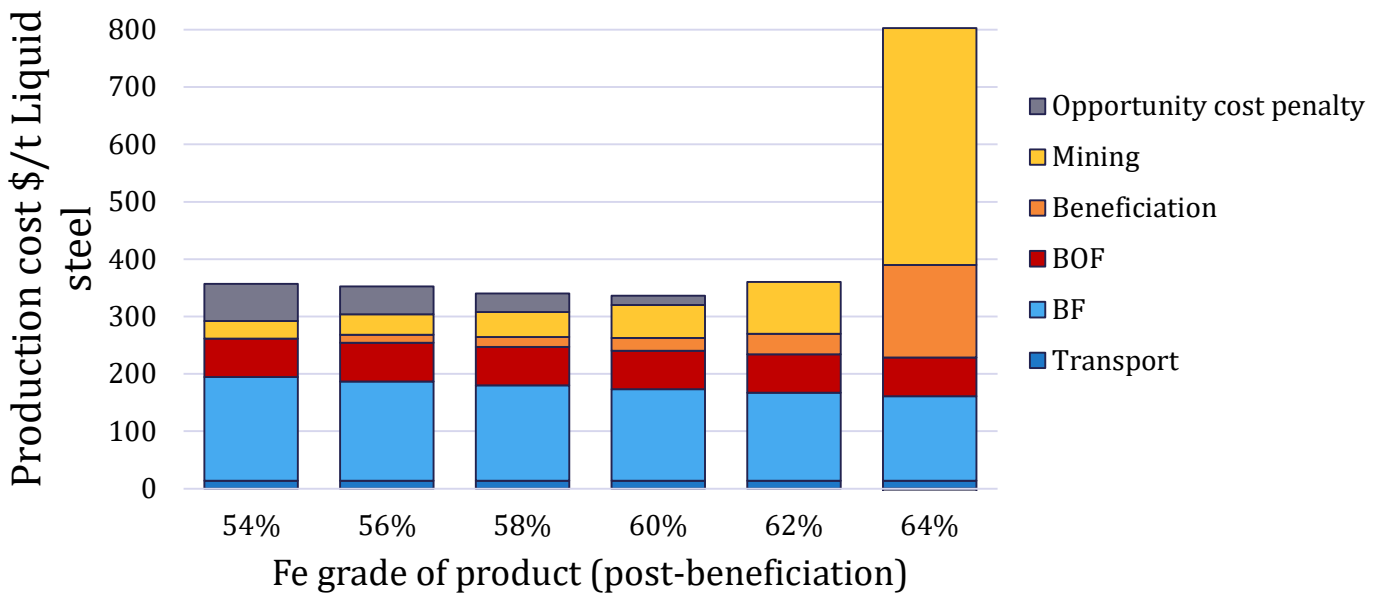

Note: y-axis is censored at $400/t; production costs at beneficiation to 64% Fe can be seen in table below.

Ton of ore mined	1.72	2.01	2.45	3.24	5.11	23.25
Ton of product	1.72	1.66	1.60	1.55	1.50	1.45
Fe grade of product	**54%**	**56%**	**58%**	**60%**	**62%**	**64%**
Mining	30.52	35.71	43.60	57.51	90.73	412.90
Beneficiation	0.00	13.94	17.01	22.44	35.41	161.12
BF	180.55	172.97	165.93	159.17	153.18	147.40
BOF	67.14	67.14	67.14	67.14	67.14	67.14
Transport	20.28	19.56	18.88	18.24	17.66	17.11
Opportunity cost penalty	64.60	48.60	32.51	15.94	0.00	-15.99
Total	**356.75**	**352.30**	**340.13**	**336.14**	**360.39**	**786.52**
Ton of ore fed into blast furnace	1.72	1.66	1.60	1.55	1.50	1.45
Steel output vs use of a 62% ore	0.87	0.90	0.93	0.97	1.00	1.03
Revenue per ton of steel	500	500	500	500	500	500
Revenue in this scenario	435.40	451.40	467.49	484.06	500.00	515.99
Revenue penalty incurred ($/tLS)	64.60	48.60	32.51	15.94	0.00	-15.99
Revenue penalty incurred ($/t ore)	37.60	29.32	20.31	10.31	0.00	-11.03

HILT CRC

hiltcrc.com.au

General enquiries
enquiries@hiltcrc.com.au

Connect with us
hiltcrc.com.au/connect

Australian Government
Department of Industry, Science and Resources

Cooperative Research Centres Program